NASA Technical Memorandum 107752

# STRUCTURAL MECHANICS DIVISION RESEARCH AND TECHNOLOGY ACCOMPLISHMENTS FOR C.Y. 1992 AND PLANS FOR C.Y. 1993

**John B. Malone**



**November 1993**

National Aeronautics and Space Administration

**Langley Research Center**
Hampton, Virginia 23681-0001

# STRUCTURAL MECHANICS DIVISION

# RESEARCH AND TECHNOLOGY ACCOMPLISHMENTS FOR C.Y. 1992 AND PLANS FOR C.Y. 1993

## SUMMARY

The purpose of this report is to present the Structural Mechanics Division's research accomplishments for C.Y. 1992 and plans for C.Y. 1993. The technical mission and goals of the Division and its constituent research branches are described. The work performed by each branch is described in terms of highlights of accomlishments during the past year and plans for the current year related to branch long-range goals. This information is useful in program coordination with other government organizations, universities, and industry in areas of mutual interest.

THIS PAGE LEFT INTENTIONALLY BLANK

## TABLE OF CONTENTS

THIS PAGE LEFT INTENTIONALLY BLANK

## ORGANIZATION

The Langley Research Center is organized into research and support directorates as shown in figure 1. The Structures Directorate, headed by Mr. Charles P. Blankenship, is one of the five research directorates shown in the figure. The research organizations are the Aeronautics, Structures, Flight Systems, Electronics and Space Directorates. The Structures Directorate organization, shown in figure 2, consists of the Structural Mechanics Division (SMD), the Materials Division (MD), the Structural Dynamics Division (SDyD), the Acoustics Division (AD), and the Structures Technology Program Office (STPO).

The Structural Mechanics Division conducts analytical studies, develops computational methods, and performs experimental research in a variety of areas to meet the technical requirements of advanced aerospace vehicles and spacecraft configurations. The Division consists of 62 NASA civil servants and 4 members of the Vehicle Structures Directorate, US Army Research Laboratory, who are collocated within two of the SMD branches. Four primary technical areas emphasized in the SMD are illustrated in figure 3. Division personnel are organized into four branches, as shown on figure 4, and focus their work along research thrusts related to these four technical areas. The SMD branches are: the Aircraft Structures Branch (ASB), headed by Dr. James H. Starnes, Jr.; the Spacecraft Structures Branch (SSB), headed by Mr. Harold G. Bush; the Computational Mechanics Branch (CMB), headed by Dr. Jerrold M. Housner; and the Aerothermal Loads Branch (ALB), headed by Dr. Allan R. Wieting. Each branch has the lead responsibility for a number of related technical thrusts, several of which are indicated in figure 4.

There have been some changes in the Division management personnel during the past year: Dr. John B. Malone, formerly Head, Unsteady Aerodynamics Branch, SDyD, was appointed Chief, Structural Mechanics Divison; and Dr. Mark J. Shuart, formerly Assistant Head, Aircraft Structures Branch, SMD, was appointed Assistant Chief, Structural Mechanics Division.

## FUNCTIONS AND RESPONSIBILITIES

The primary goal of the Structural Mechanics Division is to conduct analytical and experimental research that provides for reliable structural concepts which meet functional requirements of advanced atmospheric and space flight vehicles. In support of this goal, the Division develops and validates new analytical and computational structural analysis and design methods for predicting stresses, deformation, structural strength, thermal loads and thermoelastic phenomena. In addition, the Division develops, fabricates, tests and evaluates structural components embodying new material systems and/or advanced design concepts for general application and for specific classes of aerospace vehicles. The Division also performs unique structural tests to provide data required to validate computational methods. In conducting

experimental research, the Division uses a broad spectrum of test facilities and develops new experimental techniques.

In addition to conducting a core research program which address longer-term discipline topics, the Division also participates in a number of shorter-term, focused, systems technology programs. These focused programs include the Advanced Composites Technology (ACT) program, the High Speed Research (HSR) program, the Aircraft Structural Integrity Program (ASIP), the National Aero-Space Plane (NASP) program, and the High Performance Computing and Communications (HPCC) program. These focused programs are conducted as team activites, combining the efforts of NASA research centers, industry and university participants.

## FOCUSED TECHNOLOGY PROGRAMS

The ACT, HSR and ASIP programs, to which the SMD provides major support in both planning and execution, are described briefly in the following paragraphs.

### Advanced Composites Technology Program

The objective of the Advanced Composites Technology Program is to develop an integrated composites structures and materials technology that will provide the impetus for a more rapid and timely transition of this technology into production aircraft. This program focuses on enabling research for the application of cost-effective composites in primary structures of future commerical transport aircraft designs. The development of this integrated technology involves a cooperative and coordinated research effort between government, industry and universities which encourages innovation, verification, and dissemination throughout the United States composites industry. The major research elements of the ACT program are illustrated in figure 5. The three phases of this multi-year research effort are shown in figure 6.

### High Speed Research Program

The objective of the High Speed Research Program is to develop the technology for enabling an economically viable supersonic transport. The initial phase of this program has been developing solutions for critical environmental issues. These issues deal with acceptable airport noise level, feasibility of supersonic flight overland, and reduction of engine emissions for minimum impact on atmospheric ozone. The second phase of the HSR Program deals with the development of critical technologies in a number of areas including, aerodynamics, structures and materials, propulsion and flight deck design. The focused technology development in airframe structures and materials will provide the foundation for the development of low-weight, high-durability materials and structural concepts capable of withstanding the temperature and external loads associated with the sustained supersonic flight of a high-speed civil transport. Specifically, polymer matrix composites, metal matrix composites, and advanced metals will be developed through a combined industry, NASA and academia program.

Additionally, structural concepts which are appropriate for these material systems will be developed and verified. The major research elements of the HSR airframe materials and structures technology program are illustrated in figure 7.

### Aircraft Structural Integrity Program

The FAA and NASA have developed a cooperative research effort aimed at providing a technological basis for ensuring the continued safe operation of the US commerical airplane fleet. The two agencies' efforts concentrate on research and development in fatigue and fracture behavior of materials, structural integrity, corrosion, flight loads, nondestructive inspection and evaluation, human factors, and maintenance and repair. NASA's contribution to this effort, the Aircraft Structural Integrity Program, is developing: 1) a fatigue crack growth prediction methodology and incorporating this methodology into advanced structural analysis methods to permit determination of the residual strength of complex built-up structures; 2) an experimental data base suitable for verifying computational methods; and 3) nondestructive evaluation technologies to detect fatigue cracks, corrosion, and disbonds in adhesively bonded joints. The major research elements of the ASIP Program are illustrated in figure 8.

## FACILITIES

The Structural Mechanics Division has three major experimental facilities to support its research activities, as shown in figure 9. These facilities are the Structures and Materials Laboratory, the 8-foot High Temperature Tunnel, and the Automated Structural Assembly Laboratory. In addition, there are several other facilities, both experimental and computational, which support Division research. These additional facilities are the Thermal Structures Laboratory, the 7-inch High Temperature Tunnel, the Aerothermal Arc Tunnels, and the Convex computer system. A new structural test facility, the Combined Loads Test System (COLTS), is currently being designed to provide a unique test facility for large-scale, primary aircraft structural components. The SMD test facilities are located on the west side of the NASA Langley Research Center, as shown in figure 10.

### Structures and Materials Laboratory

The Structures and Materials Laboratory, located in NASA Langley Building 1148, supports the research activities of the Aircraft Structures Branch and the Spacecraft Structures Branch. Laboratory equipment, as shown in figure 11, includes a 1,200,000-lb.-capacity testing machine for tensile and compressive specimens up to 6 feet wide and 18 feet long; lower capacity testing machines of 300,000 lb. and 120,000 lb. capacity; a torsion machine of approximately 60,000 lb. capacity; hydraulic and pneumatic pressurization equipment; impact testing equipment; a cylinder bending test fixture; and a vertical abutment-type backstop for supporting and/or anchoring large structural test specimens.

## 8-foot High Temperature Tunnel

The 8-foot High Temperature Tunnel (8'HTT), located in NASA Langley Building 1265, is operated by the Aerothermal Loads Branch. The tunnel, shown in figure 12, is a unique hypersonic Mach 7 blowdown wind tunnel with an 8-ft.-diameter test section. Elevated temperatures are attained by burning a mixture of air and methane under pressure in a combustor, and then using the products of combustion as a test medium (fig. 13). The tunnel operates at dynamic pressures of 250 to 1800 psf, temperatures of 2400$^{o}$R to 3600$^{o}$R and Reynolds numbers of 0.3 to 2.2 x $10^{6}$/ft. The tunnel is used to test 2-D and 3-D type models to determine aerothermal loads and to evaluate new high temperature structural concepts. A major Construction of Facility (CoF) activity is currently under way to provide Mach 4 and Mach 5 capability, to verify a transpiration-cooled primary nozzle, and to add oxygen enrichment to the test medium. This is being done primarily to permit testing of models that have hypersonic air-breathing propulsion applications.

## Automated Structural Assembly Laboratory

The Automated Structural Assembly Laboratory (ASAL), located in NASA Langley Building 1220, is operated jointly by the Spacecraft Structures Branch and the Automated Technology Branch, of the Information Systems Division, Flight Systems Directorate. The ASAL, shown in figure 14, is composed of a robot arm, a planar X-Y motion base platform, and a rotating motion base. The facility hardware was designed as a ground-based system to permit initial evaluation of in-space assembly concepts. The facility also has an integrated video subsystem to permit the operator to view, at close range, the operations of the robot and end-effector.

## Thermal Structures Laboratory

The Thermal Structures Laboratory (TSL), located in NASA Langley Building 1267, is operated by the Aircraft Structures Branch. The facility provides a capability for testing panel-size structural elements, which are representative of supersonic and hypersonic structural components, subjected to combined mechanical and thermal loadings (fig. 15). Three test machines (22,000-lb. capacity; 110,000-lb. capacity; and 550,000-lb. capacity) are available for applying compressive and tensile mechanical loads to test specimens. In addition, the TSL has two chambers for thermal conditioning and for apparent strain measurement of instrumented structural panels at temperatures up to 2000$^{o}$F and 3000$^{o}$F, respectively, two clamshell chambers for structural joint and material property testing, two chambers for panel testing with mechanical loads at elevated temperature, an IR camera for full-field temperature measurement, and a collumnated coherent light source to obtain full-field out-of-plane deformation of panels using the Moire' strain technique. Two complete PC-based data acquisition systems, software, and signal conditioning equipment are available which allow for simultaneous mechanical and thermal loads testing and provide a total collection capability of 256 strain channels, 700 temperature channels, and 50 displacement channels.

## 7-inch High Temperature Tunnel

The Aerothermal Loads Branch also operates a 7-inch High Temperature Tunnel (7"HTT). This facility is a nearly 1/12th scale of the 8'HTT with basically the same capabilities as the larger tunnel. The 7"HTT is used primarily as an aid in the design of larger models for the 8'HTT and for aerothermal loads tests on subscale models.

## Aerothermal Arc Tunnels

The Aerothermal Loads Branch is also responsible for the operation of two Aerothermal Arc Tunnels (20 MW and 5 MW) which are used to test models in an environment that simulates the flight reentry envelope for high-speed vehicles such as the Space Shuttle. The amount of usable energy to the test medium in these facilities is 9 MW and 2 MW. The 5 MW facility uses a three-phase AC arc heater while the 20 MW facility uses a DC arc heater. Test conditions can support a wide range of temperature, flow rate, and enthalpy using a variety of nozzles, throats and model sizes (3-in. diameter to 1-ft. x 2-ft. panels). Although heavily utilized in the past, the Arc Tunnel facilities are now kept in a standby mode due to present decreased testing requirements at Langley.

## Computer Systems

The SMD Convex C240 (fig. 16), designated as blackbird, provides the cornerstone of the computer resources for the Structural Mechanics Division. This system provides a four-processor mini-super computer with 512 megabytes of main memory, 22 Gigabytes of secondary storage, and an aggregate processing speed of 200 megaflops. This resource enables research in advanced computational algorithms, using both parallel and vector techniques, to be directly applied to current research in the development of advanced structural analysis methods. From the Convex C240 the shared computational environment extends to a variety of workstations and other computers that provide graphical tools for preparation and visualization of finite element structural models and a user interface for program development using the ethernet network for communication.

In addition to the Convex system, SMD has access to a number of super computer facilites. These facilites include Cray 2's and Cray YMP's at both NASA Langley and NASA Ames, a Cray-C90 at NASA Ames, as well as several computer systems of the massively-parallel-type of architecture located at various sites around the United States. These super computer facilities are used for the development computational mechanics methods which take advantage of multi-processor capability, and for applications where structural models consist of large numbers of degrees-of-freedom (>100,000).

### Combined Loads Test System

A unique facility for the testing of large-scale stiffened shells and curved stiffened panels (fig. 17) is currently in the design stage, and is planned to be available for initial operation in 1996. When completed, the Combined Loads Test System (COLTS) will permit the testing of shell components of up to 14 ft. in diameter directly, or panel components of up to 10 ft. in radius (i.e., 20 ft. diameter) using a special fixture. When completed, COLTS will allow specimens to be tested under combined mechanical, thermal, pressure, and cyclic loads. An auxillary test site will also be available for testing larger shells of up to 20 ft. in diameter under combined mechanical and pressure loads. The first test fixture of the COLTS facility to be completed, a pressure-box test machine, has been delivered to NASA and is currently scheduled to be operational in 1993. The pressure box, shown in figure 18, will provide biaxial tension and pressure loading test capability for curved stiffened panels having approximately a 125 in. radius, 72 in. long and 63 in. wide. This test facility will support research into shell and panel structural response, damage tolerance, durability and failure mechanisms. The COLTS will be operated as a National facility, in that it will be used to support US industry, as well as NASA testing requirements. The facility will initially be used to test subcomponents and components fabricated by US industry under the ACT, HSR and ASIP focused programs.

## ACCOMPLISHMENT HIGHLIGHTS

Specific research goals and selected highlights of technical activities recently completed by each SMD organization are presented in the following paragraphs.

### Aircraft Structures Branch

The primary goal of the Aircraft Structures Branch (fig. 19), is to develop verified structural mechanics technology and innovative structural concepts for structurally-efficient, cost effective primary aircraft structures. In support of this goal, the ASB conducts analytical and experimental research on the response and failure of complex structures subject to static and dynamic loads. Studies are made of basic structural behavior, advanced methods of analysis and design are developed, and the validity of analyses are confirmed by conducting tests of elements and large-scale structural models at room temperature and at high and low temperatures as required. The ASB develops efficient structural concepts that exploit the benefits of advanced-composite and metallic materials for future low-speed and high-speed aircraft and space transportation systems. Typical studies investigate primary airframe structural behavior and concepts, structural stability, failure analysis, residual strength, damage tolerance, tailoring of structures made of composite materials, thermal protection systems, reusable cryogenic tanks, cooled structural concepts, and thermal effects on structural behavior. Special emphasis is focused on identification of structural deformations and failure modes, development of structurally efficient advanced-composite and metallic structural concepts, and prediction of nonlinear and linear response phenomena due to

mechanical, pressure and thermal loads. The ASB studies response of advanced-composite and metallic structures with local gradients, discontinuities and eccentricities. New static and dynamic test techniques are conceived and used in the Structures and Materials Research Laboratory, the Thermal Structures Laboratory and other high temperature and cryogenic test facilities.

Recent Aircraft Structures Branch accomplishments listed below are highlighted in figures 20 through 26.

Composite Structures

- Stiffness Tailoring Concept Improves Compression Buckling and Postbuckling Response for Composite Plates (fig. 20)

- Composite Materials Shown to Retain Residual Strength After 10 Years of Outdoor Exposure (fig. 21)

- Cost Effective Composite Wing Concept Developed for Civil Tilt Rotor (fig. 22)

- Cost Effective Composite Fuselage Concept Developed for Civil Tilt Rotor (fig. 23)

Thermal Structures

- Langley Heat-Pipe Concept Selected as Candidate for the NASP Wing Leading Edge (fig. 24)

- Preliminary Design Thermal Structural Analysis Reduces Modeling and Computational Time for Beam and Plate Structures (fig. 25)

- Conceptual Studies Initiated for HSR Wing Structures (fig. 26)

**Spacecraft Structures Branch**

The primary goal of the Spacecraft Structures Branch (fig. 27) is to develop enabling spacecraft structures technologies and concepts which support current and future earth orbit, lunar and planetary missions. In support of this goal, the SSB develops technology required to design advanced spacecraft structures for application to, and including, erectable and deployable precision antennas, extra-vehicular-activity (EVA) and robotic assembly procedures, space cranes, lightweight spacecraft, and launch vehicles. Spacecraft research encompasses structural concepts, deployment mechanism design and analysis, packaging for small launch vehicles, deployment simulation, joint development, and advanced composite and metallic structures. Concepts are verified by analysis, ground test and/or spaceflight experiment. Launch vehicle research encompasses analysis and design of efficient, producible structural

concepts using contemporary material systems. Structural concepts are verified by appropriate component ground tests.

Recent Spacecraft Structures Branch accomplishments listed below are highlighted in figures 28 through 33.

Flight Demonstrations

- LaRC Erectable Truss Hardware Enables Space Construction Flight Demonstration and *INTELSAT* Retrieval (fig. 28)

Precision Segmented Reflectors

- Precision Segmented Reflector Panel-to-Truss Attachment Hardware and Procedures Verified in Neutral Buoyancy Tests (fig. 29)

- EVA Assembly Procedure for 14-Meter-Diameter Precision Reflector Verified in Neutral Bouyancy Tests (fig. 30)

Robotic Assembly

- Development of a Machine Vision Guidance System for Automated Assembly of Space Structures (fig. 31)

Space Cranes

- Static and Dynamic Characterization Completed for Space Crane Reference Truss (fig. 32)

- Simulation Shows Passive Damping Structural Elements Effective in Reducing Space Crane Vibration Response (fig. 33)

## Computational Mechanics Branch

The primary goal of the Computational Mechanics Branch (fig. 34) is to provide efficient and practical structural analysis and design computational mechanics methods for the US aerospace industry using evolving supercomputer technology. In support of this goal, the CMB conducts analytical research in the development of advanced computational methods for predicting the response of complex aerospace vehicles subject to static, dynamic and thermal loads using new and evolving computer hardware and software technology. The CMB develops methods which utilize the physics of structural mechanics and materials behavior which are applicable to aerospace vehicle analysis and design, especially in a concurrent engineering environment. Special emphasis is placed on modeling methods for predicting composite and metallic component failure and integrity, global/local and macro to micro response behavior, nonlinear structural response, finite element methods (FEM), boundary element

methods (BEM) and integrated thermal and mechanical behavior. New equation solvers, eigenvalue extraction algorithms, and stiffness and mass matrix assembly techniques are developed to enhance computational efficiency of new or existing methods on present and future computer systems using modern software architecture, including massively parallel computer architecture. New analytical methods developed by the CMB are validated through comparison with other, available methods, and through experiments performed by other organizations.

Recent Computational Mechanics Branch accomplishments listed below are highlighted in figures 35 through 41.

Advanced FEM and BEM Methods

- Functional Interface Method Accurately Joins Incompatible Finite Element Models (fig. 35)

- Iterative Method Developed for Calculating Fracture Parameters (fig. 36)

Adaptive FEM Methods

- Performance of Adaptive Mesh Refinement Demonstrated on Composite Fuselage-Like Compression Panel (fig. 37)

- Superposition Adaptive Refinement Technique Demonstrated on Built-Up Structures (fig. 38)

Efficient Equation Solvers

- Advanced Reduced-Basis Methods Reduce Computational Requirements for Linear, Transient Structural Analysis (fig. 39)

Applications

- Potential Improvement in Elliptical Bolted Composite Joints Demonstrated (fig. 40)

- Nonlinear Finite Element Analysis Accurately Predicts Strain in Stiffened Composite Wing Panel (fig. 41)

**Aerothermal Loads Branch**

The primary goal of the Aerothermal Loads Branch (fig. 42) is to develop enabling aerothermal loads analysis methods and to conduct fundamental experiments which support the design and successful operation of current and future high-speed vehicles. In support of this goal, the ALB conducts analytical and experimental research to identify and understand flow phenomena and flow/surface interaction parameters

required to define detailed aerothermal loads for thermal protection systems and structural designs for high-speed flight vehicles. The ALB devises and evaluates techniques for testing in high-energy true-temperature wind tunnels. The Branch also develops fluid-thermal-structural analysis methods and applies them to support experimental aerothermal loads investigations and to evaluate new structural concepts. The ALB operates the 8-Foot High Temperature Tunnel, the Aerothermal Arc Tunnels (20 and 5 MW), and the 7-Inch High Temperature Tunnel. The Experimental Facilities and Techniques Section (EFTS) within the ALB is responsible for operating and maintaining these facilities.

The primary goal of the EFTS is the continued safe and efficient operation of these highly complex high energy facilities. The EFTS directs the operation and maintenance and effects improvements of equipment and operational techniques of the 8' High Temperature Tunnel, 5 MW, and 20 MW Aerothermal Arc Tunnels, and the 7" High Temperature Tunnel. This Section improves wind-tunnel technology, test techniques, and instrumentation for experimental determination of aerospace vehicle aerothermal loads, structural performance characteristics, and airbreathing engine performance. The facilities support (1) the Structural Mechanics Division research program in the areas of aerothermal loads and development of durable thermal protection systems for space transportation systems and high-speed vehicles, and (2) the Fluid Mechanics Division research program in the development of airbreathing propulsion systems.

Recent Aerothermal Loads Branch accomplishments listed below are highlighted in figures 43 through 48.

Methods for Integrated Fluid-Thermal-Structural Analysis

- A P=1 Runge-Kutta Discontinuous Galerkin Method Applied to Transient Compressible Flows (fig. 43)

- Adaptive Unstructured Meshing Demonstrated for Thermal Stress Analysis of Built-Up Structures (fig. 44)

- Transient Adaptive Meshing Improves Accuracy and Efficiency of Plate Thermal Analysis (fig. 45)

Experiments

- New Shock-Shock Interference Pattern Identified Concomitant Supersonic Jets (fig. 46)

- Buff Airfoil Shaped Fuel Injector is Exceptionally Quiet and Provides Stable Combustion (fig. 47)

Applications

- Computations Show Fluid Spike Effective in Reducing Shock-Shock Interference Heating on a Cylindrical Leading Edge (fig. 48)

## FUTURE PLANS

Figures 49 to 64 give SMD long range plans for the four research Branches. Each Branch research program is presented in terms an overarching technical goal and three major research thrust areas which support that goal. The research objectives for each thrust area are given in the figures, followed by the technical approach taken during 1993 in terms of specific research activities. Finally, the highlights of a proposed 5-year research effort are indicated at the bottom of each figure. The Aircraft Structures plan is given in figures 49 to 52, while the Spacecraft Structures, Computational Mechanics and Aerothermal Loads plans are given in figures 53 to 56, figures 57 to 60, and figures 61 to 64, respectively. For the Spacecraft Structures Branch, the 1993 research plan marks the start of a new research direction, the development of deployable structural concepts for application to small-to-moderate size spacecraft applications.

## PUBLICATIONS AND PRESENTATIONS

The 1992 research activities of the Structural Mechanics Division resulted in a number of publications. The publications are listed in the References section by organization in the categories of journal publications, formal NASA reports, conference presentations, contractor reports, techical briefs, and patents.

## CONCLUDING REMARKS

This document describes the experimental test facilities, computer facilities, recent research accomplishments, publications and future research plans of the Structural Mechanics Division. Further information can be obtained by contacting the following Division offices:

Structural Mechnics Division (804) 864-2902
Aircraft Structures Branch (804) 864-3168
Spacecraft Structures Branch (804) 864-3102
Computational Mechanics Branch (804) 864-2906
Aerothermal Loads Branch (804) 864-1359

## REFERENCES

### AIRCRAFT STRUCTURES BRANCH


**Formal NASA Reports:**

1. Farley, G. L.: Relationship Between Mechanical-Property and Energy-Absorption Trends for Composite Tubes. NASA TP-3284, ARL-TR-29, December 1992, 14 p.

2. Jegley, D. C.: Study of Compression-Loaded and Impact-Damaged Structurally Efficient Graphite-Thermoplastic Trapezoidal-Corrugation Sandwich and Semi-Sandwich Panels. NASA TP-3264, November 1992, 29 p.

3. Jegley, D. C.: Effect of Low-Speed Impact Damage and Damage Location on Behavior of Composite Panels. NASA TP-3196, May 1992, 26 p.

4. McGowan, D. M.; Camarda, C. J.; and Scotti, S. J.: A Simplified Method for Thermal Analysis of a Cowl Leading Edge Subject to Intense Local Shock-Wave-Interference Heating. NASA TP-3167, March 1992, 37 p.

5. Nemeth, M. P.: Buckling Behavior of Long Symmetrically Laminated Plates Subjected to Combined Loadings. NASA TP-3195, May 1992, 29 p.

6. Scotti, S. J. (Compiler): Current Technology for Thermal Protection Systems. NASA CP-3157, October 1992, 326 p.

7. Shideler, J. L.; Fields, R. A.; Reardon, L. F.; and Gong, L.: Thermal and Structural Tests on a Rene' 41 Honeycomb Integral-Tank Concept for Future Space Transporation Systems. NASA TP-3145, May 1992, 75 p

**High-Numbered Technical Memorandums:**

8. Polesky, S. P.: Hierachical Flux-Based Thermal-Structural Finite Element Analysis Method. NASA TM-107574, April 1992, 112 p.

9. Sawyer, J. W.; and Rothgeb, T. M.: Carbon-Carbon Joint and Fastener Results at Room and Elevated Temperatures. NASA TM-107638, July 1992, 32 p.

10. Scotti, S. J.: Structural Design Using Equilibrium Programming. NASA TM-107593, October 1992, 19 p.

**Conference Presentations:**

11. Ambur, D. R.: Design and Evaluation of a Foam-Filled, Hat-Stiffened Panel Concept for Aircraft Primary Structural Applications. Presented at Third NASA

Advanced Composites Technology Conference, June 8-11, 1992, Long Beach, California. In NASA CP-3178, Volume I.

12. Camarda, C. J.; and Glass, D. E.: Thermostructural Applications of Heat Pipes for Cooling Leading Edges of High-Speed Aerospace Vehicles. Presented at Current Technology for Thermal Protection Systems Workshop, February 11-12, 1992, Hampton, Virginia. In NASA CP-3157, p. 291-318.

13. Cohen, D.; Do, L. Q.; Hyer, M. W.; Griffin, O. H.; Yalamanchili, S. R.; Shuart, M. J.; and Prasad, C. B.: Failure Criterion for Thick Multi-Fastener Graphite/Epoxy Composite Joints. Presented at Sixth Japan-United States Conference on Composite Materials, June 22-25, 1992, Orlando, Florida. In Proceedings.

14. Cruz, J. R.: Buckling Analysis of Curved Composite Sandwich Panels Subjected to Inplane Loadings. Presented at Third NASA Advanced Composites Technology Conference, June 8-11, 1992, Long Beach, California. In NASA CP-3178, Volume I.

15. Elishakoff, I.; Arbocz, J.; and Starnes, J. H., Jr.: Buckling of Stiffened Shells With Random Initial Imperfections, Thickness and Boundary Conditions. Presented at 33rd AIAA/ASME/ASCE/AHS/ASC Structures, Structural Dynamics, and Materials Conference, April 13-15, 1992, Dallas, Texas. AIAA Paper No. 92-2233-CP.

16. Farley, G. L.: Crushing Response of Energy Absorbing Composite Structure. Presented at ASCE Engineering Mechanics Specialty Conference, May 24-27, 1992, College Station, Texas.

17. Griffin, O. H.; Hyer, M. W.; Yalamanchili, S. R.; Shuart, M. J.; Prasad, C. B.; and Cohen, D.: Analysis of Multifastener Composite Joints. Presented at 33rd AIAA/ASME/ASCE/AHS/ASC Structures, Structural Dynamics, and Materials Conference, April 13-15, 1992, Dallas, Texas. AIAA Paper No. 92-2542-CP.

18. Jegley, D. C.: A Study of Structurally Efficient Graphite-Thermoplastic Trapezopidal-Corrugation Sandwich and Semi-Sandwich Panels. Presented at Third NASA Advanced Composites Technology Conference, June 8-11, 1992, Long Beach, California. In NASA CP-3178, Volume I.

19. Kelly, H. N.; and Blosser, M. L.: Active Cooling From the Sixties to NASP. Presented at Current Technology for Thermal Protection Systems Workshop, February 11-12, 1992, Hampton, Virginia. In NASA CP-3157, p. 189-249.

20. Nagendra, S.; Gurdal, Z.; Haftka, R. T.; and Starnes, J. H., Jr.: Buckling and Failure Characteristics of Compression-Loaded Stiffened Composite Panels With a Hole. Presented at ACS Seventh Technical Conference on Composite Materials, October 13-15, 1992, University Park, Pennsylvania.

21. Nemeth, M. P.: Buckling Behavior of Long Symmetrically Laminated Plates Subjected to Compression, Shear, and Inplane Bending Loads. Presented at 33rd AIAA/ASME/ASCE/AHS/ASC Structures, Structural Dynamics, and Materials Conference, April 13-15, Dallas, Texas. AIAA Paper No. 92-2286-CP.

22. Noor, A. K.; Starnes, J. H., Jr.; and Peters, J. M.: Thermomechanical Buckling and Postbuckling of Multilayered Composite Panels. Presented at 33rd AIAA/ASME/ASCE/AHS/ASC Structures, Structural Dynamics, and Materials Conference, April 13-15, 1992, Dallas, Texas. AIAA Paper No. 92-2541-CP.

23. Prasad, C. B.; and Shuart, M. J.: Effects of Cutouts on the Behavior of Symmetric Composite Laminates Subjected to Bending and Twisting Loads. Presented at Third NASA Advanced Composites Technology Conference, June 8-11, 1992, Long Beach, California. In NASA CP-3178, Volume I.

24. Sawyer, J. W.; and Rothgeb, T. M.: Carbon-Carbon Joint and Fastener Test Results at Room and Elevated Temperatures. Presented at 16th Annual Conference on Composites, Materials, and Structures, January 12-15, 1992, Cocoa Beach, Florida. In NASA CP-3175.

25. Sawyer, J. W.; and Rothgeb, T. M.: An Instrumented Fastener for Shear Force Measurements in Joints. Presented at 1992 SEM VII International Congress on Experimental Mechanics, June 8-11, 1992, Las Vegas, Nevada. In Proceedings.

26. Sawyer, J. W.; and Vause, R. F.: Test and Analysis of Carbon-Carbon Control Surface Torque-Tube/Attachment-Ring Joint. Presented at NASP Mid-Term Technology Review, April 21-24, 1992, Monterey, California. In NASP CP-11064, Volume 6, p. 397.

27. Scotti, S. J.: Structural Design Using Equilibrium Programming. Presented at 33rd AIAA/ASME/ASCE/AHS/ASC Structures, Structural Dynamics, and Materials Conference, April 13-15, 1992, Dallas, Texas, AIAA Paper No. 92-2365.

28. Segobiano N. B.; Rothgeb, T. M.; and Sawyer, J. W.: Titanium Matrix Composite High Temperature Bolted Joint Test. Presented at 16th Annual Conference on Composites, Materials, and Structures, January 12-15, 1992, Cocoa Beach, Florida. In NASA CP-3175.

29. Shideler, J. L.: Predicted and Tested Performance of Durable TPS. Presented at Current Technology for Thermal Protection Systems Workshop, February 11-12, 1992, Hampton, Virginia. In NASA CP-3157, p. 97-129.

30. Shuart, M. J.; Ambur, D. R.; Davis, D. D., Jr.; Davis, R. C.; Farley,. G. L.; and Wang, J. T.: Technology Integration Box Beam Failure Study. Presented at Third NASA Advanced Composites Technology Conference, June 8-11, 1992, Long Beach, California. In NASA CP-3178, Volume I.

31. Starnes, J. H., Jr.; and Britt, V. O.: Nonlinear Analysis of Stiffened Fuselage Shells With Local Damage. Presented at International Workshop on Structural Integrity of Aging Airplanes, March 31-April 2, 1992, Atlanta, Georgia.

**Journal Articles and Other Publications:**

32. Curry, J. M; Johnson, E. R.; and Starnes, J. H., Jr.: Effect of Dropped Plies on the Strength of Graphite-Epoxy Laminates. *AIAA Journal,* Volume 30, No. 2, February 1992, p. 449-456.

33. Jegley, D. C.; and Lopez, O. F.: Effect of Composite Fabrication Method on Structural Response and Impact Damage. *AIAA Journal,* Volume 30, No. 1, January 1992, p. 205-213.

34. Librescu, L.; and Stein, M.: A Geometrically Nonlinear Theory of Transversely Isotropic Laminated Composite Plates and Its Use in the Postbuckling Analysis. *Thin-Walled Structures,* Volume 11, 1991, p. 177-201.

35. Nemeth, M. P.: Buckling of Symmetrically Laminated Plates With Compression, Shear, and Inplane Bending. *AIAA Journal,* Volume 30, No. 12, 1992, p. 2959-2966.

36. Noor, A. K.; Starnes, J. H., Jr.; and Waters, W. A., Jr.: Numerical and Experimental Simulation of the Postbuckling Response of Laminated Anisotropic Panels. *ASCE Journal of Aerospace Engineering,* Volume 5, No. 3, July 1992, p. 347-368.

37. Polesky, S. P.; Dechaumphai, P.; Glass, C. E.; and Pandey, A. K.: Three-Dimensional Thermal Structural Analysis of a Swept Cowl Leading Edge Subjected to Skewed Shock-Shock Interference Heating. *Journal of Thermophysics and Heat Transfer,* Volume 6, No. 1, January-March 1992 p. 48-54.

38. Sridharan, S.; Zeggane, M.; and Starnes, J. H., Jr.: Postbuckling Response of Stiffened Composite Cylindrical Shells. *AIAA Journal,* Volume 30, No. 12, December 1992, p. 2897-2905.

39. Wieland, T. M.; Morton, J.; and Starnes, J. H., Jr.: Scale Effects on Buckling, Postbuckling and Crippling of Graphite-Epoxy Z-Section Stiffeners. *AIAA Journal,* Volume 30, No. 11, November 1992, p. 2750-2757.

**Contractor Reports:**

40. Blackburn, C. L.: Preliminary Structural Sizing of a Mach 3.0 High Speed Civil Transport Model. Analytical Services & Materials, Inc., NASA CR-189631, April 1992, 49 p.

41. Rehfield, L. W.; Chang, S.; and Zischka, P. J.: Modeling and Analysis Methodology for Aeroelastically Tailored Chordwise Deformable Wings. University of California at Davis, NASA CR-189620, July 1992, 82 p.

42. Santare, M. H.; and Pipes, R. B.: Continuation of Tailored Composite Structures of Ordered Staple Thermoplastic Material. University of Delaware, NASA CR-189671, September 1992, 87 p.

**Technical Briefs:**

43. Jegley, D. C.: A Study of the Structural Efficiency of Fluted Core Graphite-Epoxy Panels. NASA Tech Brief LAR-14539.

**Patents:**

44. Scotti, S. J.; Blosser, M. L.; and Camarda, C. J.: Heat Exchanger With Oscillating Flow. U. S. Patent 5,107,790. Issued April 28, 1992.

## SPACECRAFT STRUCTURES BRANCH

**Formal NASA Reports:**

45. Dorsey, J. T.; and Dyess, J. W.: Structural Performance of Two Aerobrake Hexagonal Heat Shield Panel Concepts. NASA TM-4372, May 1992, 30 p.

46. Dorsey, J. T.; Sutter, T. R.; and Wu, K. C.: Structurally Adaptive Space Crane Concept for Assembling Space Systems on Orbit. NASA TP-3307, November 1992, 19 p.

47. Heard, W. L., Jr.; Lake, M. S.; Bush, H. G.; Jensen, J. K.; Phelps, J. E.; and Wallsom, R. E.: Extravehicular Activity Compatibility Evaluation of Developmental Hardware for Assembly and Repair of Precision Reflectors. NASA TP-3246, September 1992, 60 p.

48. Heard, W. L., Jr.; Watson, J. J.; Lake, M. S.; Bush, H. G.; Jensen, J. K.; Wallsom, R. E.; and Phelps, J. E.: Tests of an Alternate Mobile Transporter and Extravehicular Activity Assembly Procedure for the Space Station Freedom Truss. NASA TP-3245, October 1992, 32 p.

49. Herstrom, C. L.; Grantham,. C.; Allen, C. L.; Doggett, W. R.; and Will, R. W.: Software Design for Automated Assembly of Truss Structures. NASA TP-3198 June 1992, 45 p.

50. Lake, M. S.: Stiffness and Strength Tailoring in Uniform Space-Filling Truss Structures. NASA TP 3210, April 1992 28 p.

51. Sutter, T. R.; Wu, K. C.; Riutort, K. T.; Laufer, J. B.; and Phelps, J. E.: Structural Characterization of a First-Generation Articulated-Truss Joint for Space Crane Application. NASA TM-4371, May 1992, 22 p.

52. Sydow, P. D.; and Cooper, E. G.: Development of a Machine Vision System for Automated Structural Assembly. NASA TM-4366, May 1992, 28 p.

53. Sydow, P. D; and Shuart, M. J.: Experimental Behavior of Graphite-Epoxy Y-Stiffened Specimens Loaded in Compression. NASA TP-3171, May 1992, 18 p.

54. Wu, K. C.; and Sutter, T. R.: Structural Analysis of Three Space Crane Articulated-Truss Joint Concepts. NASA TM-4373, May 1992, 30 p.

**Conference Presentations:**

55. Dorsey, J. T.; and Dyess, J. W.: Structural Studies of Two Aerobrake Heatshield Panel Concepts. Presented at Third International Conference on Engineering, Construction and Operations in Space, May 31-June 4, 1992, Denver, Colorado.

56. Dorsey, J. T.; Sutter, T. R.; and Wu, K. C.: A Structurally Adaptive Space Crane Concept for Assembling Space Systems on Orbit. Presented at Third International Conference on Adaptive Structures, November 9-11, 1992, San Diego, California.

57. Sutter, T. R.; Wu, K. C.; Riutort, K. T.; Laufer, J. B.; and Phelps, J. E.: Structural Characterization of an Articulated-Truss Joint. Presented at Third International Conference on Engineering, Construction and Operations in Space, May 31-June 4, 1992, Denver, Colorado.

58. Wu, K. C.; and Sutter, T. R.: Analysis of Space Crane Articulated-Truss Joints. Presented at Third International Conference of Engineering, Construction and Operations in Space, May 31-June 4, 1992, Denver, Colorado.

59. Doggett, William R.; Quach, Cuong; Will, Ralph W.; and Rhodes, Marvin D.: The Automated Assembly of a Panelled, Truss-Supported Planar Surface. Presented at the SPIE's OE/Technology '92 Conference, November 15-20, 1992, Boston, Massachusetts.

**Journal Articles and Other Publications:**

60. Lake, M. S.; and Klang, E. C.: Generation and Comparison of Globally Isotropic Space-Filling Truss Structures. *AIAA Journal,* Volume 30, No. 5, May 1992, p. 1416-1424.

61. Watson, J. J.; Bush, H. G.; Heard, W. L., Jr.; Lake, M. S.; Jensen, J. K.; Wallsom, R. E.; and Phelps, J. E.: Mobile Transporter Concept for Extravehicular Activity Assembly of Future Spacecraft. *Journal of Spacecraft and Rockets*, Volume 29, No. 4, July-August 1992, p. 437-443.

## COMPUTATIONAL MECHANICS BRANCH

### Formal NASA Reports:

62. Noor, A. K.; Housner, J. M.; Starnes, J. H., Jr.; Hopkins, D. A.; and Chamis, C. C. (Compilers): Computational Structures Technology for Airframes and Propulsion Systems. NASA CP-3142, May 1992, 527 p.

### High-Numbered Technical Memorandums:

63. Ransom, J. B.; McCleary, S. L.; Aminpour, M. A.; and Knight, N. F., Jr.: Computational Methods for Global/Local Analysis. NASA TM-107591, August 1992, 23 p.

64. Stroud, W. J.; Davis, D. D., Jr.; Maring, L. D.; Krishnamurthy, T.; and Elishakoff, I.: Reliability of Stiffened Structural Panels: Two Examples. NASA TM-107687, ATCOM TR-92-B-015, December 1992, 19 p.

### Conference Presentations:

65. Aminpour, M. A.; McCleary, S. L.; and Ransom, J. B.: A Global/Local Analysis Method for Treating Details in Structural Design. Presented at Third NASA Advanced Composites Technology Conference, June 8-11, 1992, Long Beach, California. In NASA CP-3178, Volume I.

66. Aminpour, M. A.; McCleary, S. L.; Ransom, J. B.; and Housner, J. M.: A Global/Local Analysis Method for Treating Details in Structural Design. Presented at 1992 ASME Winter Annual Meeting, November 8-13, 1992, Anaheim, California.

67. Aminpour, M. A.; Ransom, J. B.; and McCleary, S. L.: Coupled Analysis of Independently Modeled Finite Element Subdomains. Presented at 33rd AIAA/ASME/.ASCE/AHS/ASC Structures, Structural Dynamics, and Materials Conference, April 13-15, 1992, Dallas, Texas. AIAA Paper No. 92-2235-CP.

68. Housner, J. M; Aminpour, M. A.; Ransom, J. G.; McCleary, S. L.; Kao, P. J.; and Lotts, C. G.: Development and Application of Integrated Multiple Methods for Structural Analysis and Design. Presented at 1992 ASME Winter Annual Meeting, November 8-13, 1992, Anaheim, California. In Proceedings, Volume 157, p. 119-137.

69. Ransom, J. B.; McCleary, S. L.; Aminpour, M. A.; and Knight, N. F., Jr.: Computational Methods for Multilevel Analysis of Composite Structures. Presented at 1992 ASME Summer Mechanics and Materials Meeting, April 28-May 1, 1992, Tempe, Arizona.

70. Stroud, W. J.; Maring. L. D.; Davis, D. D., Jr.; and Anderson, M. S. : Reliability of Stiffened Structural Panels: Two Examples. Presented at 1992 ASME Winter Annual Meeting, November 8-13, 1992, Anaheim, California.

71. Tessler, A.; Saether, E. ; and Tsui, T: Vibration of Thick Composite Laminates: Analytical Theory and Finite Element Approximations. Presented at 33rd AIAA/ASME/ASCE/AHS/ASE Structures, Structural Dynamics, and Materials Conference, April 13-15, 1992, Dallas, Texas. AIAA Paper No. 92-2415-CP.

72. Wang, J. T.; Lotts, C. G.; Davis, D. D., Jr.; and Krishnamurthy T.: Coupled 2D/3D Finite Element Methods for Analysis of a Skin Panel With a Discontinuous Stiffener. Presented at 33rd AIAA/ASME/ASCE/AHS/ASC Structures, Structural Dynamics, and Materials Conference, April 13-15, 1992, Dallas, Texas. AIAA Paper No. 92-2474-CP.

**Contractor Reports:**

73. Averill, R. C.; and Reddy, J. N.: Nonlinear Analysis of Laminated Composite Shells Using a Micromechanics-Based Progressive Damage Model. Virginia Polytechnic Institute and State University, NASA CR-189675, August 1992, 180 p.

74. Raju, I. S.; and Krishnamurthy, T.: A Boundary Element Alternating Method for Two-Dimensional Mixed-Mode Fracture Problems. Analytical Services & Materials, Inc., NASA CR-4460, August 1992, 36 p.

**Journal Articles and Other Publications:**

75. Wu, S. C.; Chang, C. W.; and Housner, J. M.: A Finite Element Approach for Transient Analysis of Multibody Systems. *Journal of Guidance, Control, and Dynamics*, Volume 15, No. 4, July-August 1992, p. 847-854.

## AEROTHERMAL LOADS BRANCH

**Formal NASA Reports:**

76. Venkateswaran, S.; Hunt, L. R.; and Prabhu, R. K.: Computational Method to Predict Thermodynamic, Transport, and Flow Properties for the Modified Langley 8-Foot High Temperature Tunnel. NASA TM-4374, July 1992, 35 p.

**High-Numbered Technical Memorandums:**

77. Dechaumphai, P.: Adaptive Unstructured Meshing for Thermal Stress Analysis of Built-Up Structures. NASA TM-104221, February 1992 10 p.

**Conference Presentations:**

78. Dechaumphai, P.: Adaptive Unstructured Meshing for Thermal Stress Analysis of Built-Up Structures. Presented at 33rd AIAA/ASME/ASCE/AHS/ASC Structures, Structural Dynamics, and Materials Conference, April 13-15, 1992, Dallas, Texas. AIAA Paper No. 92-2542-CP.

79. Pandey, A. K.; and Dechaumphai, P.: Thermo-Viscoplastic Analysis of Leading Edges Subjected to Oscillating Shock-Shock Interaction. Presented at 33rd AIAA/ASME/ASCE/AHS/ASC Structures, Structural Dynamics, and Materials Conference, April 13-15, 1992, Dallas, Texas. AIAA Paper No. 92-2537.

80. Puster, R. L.; Brown, R. D.; and Borg, S. E.: Fuel Injectors, Flameout Detectors, and Oxygen System Monitors for the Langley 8-Foot High Temperature Tunnel. Presented at 78th Semi-Annual STA Meeting, October 19-20, 1992, Long Island, New York.

**Journal Articles and Other Publications:**

81. Paney, A. K.; Dechaumphai, P.; and Wieting, A. R.: Thermal-Structural Finite Element Analysis Using Linear Flux Forumation. *Journal of Thermophysics and Heat Transfer*, Volume 6, No. 2, April-June 1992, p. 341-348.

82. Venkateswaran, S.; Witte, D. W.; and Hunt, L. R.: Axial Compression Corner Flow With Shock Impingement. *Journal of Spacecraft and Rockets*, Volume 29, No. 2, March-April 1992, p. 288-289.

83. Wieting, A. R.: Multiple Shock-Shock Interference on a Cylindrical Leading Edge. *AIAA Journal*, Volume 30, No. 8, August 1992, p. 2073-2079.

**Contractor Report:**

84. Holden, M. S.; and Rodriquez, K. M.: Studies of Shock/Shock Interaction on Smooth and Transpiration-Cooled Hemispherical Nosetips in Hypersonic Flow. Lockheed Advanced Development Company; Calspan Advanced Technology Center, NASA CR-189585, April 1992, 290 p.

**Technical Brief**:

85. Puster, R. L.; Franke, J. M.; West, J. W.; Adcock, E. E.; Chapman, J. J.; Sealey, B. S.; Petty, J. L.; and Venkateswaran, S.: Acoustic Flameout Detector. NASA Tech Brief LAR-14900.

# Langley Research Center

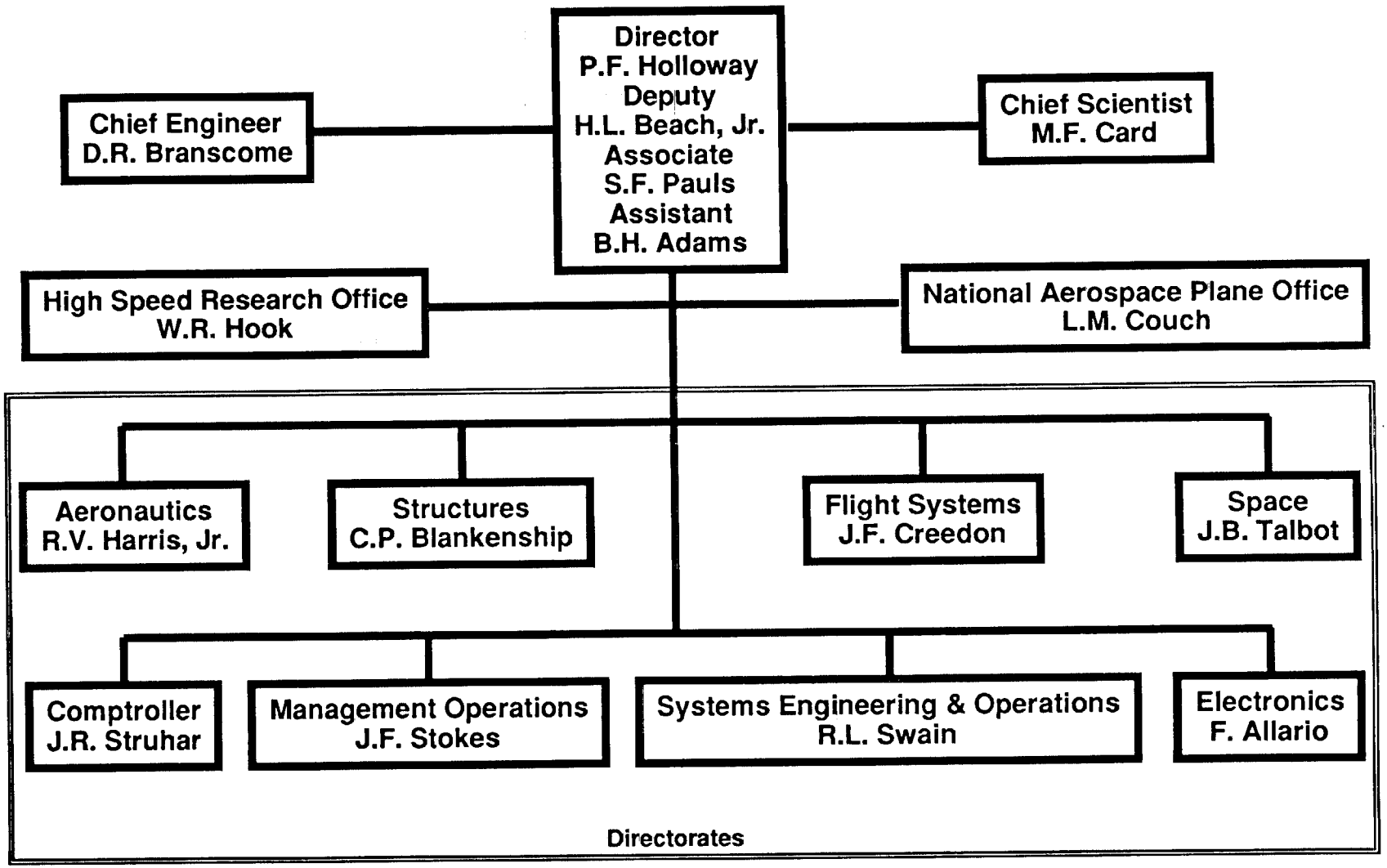


Figure 1

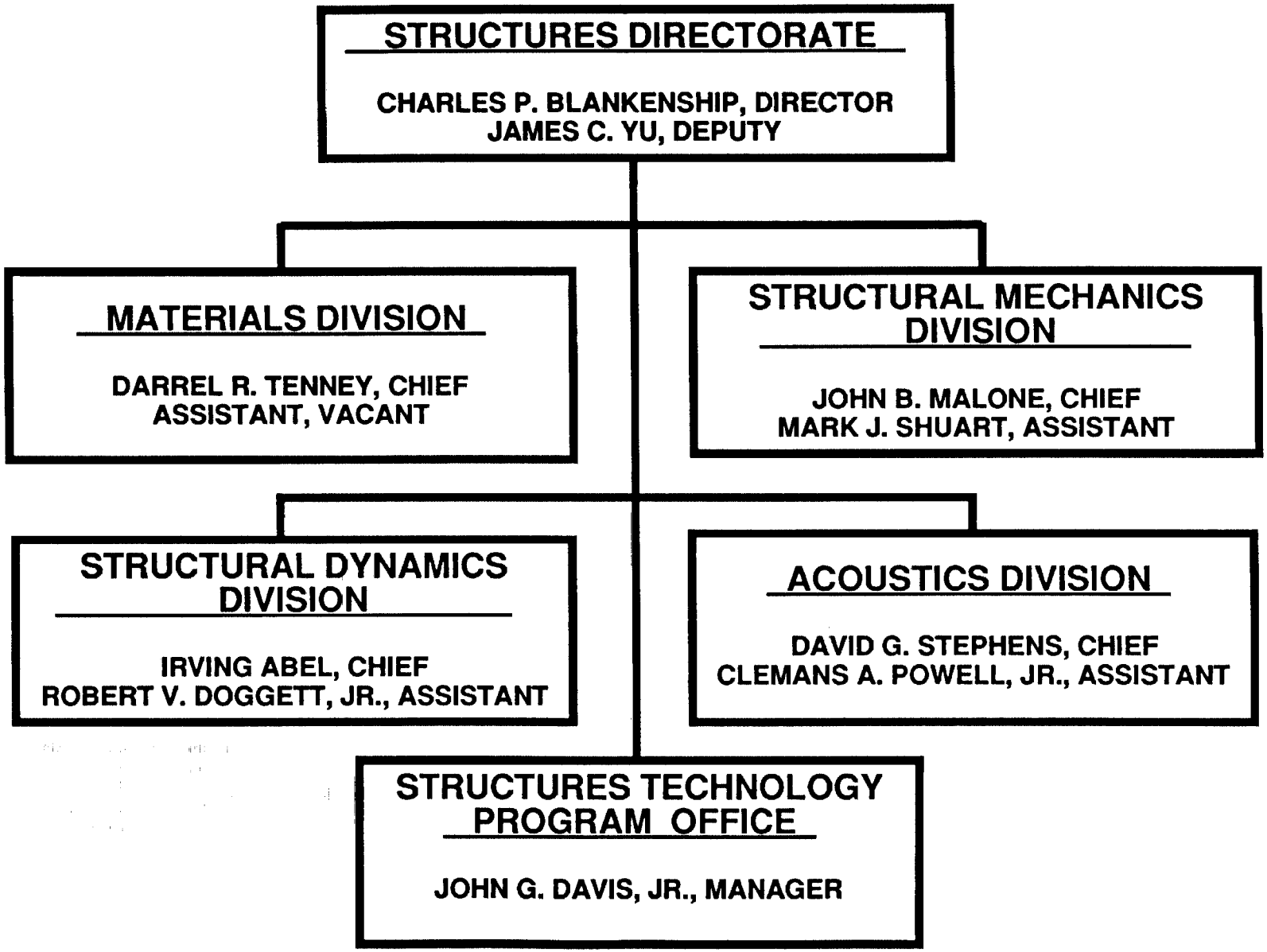
STRUCTURES DIRECTORATE
CHARLES P. BLANKENSHIP, DIRECTOR
JAMES C. YU, DEPUTY
MATERIALS DIVISION
DARREL R. TENNEY, CHIEF
ASSISTANT, VACANT
STRUCTURAL MECHANICS DIVISION
JOHN B. MALONE, CHIEF
MARK J. SHUART, ASSISTANT
STRUCTURAL DYNAMICS DIVISION
IRVING ABEL, CHIEF
ROBERT V. DOGGETT, JR., ASSISTANT
ACOUSTICS DIVISION
DAVID G. STEPHENS, CHIEF
CLEMANS A. POWELL, JR., ASSISTANT
STRUCTURES TECHNOLOGY PROGRAM OFFICE
JOHN G. DAVIS, JR., MANAGER

Figure 2

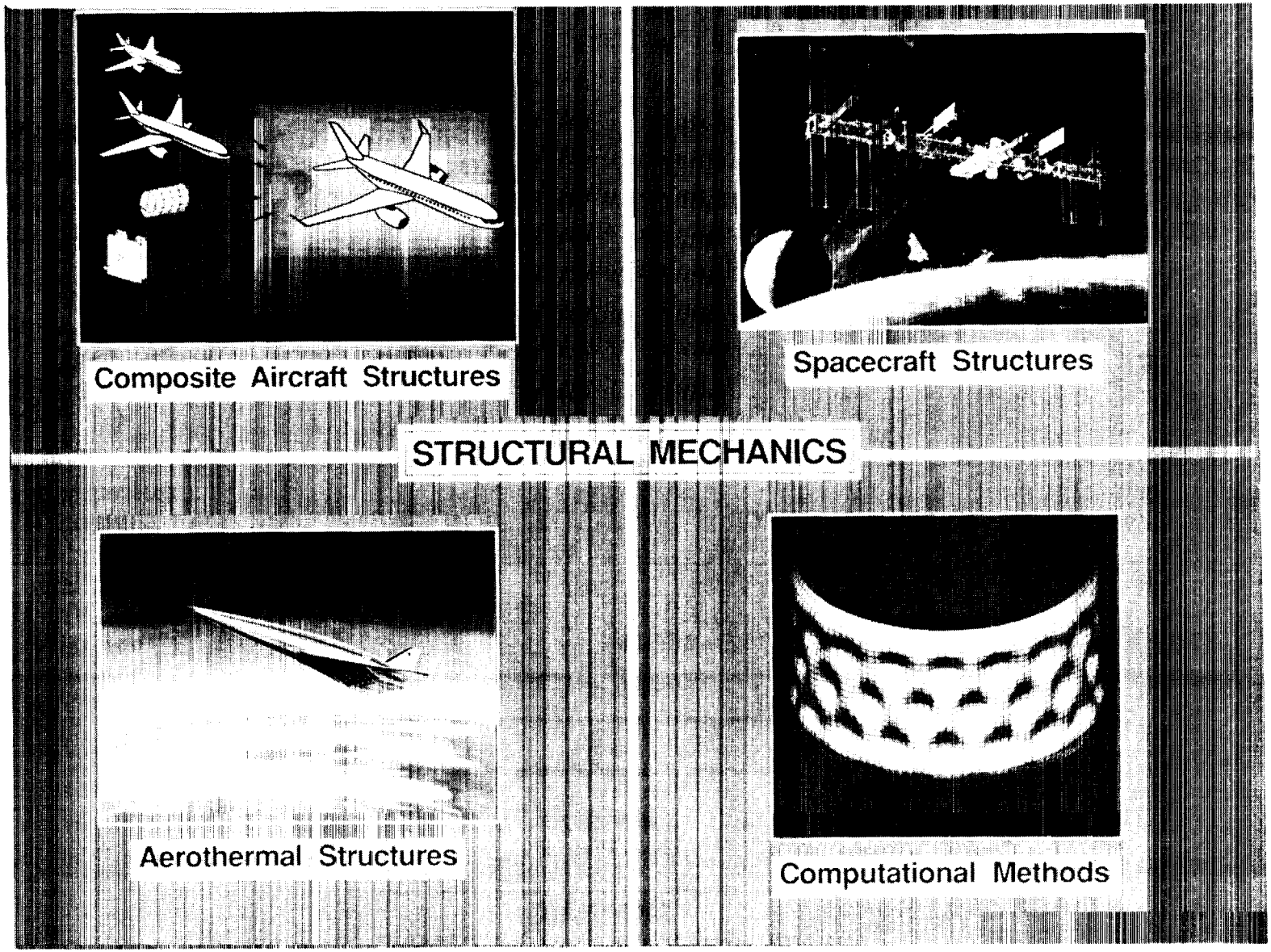
Composite Aircraft Structures
Spacecraft Structures
STRUCTURAL MECHANICS
Aerothermal Structures
Computational Methods

Figure 3

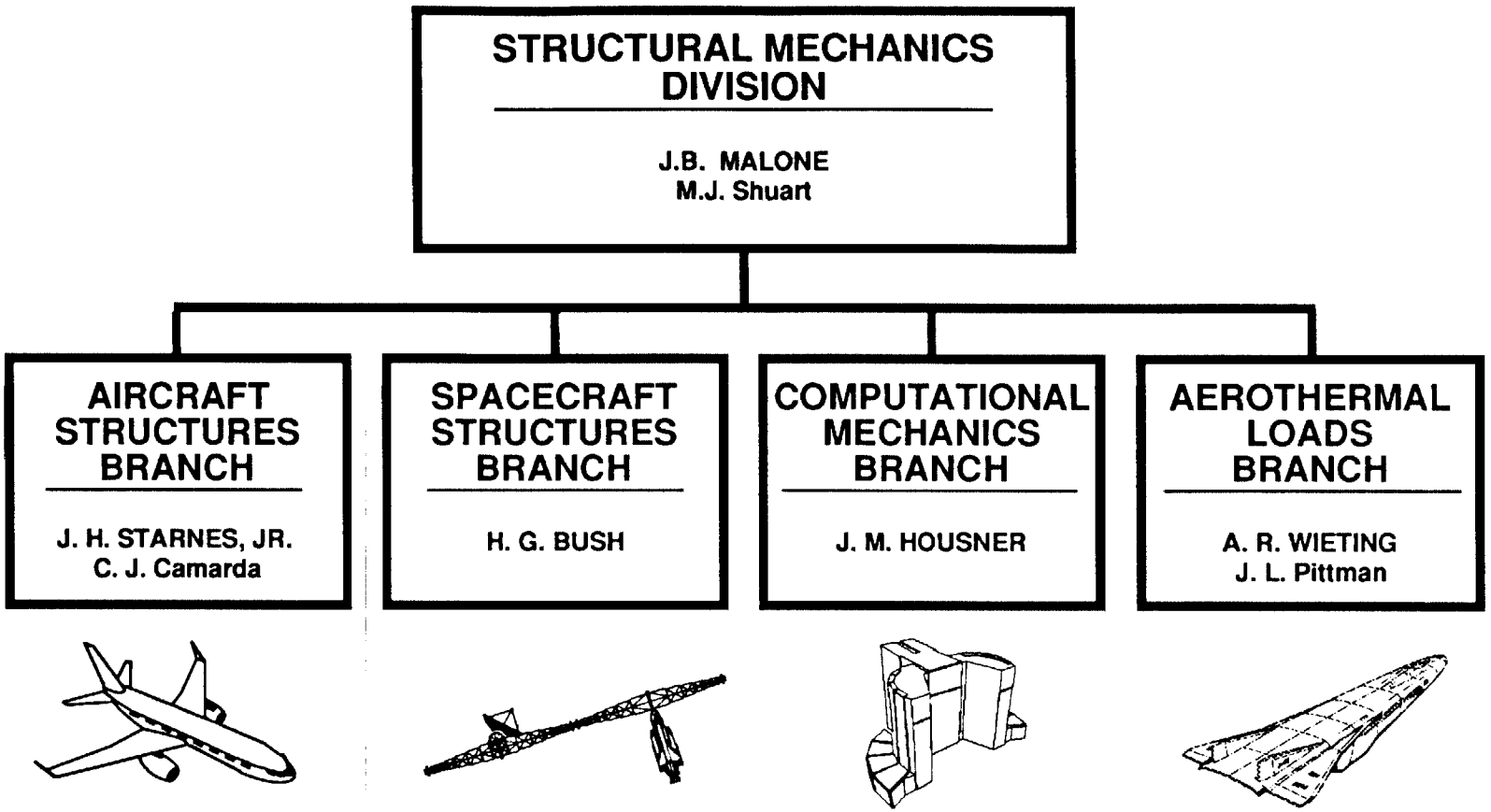
STRUCTURAL MECHANICS DIVISION
J.B. MALONE
M.J. Shuart
AIRCRAFT STRUCTURES BRANCH
J. H. STARNES, JR.
C. J. Camarda
SPACECRAFT STRUCTURES BRANCH
H. G. BUSH
COMPUTATIONAL MECHANICS BRANCH
J. M. HOUSNER
AEROTHERMAL LOADS BRANCH
A. R. WIETING
J. L. Pittman
- Composites
- Thermal effects
- Design methods
- Structural test
- Precision Reflectors
- Robotic Assembly
- Spacecrane
- Deployables
- FEM methods
- Parallel computing
- Multidisciplinary analysis
- CFD methods
- Integrated Fluid-Thermal-Structures analysis methods
- Wind tunnel tests

Figure 4

# Advanced Composites Technology

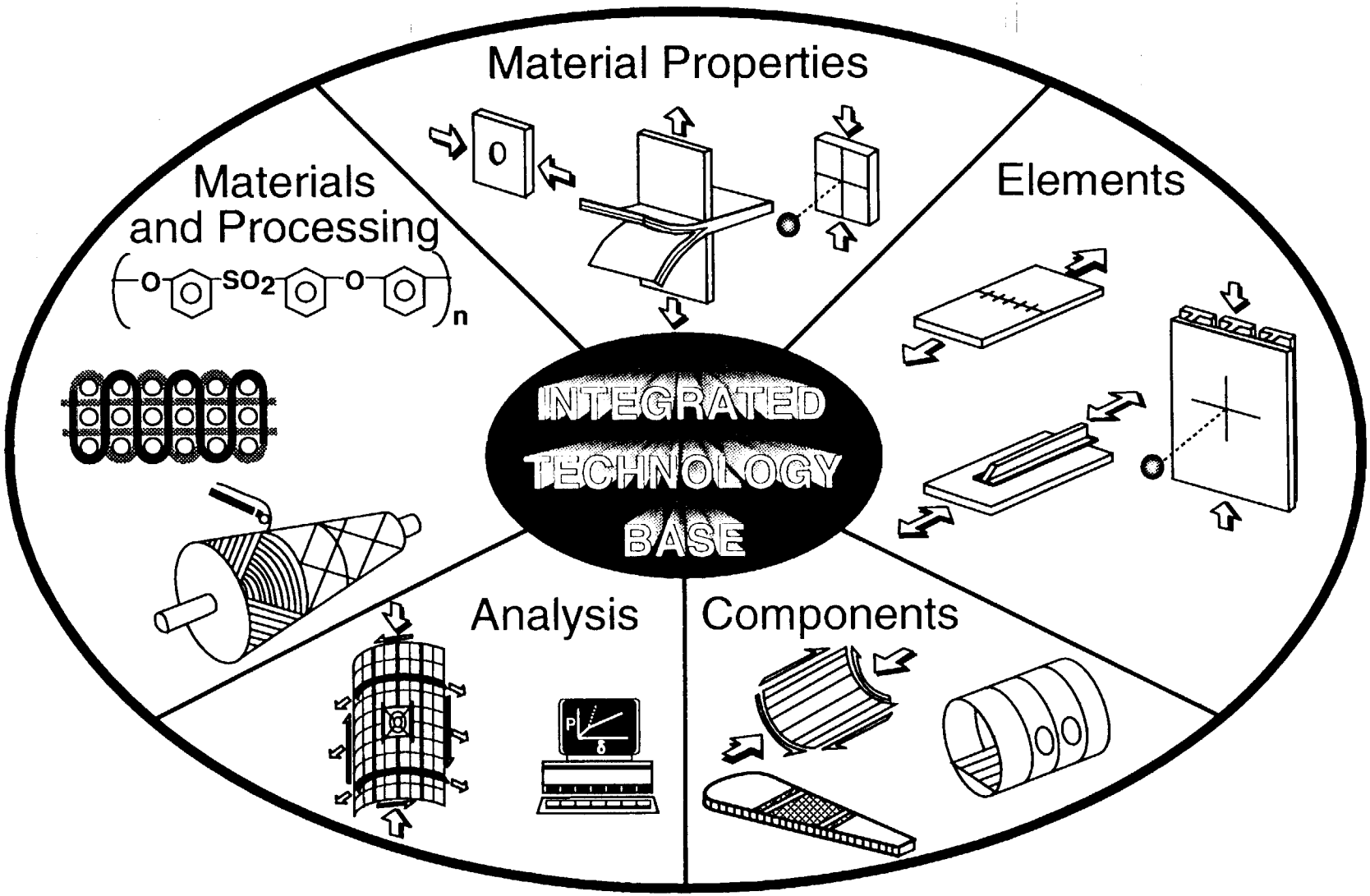


Figure 5

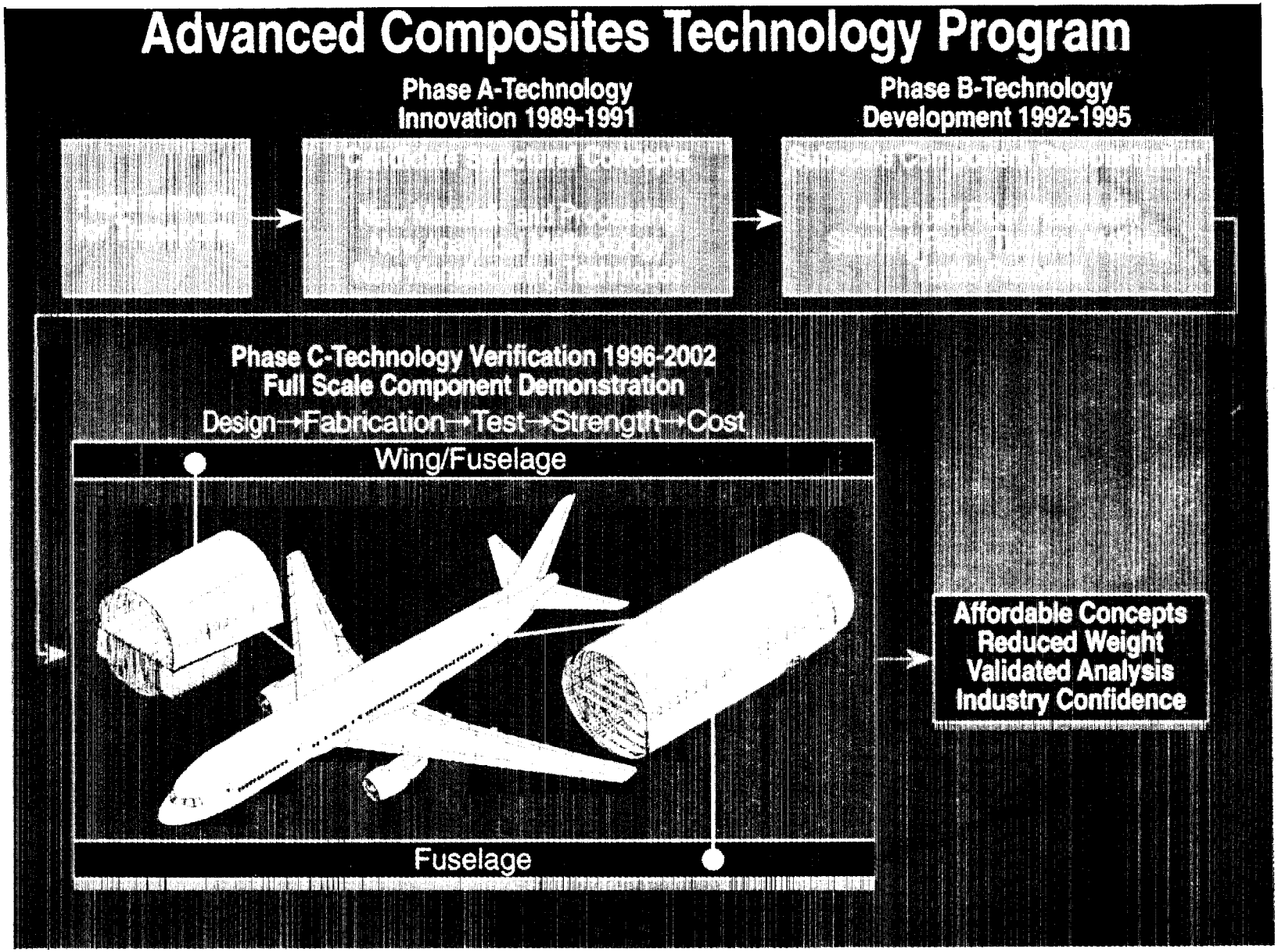
Advanced Composites Technology Program
Phase A-Technology
Innovation 1989-1991
Phase B-Technology
Development 1992-1995
Phase C-Technology Verification 1996-2002
Full Scale Component Demonstration
Design→Fabrication→Test→Strength→Cost
Wing/Fuselage
Fuselage
Affordable Concepts
Reduced Weight
Validated Analysis
Industry Confidence

Figure 6

# Airframe Materials and Structures Technology

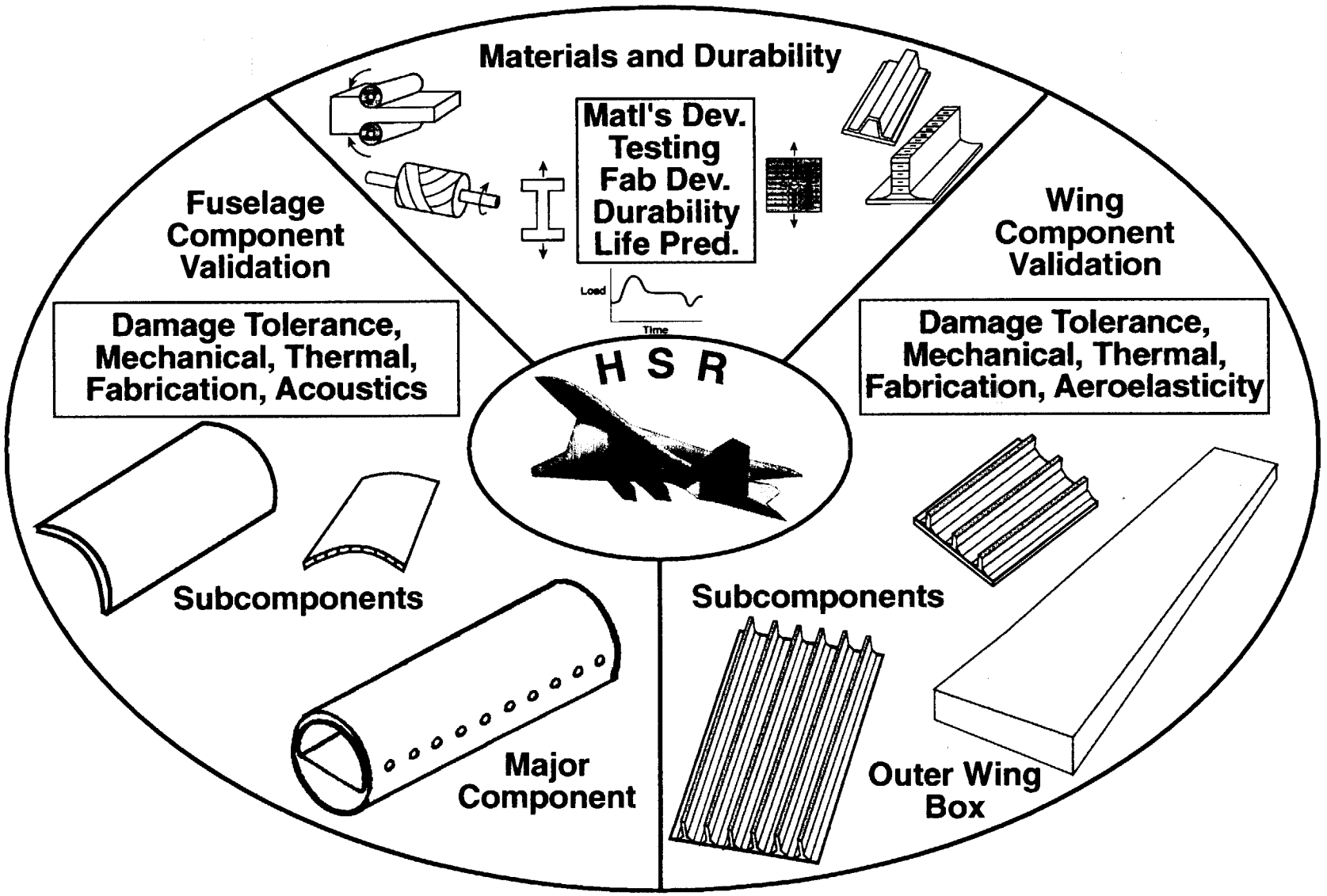


Figure 7

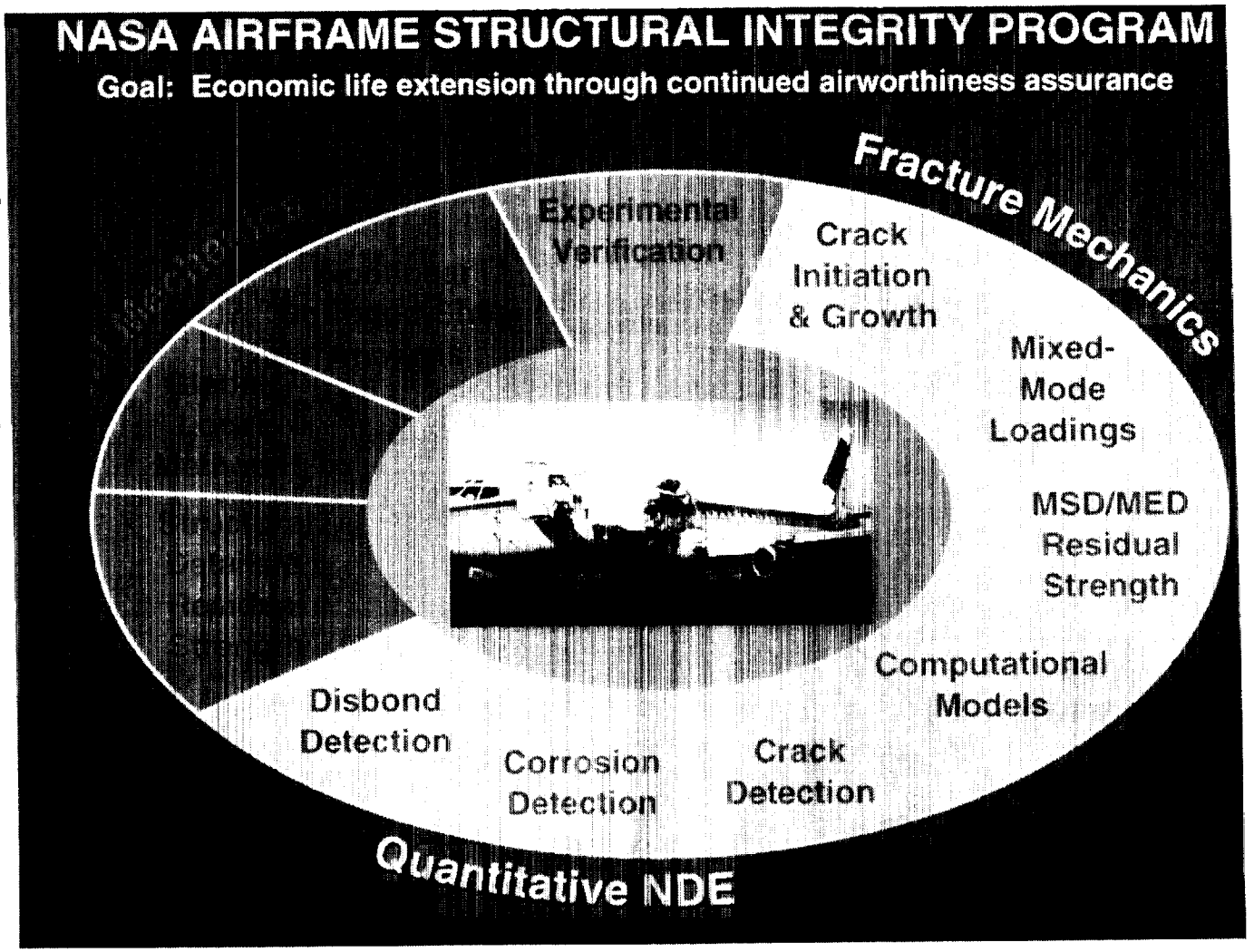
NASA AIRFRAME STRUCTURAL INTEGRITY PROGRAM
Goal: Economic life extension through continued airworthiness assurance
Fracture Mechanics
Experimental Verification
Crack Initiation & Growth
Mixed-Mode Loadings
MSD/MED Residual Strength
Computational Models
Crack Detection
Corrosion Detection
Disbond Detection
Quantitative NDE

Figure 8

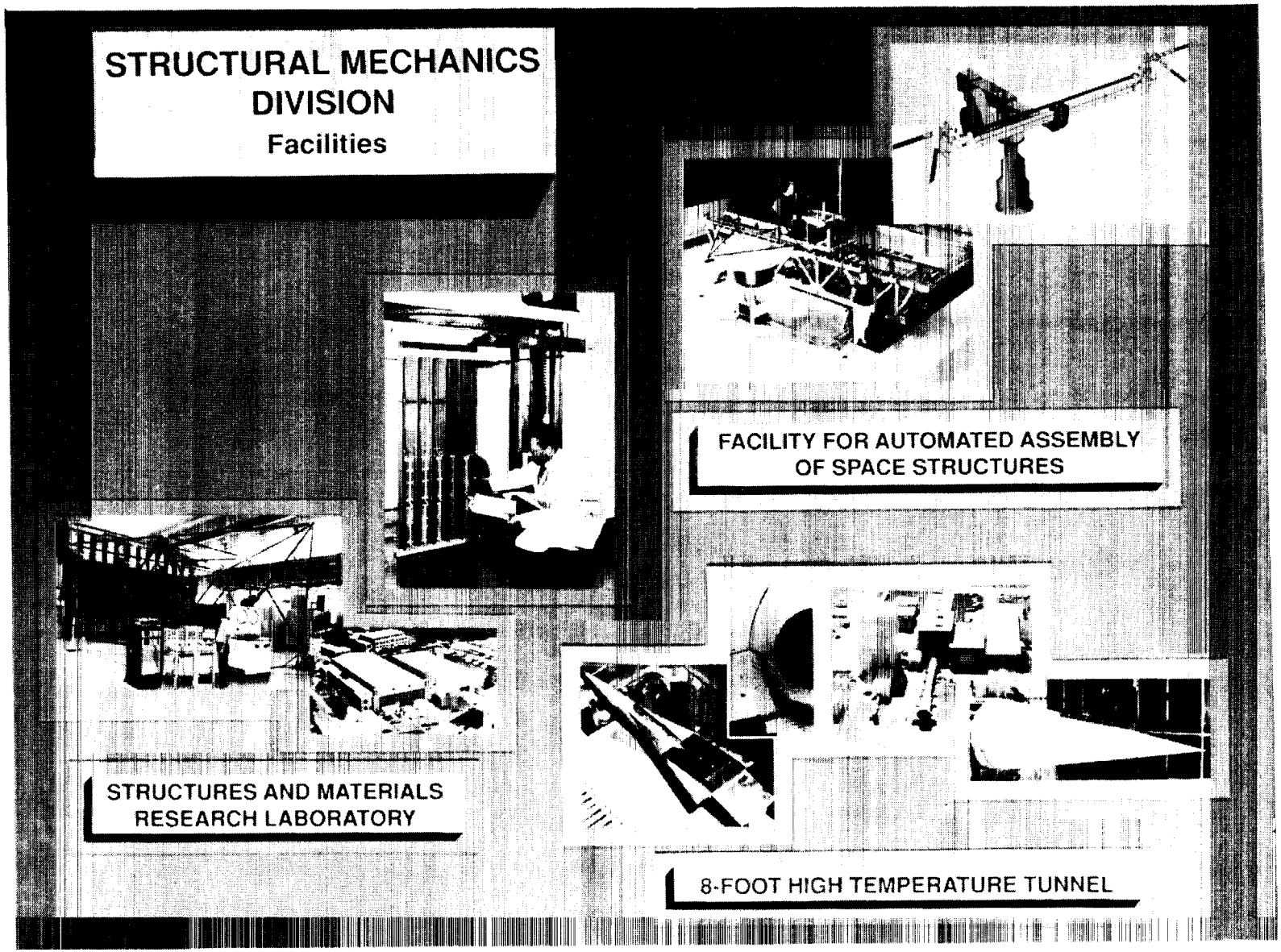
STRUCTURAL MECHANICS
DIVISION
Facilities
FACILITY FOR AUTOMATED ASSEMBLY
OF SPACE STRUCTURES
STRUCTURES AND MATERIALS
RESEARCH LABORATORY
8-FOOT HIGH TEMPERATURE TUNNEL

Figure 9

# SMD Locater

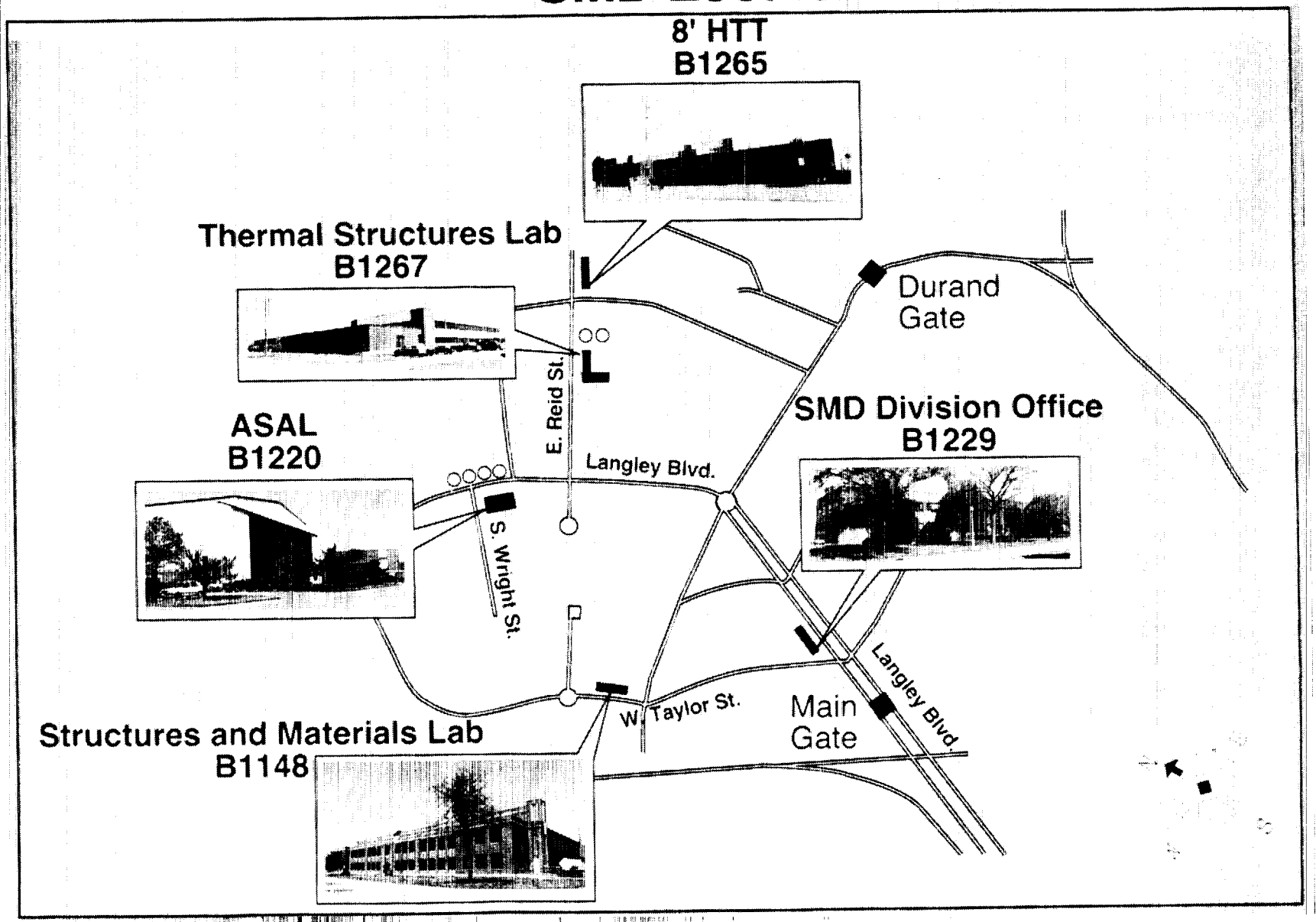


Figure 10

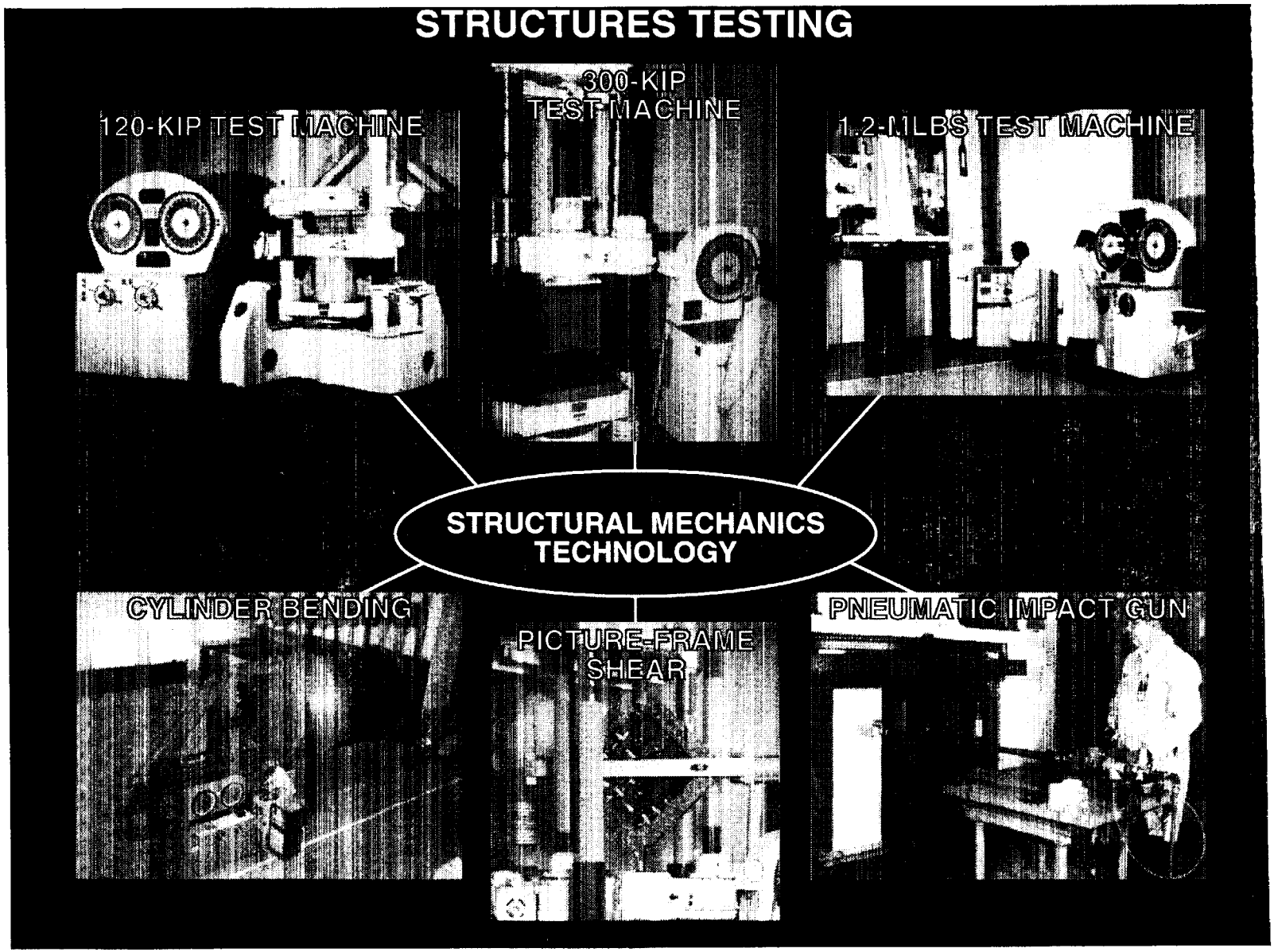
STRUCTURES TESTING
120-KIP TEST MACHINE
300-KIP TEST MACHINE
1.2-MLBS TEST MACHINE
STRUCTURAL MECHANICS TECHNOLOGY
CYLINDER BENDING
PICTURE-FRAME SHEAR
PNEUMATIC IMPACT GUN

Figure 11

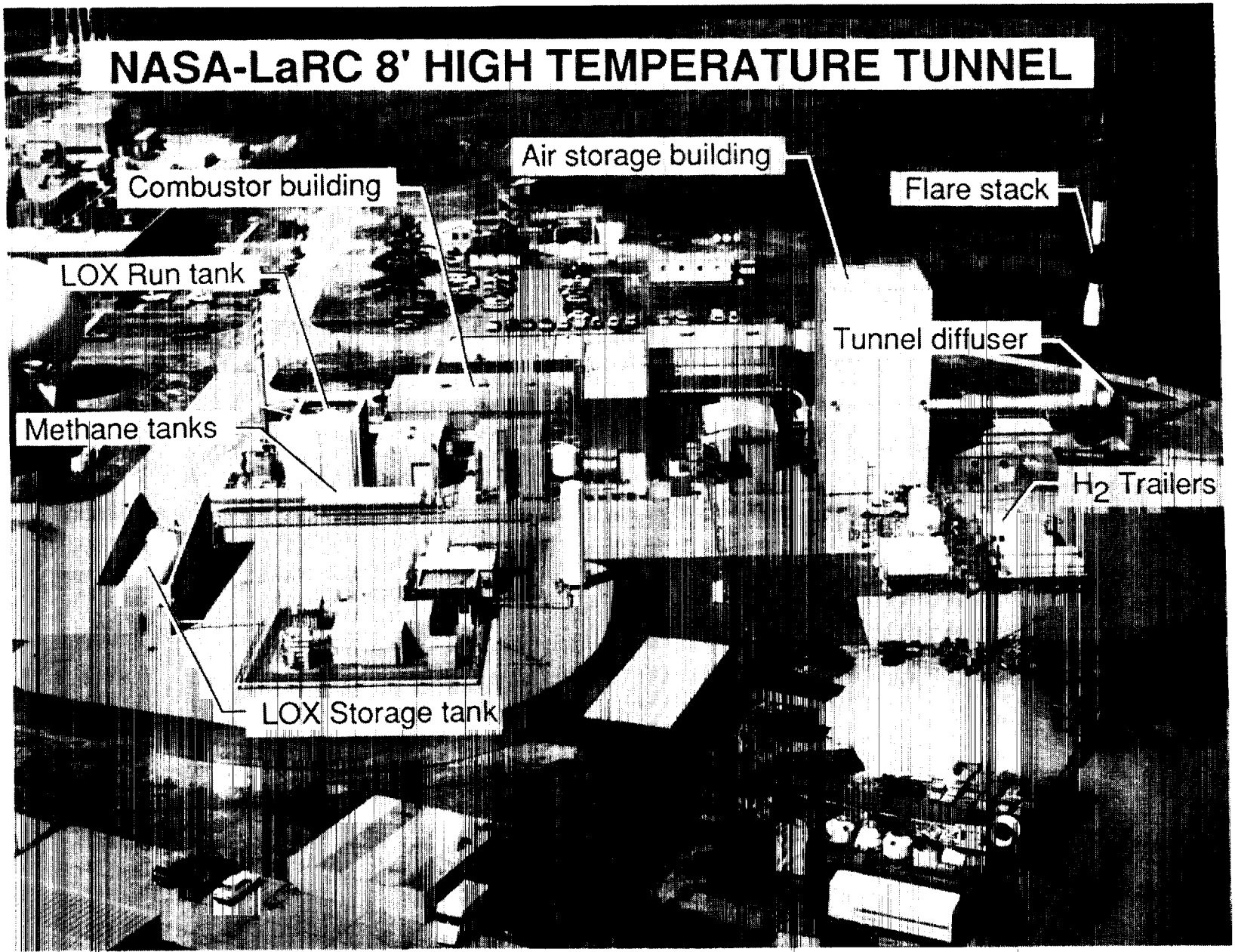
NASA-LaRC 8' HIGH TEMPERATURE TUNNEL
Air storage building
Combustor building
Flare stack
LOX Run tank
Tunnel diffuser
Methane tanks
$H_2$ Trailers
LOX Storage tank

Figure 12

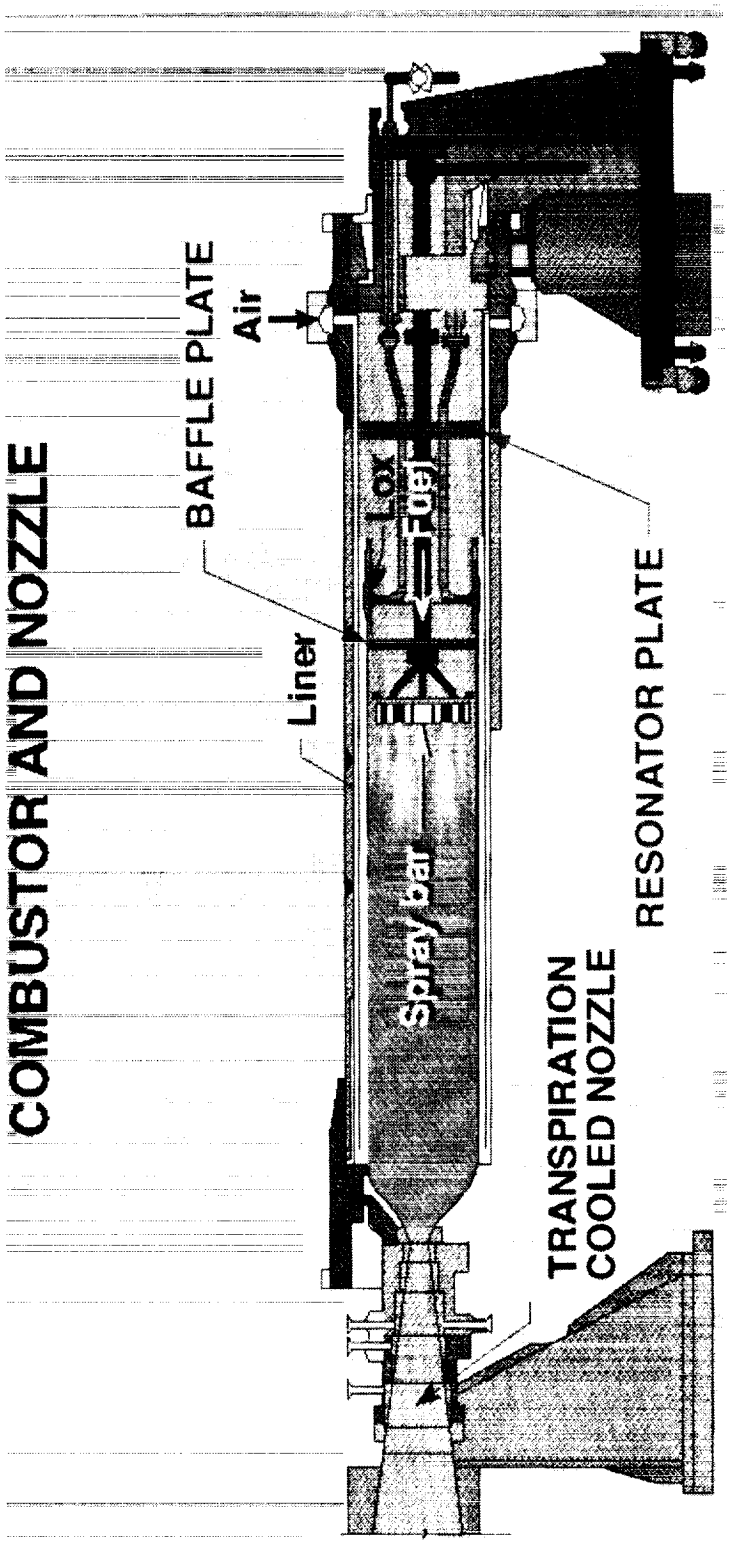
COMBUSTOR AND NOZZLE
BAFFLE PLATE
Air
LOx
Fuel
Liner
Spray bar
RESONATOR PLATE
TRANSPIRATION
COOLED NOZZLE

Figure 13

# TELEROBOTIC ASSEMBLY FACILITY

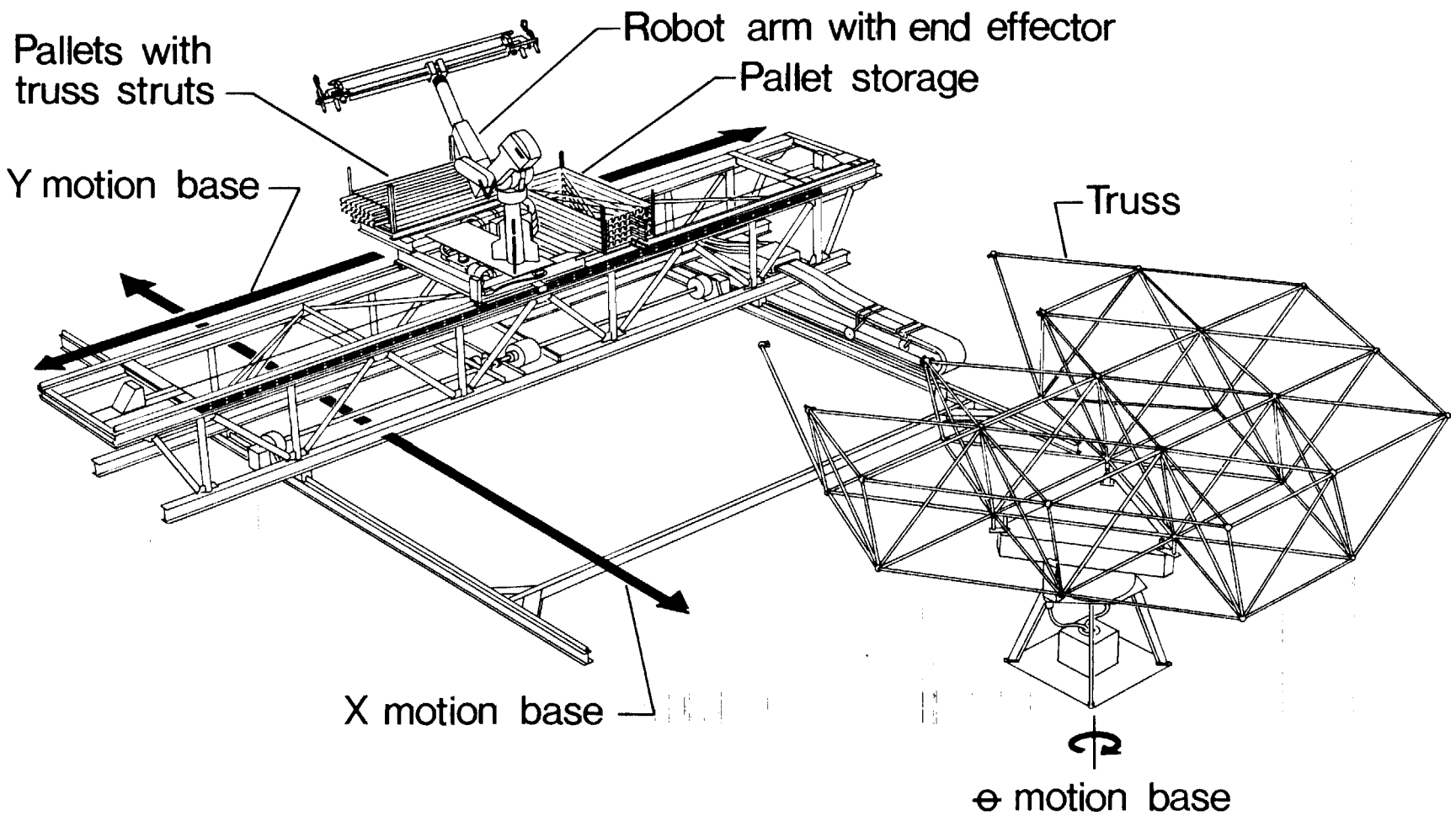


Figure 14

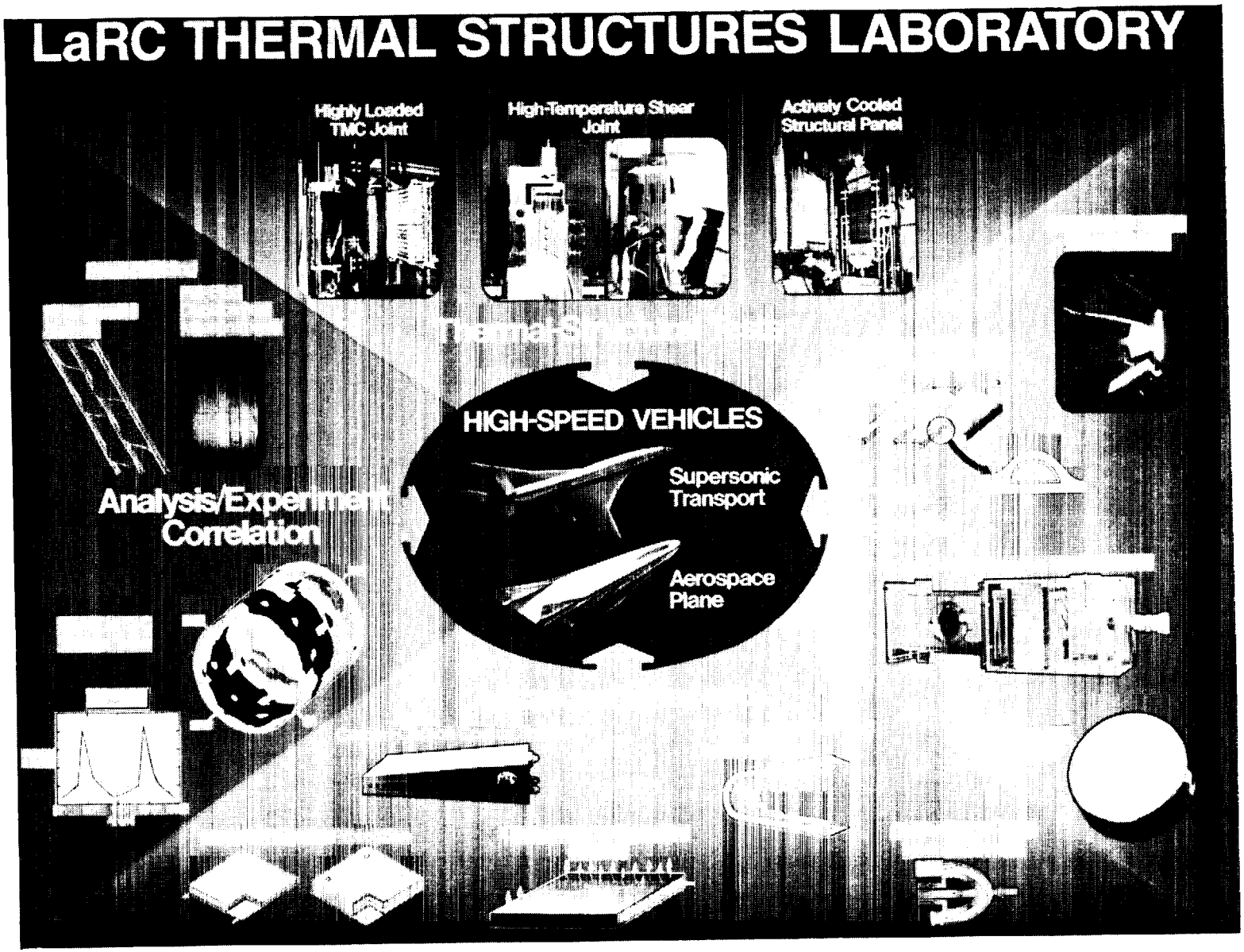
LaRC THERMAL STRUCTURES LABORATORY
Highly Loaded TMC Joint
High-Temperature Shear Joint
Actively Cooled Structural Panel
HIGH-SPEED VEHICLES
Supersonic Transport
Aerospace Plane
Analysis/Experiment Correlation

Figure 15

# Distributed Computing Environment

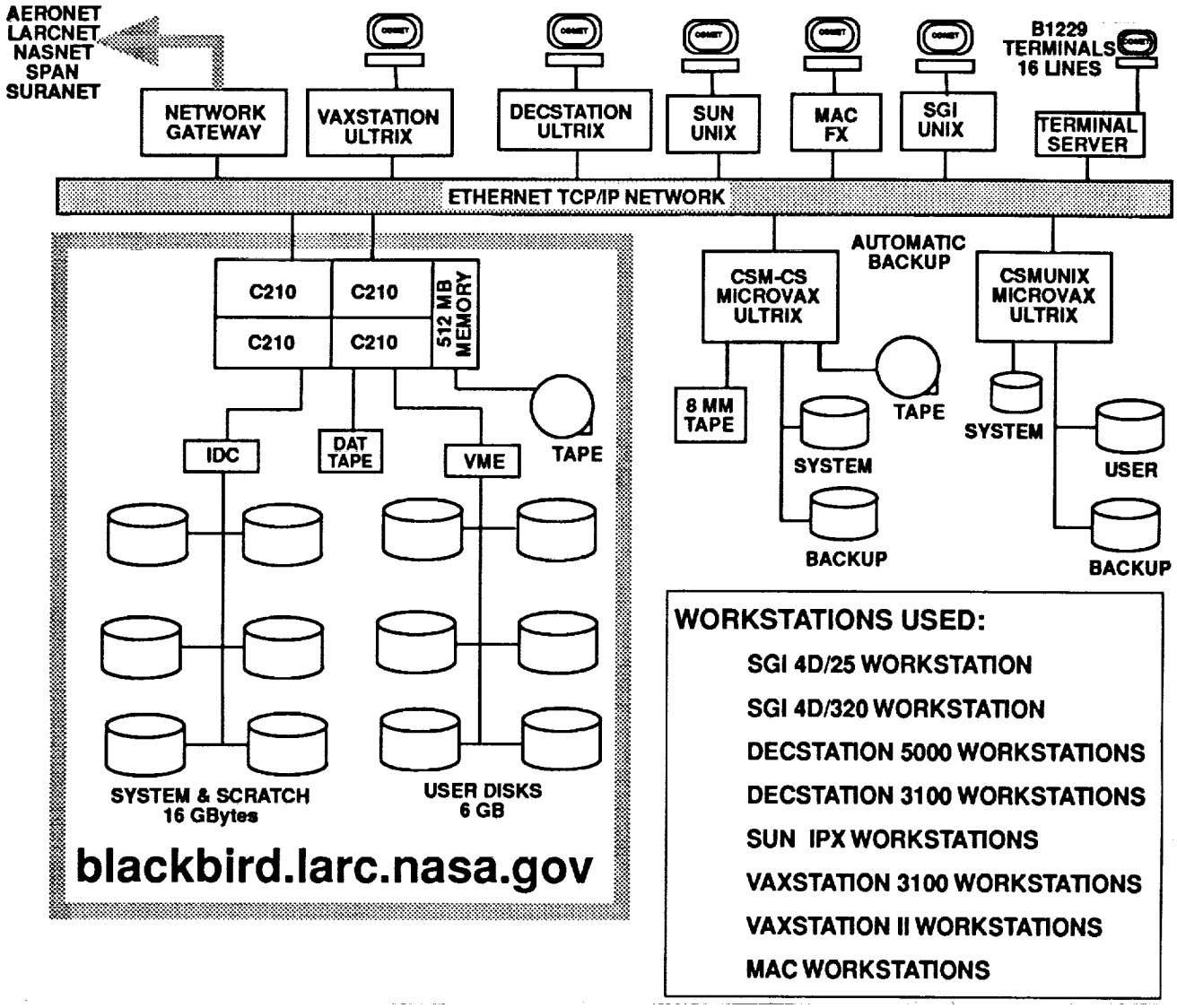


Figure 16

# COMBINED LOADS TEST MACHINE

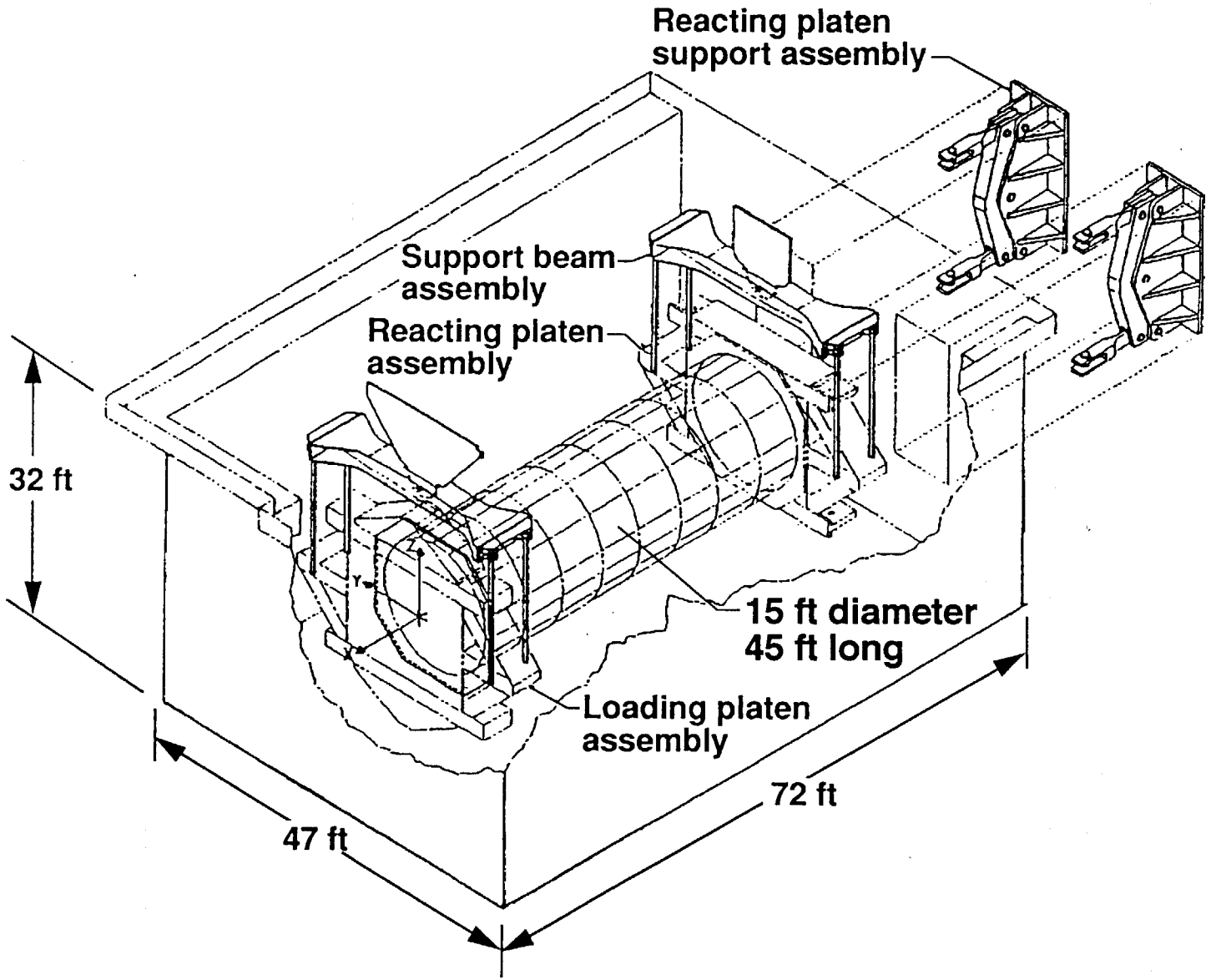


Figure 17

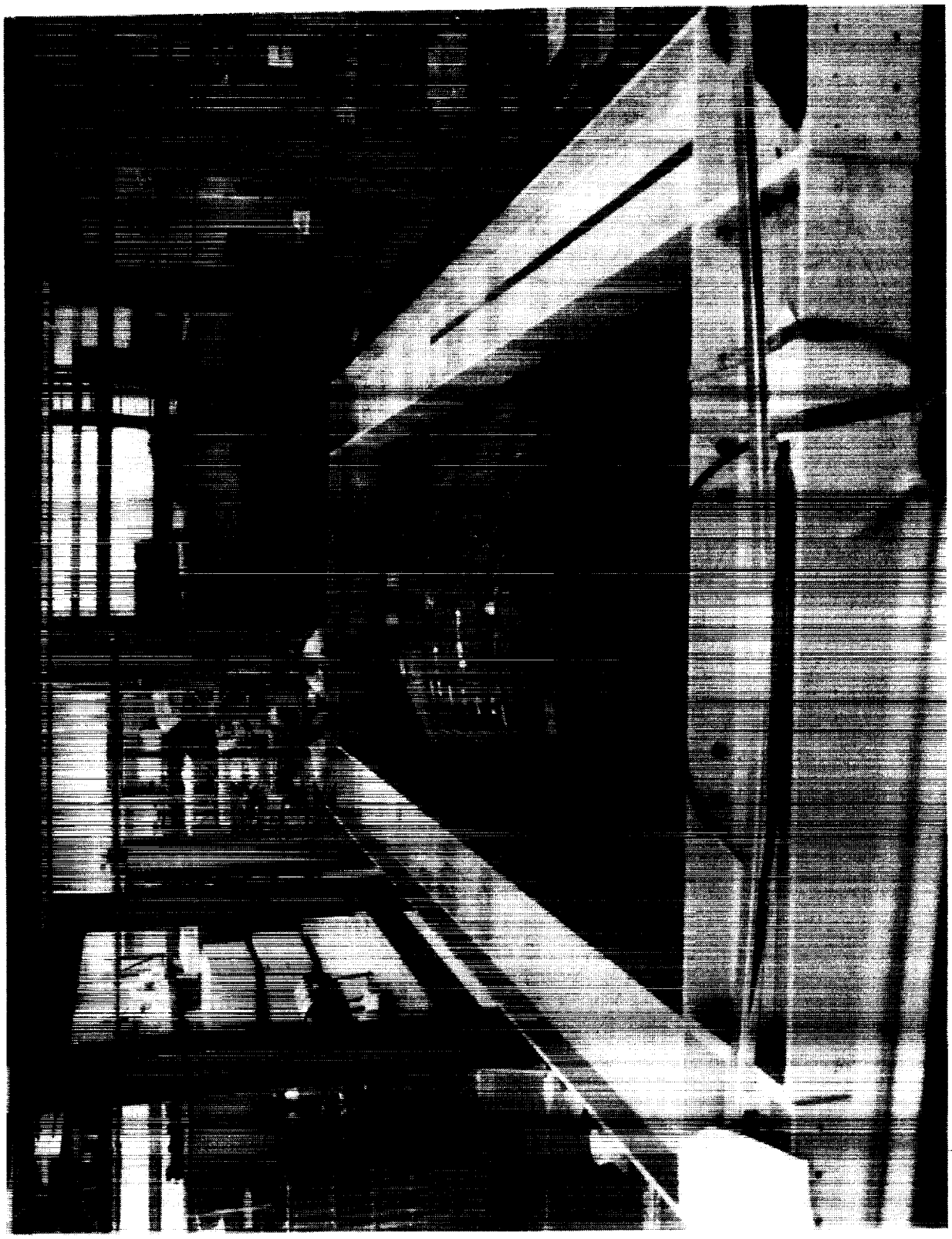

Figure 18

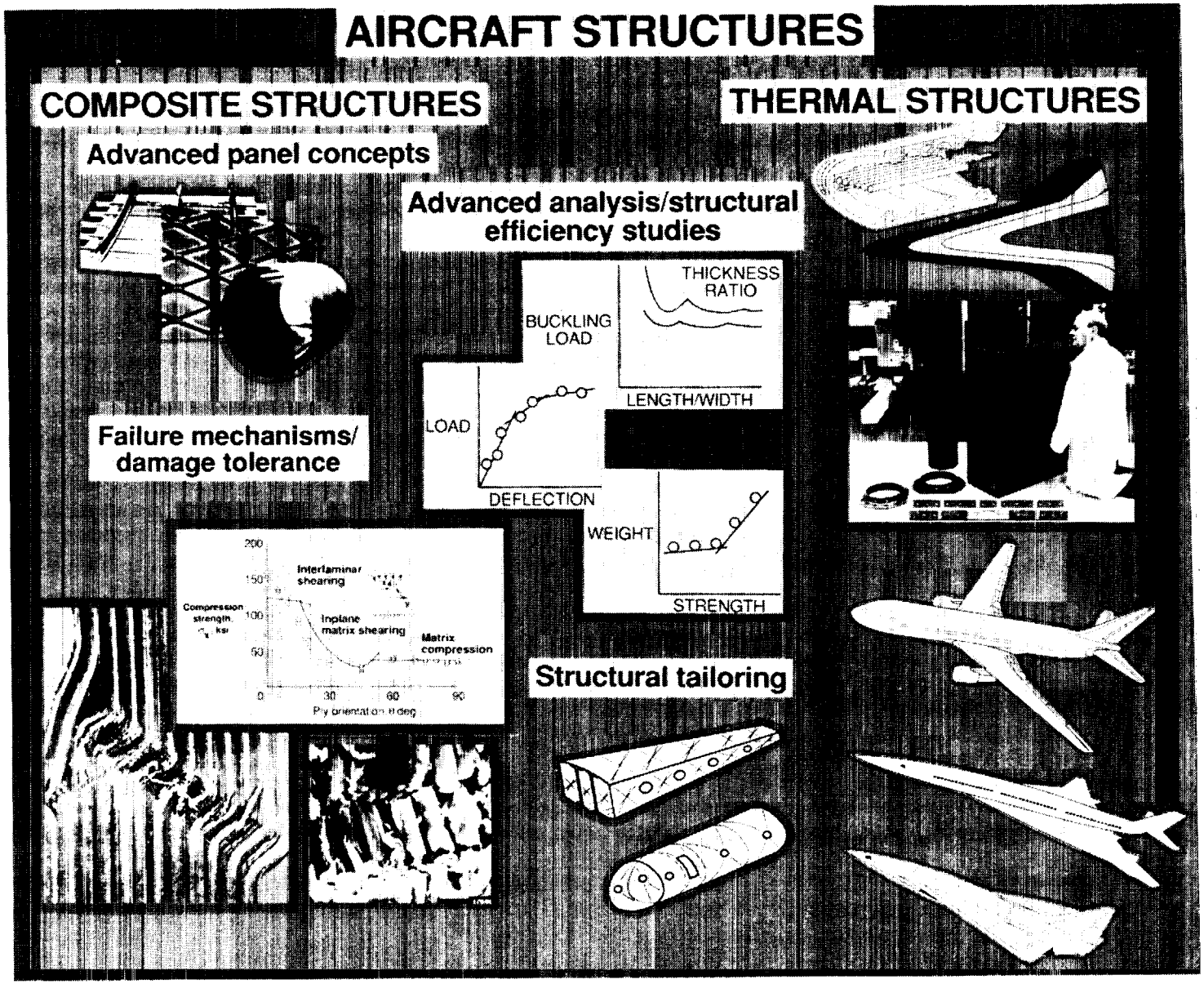
AIRCRAFT STRUCTURES
COMPOSITE STRUCTURES
THERMAL STRUCTURES
Advanced panel concepts
Advanced analysis/structural efficiency studies
Failure mechanisms/ damage tolerance
BUCKLING LOAD
THICKNESS RATIO
LENGTH/WIDTH
LOAD
DEFLECTION
WEIGHT
STRENGTH
Interlaminar shearing
Inplane matrix shearing
Matrix compression
Compression strength, ksi
200
150
100
50
0
30
60
90
Structural tailoring

Figure 19

## STIFFNESS TAILORING CONCEPT IMPROVES COMPRESSION BUCKLING AND POSTBUCKLING RESPONSE FOR COMPOSITE PLATES

**Research Objective**: To evaluate a simple stiffness tailoring concept for potential structural performance benefits through increased compression buckling load and improved postbuckling stiffness and strength.

**Approach**: Buckling resistance is often a controlling criterion in the design of structural elements. Postbuckling response is allowed in certain applications with design controls set on the postbuckling stresses and deformations. Design concepts that lead to increased buckling loads (or strains) can directly lower the structural weight and/or cost. Concepts that also increase postbuckling membrane stiffnesses and reduce out-of-plane deformations and bending stresses can further reduce weight and/or cost when postbuckling is allowed. This study quantifies the improvements that can be achieved in compression buckling loads of square and rectangular composite plates by using a simple stiffness tailoring concept. Preliminary results have also been obtained for square postbuckled plates. The approach is to position the 0° plies through the thickness and over the planform of the plate so that the buckling load is increased with no loss in in-plane stiffness or increase in weight. Finite element analyses have been used to determine the effects of tailoring on the buckling load of plates with various boundary conditions, aspect ratios, thicknesses, and membrane stiffnesses. Similar models have been used to evaluate the postbuckling response of plates optimized for maximum buckling resistance.

**Accomplishment**: A parametric study has been conducted to determine the effect of various design variables and conditions on the compression buckling loads of tailored plates. Stiffness tailoring has been shown to be especially advantageous when the plate is relatively thin, when the unloaded edges are simply supported, and when the average in-plane stiffness of the laminate is relatively high. Laminate stacking sequence and plate length have only small effects on the relative improvements due to tailoring. Buckling loads have been shown to be over 200 percent higher for some tailored plates compared to uniform plates. Significant improvements ranging from 50 to 200 percent can also be achieved in all cases, even for nonoptimum choices of design variables. An initial investigation into the postbuckling response of tailored plates has shown substantial benefits. The results shown in the figure are for a thin, square, quasi-isotropic plate with 0° plies relocated from the center to the unloaded edges of the plate. When the tailored plate is optimized for maximum buckling load, an improvement of 138 percent in the buckling load is achieved, as noted by the open circles on the plot of normalized average compressive load versus normalized edge displacement. When this plate is loaded past buckling, both the secant stiffness (a measure of the ability of the plate to carry increased load) and the tangent stiffness (a measure of the plate's contribution to the stability of a stiffened panel) are increased by similar percentages. A preliminary evaluation of the failure of the postbuckled plate has shown even larger relative improvement in the load capacity at failure.

**Significance**: A simple design concept has been shown to provide large improvements in the buckling and postbuckling response of plates loaded in compression. Weight and/or cost savings should accompany these improvements in plates and stiffened panels.

**Future Plans**: Evaluate tailoring for shear, biaxial, and combined loading. Evaluate tailoring concepts for sandwich plates and for nonrectangular plates. Define an experimental validation test plan and correlate with the analytical results.

**Point of Contact:** Mark J. Shuart, Structural Mechanics Division, (804) 864-2902

Figure 20a

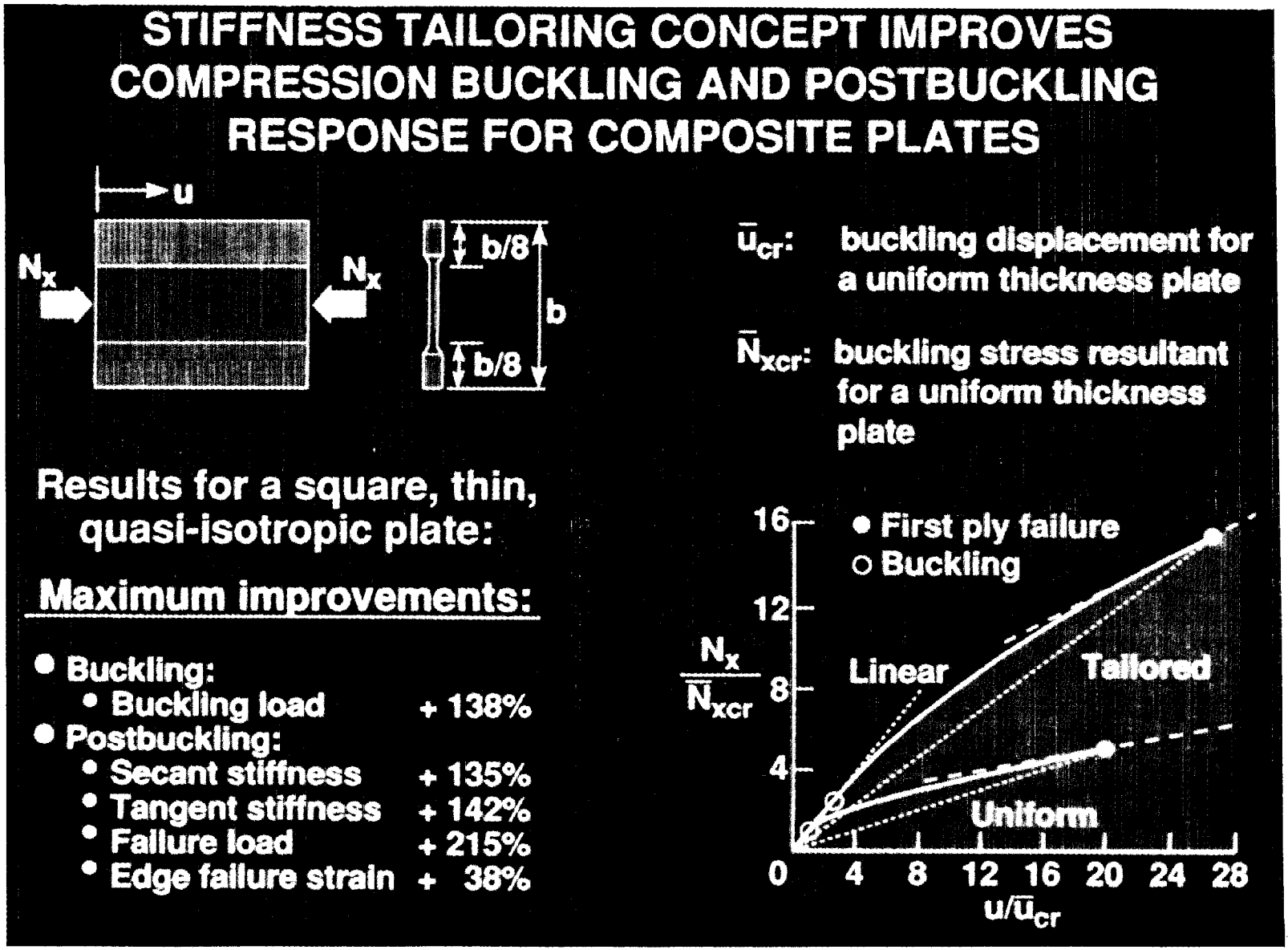
STIFFNESS TAILORING CONCEPT IMPROVES COMPRESSION BUCKLING AND POSTBUCKLING RESPONSE FOR COMPOSITE PLATES
u
$N_x$
$N_x$
b/8
b
b/8
$\bar{u}_{cr}$: buckling displacement for a uniform thickness plate
$\bar{N}_{xcr}$: buckling stress resultant for a uniform thickness plate
Results for a square, thin, quasi-isotropic plate:
Maximum improvements:
• Buckling:
• Buckling load + 138%
• Postbuckling:
• Secant stiffness + 135%
• Tangent stiffness + 142%
• Failure load + 215%
• Edge failure strain + 38%
16
12
8
4
0
$\frac{N_x}{\bar{N}_{xcr}}$
• First ply failure
○ Buckling
Linear
Tailored
Uniform
4 8 12 16 20 24 28
$u/\bar{u}_{cr}$

Figure 20b

## COMPOSITE MATERIALS SHOWN TO RETAIN RESIDUAL STRENGTH AFTER 10 YEARS OF OUTDOOR EXPOSURE

**Research Objective**: To determine the effect of outdoor exposure on the tension, compression and short beam shear strength of composite materials used in the Bell Model 206L helicopter flight service program.

**Approach**: A 10-year ground exposure program was established to support the Bell 206L helicopter flight service program. Painted tension, compression and short beam shear specimens made from the same materials as those used in the flight service program were exposed in racks at five sites on the North American continent: Fort Greely, AK; Toronto, Canada; Hampton, VA; Cameron, LA; and on an oil platform in the Gulf of Mexico. The selected locations are in the general areas where Bell Model 206L helicopter composite flight components are being flown and represent a spectrum of environmental conditions.

**Accomplishment**: Each exposure location contained a rack of specimens that was put in place in 1980 and each rack contained five trays of specimens that were removed for residual tests after 1, 3, 5, 7 and 10 years of exposure. Each tray contained 24 each of tension, compression and short beam shear specimens. The specimens were painted with a polyurethane paint. The four composite material systems and laminates used in the ground exposure program are: (1) Kevlar-49 fabric (style 281)/F-185 epoxy $[0/45/0]_S$ laminate; (2) Kevlar-49 fabric (style 120)/LRF-277 epoxy $[0/90/\pm45]_S$ laminate; (3) Kevlar-49 fabric (style 281)/CE-306 $[0/90]_S$ laminate; and (4) T-300/E-788 $[0/\pm45/0]_S$ laminate. In the summer of 1985 the exposure racks located at Cameron, LA and on the offshore oil platform were destroyed by hurricanes. The data for 5, 7 and 10 years of exposure were obtained from the remaining three sites. Six replicates of each material for each exposure site were tested for each exposure period. The baseline mean strength and data range for each specimen type and material type are shown in the figure for six as-fabricated specimens. The results shown for the exposed specimens are the mean of 30 tests for each material and specimen type that have been exposed for 10 years. The data range shown for the exposed specimens include data from 1, 3, 5, and 7 years of exposure. A total of 456 tests for each type of specimen have been completed. The residual compression strength after 10-years of exposure varies between 87 and 97 percent of the baseline strength. The short beam shear strength varies between 92 and 101 percent of the baseline strength after 10-years of exposure. The Kevlar-49/LRF-277 material exhibited the largest compression and short beam shear strength reductions and the T-300/E-788 material exhibited no strength reduction. The residual tension strengths for all four materials were within the baseline scatter band for all exposure periods up to 10 years.

**Significance**: This program to evaluate the effect of long-term outdoor exposure on the strength of selected composite materials has been completed. Painted composite materials have been exposed in ground-based racks for up to 10 years and the results do not indicate any significant strength reduction as a function of exposure time.

**Future Plans**: A summary of results through 7 years of exposure is presented in NASA TM-4195. A summary of the total 10-year program will be given at the 16th Annual Air Force Mechanics of Composites Review on November 12-13, 1991, at Dayton, Ohio. A NASA document is planned to summarize the total program.

**Point of Contact:** Donald J. Baker, (Vehicle Structures Directorate, Army Research Office) Aircraft Structures Branch, (804) 864-3171

Figure 21a

# Composite Materials Shown to Retain Residual Strength After 10 Years of Outdoor Exposure

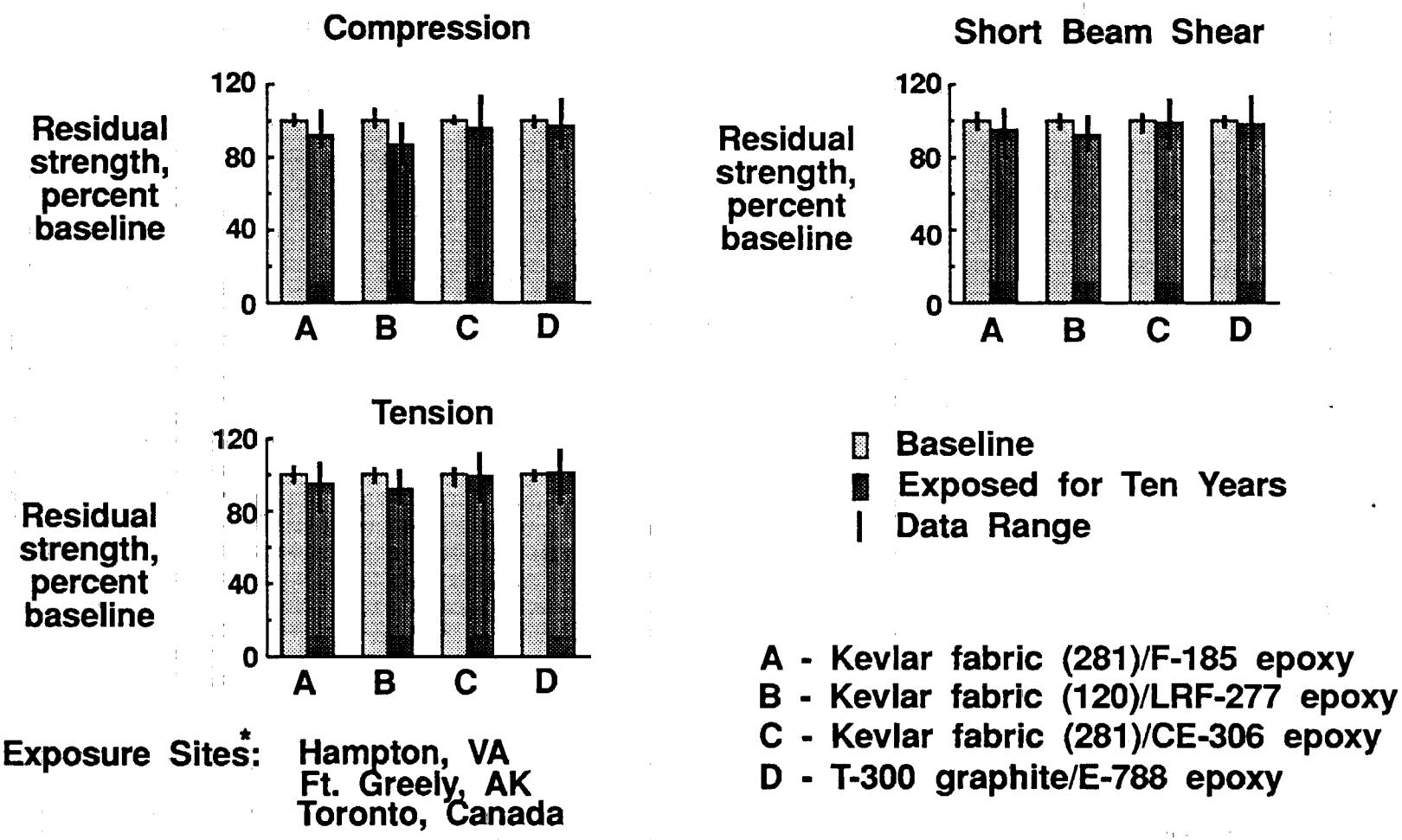


Exposure Sites*: Hampton, VA
Ft. Greely, AK
Toronto, Canada

* 1- and 3-year exposure data available for Cameron, LA and Gulf of Mexico

A - Kevlar fabric (281)/F-185 epoxy
B - Kevlar fabric (120)/LRF-277 epoxy
C - Kevlar fabric (281)/CE-306 epoxy
D - T-300 graphite/E-788 epoxy

Figure 21b

## COST EFFECTIVE COMPOSITE WING CONCEPT DEVELOPED FOR CIVIL TILT ROTOR

**Research Objective**: Develop cost-effective, advanced concepts for a civil tilt rotor wing using innovative structural and material technologies to achieve structurally efficient designs.

**Approach**: Perform a conceptual design study of a civil tilt rotor wing with the goals: to minimize part count; to develop a design and tooling concept suitable for automated fabrication methods; to improve finished part quality; and to increase material design allowables.

**Accomplishment:** As part of task assignment contract NAS1-18796, Bell Helicopter Textron, Inc. has completed a conceptual design study for the wing of a 40-passenger civil tilt rotor aircraft. This conceptual design uses the V-22 (Osprey) dynamic system thereby restricting the wing stiffness to be the same as the Osprey wing stiffness. This stiffness restriction reduces the potential for weight savings but does offer the potential for increasing the design allowables and reducing manufacturing costs. The proposed wing has the same internal structural arrangement as the Osprey. The wing is a two spar, multi-rib configuration with an integrally stiffened cover skin as illustrated on the attached figure. The ±45° cover skin laminate has constant thickness between the side-of-body rib and wing tip close-out ribs and the wing has a simple contour except at the side-of-body rib where a 6° dihedral and forward sweep occurs. Access to the wing interior for assembly or maintenance will be through the spar webs. Each of the five cover skin stiffeners, shown in the attached figure, is a very stiff beam with pultruded graphite-epoxy rods embedded in a syntactic foam. The rods provide the bending material for the stiffener. Angle-ply laminates entrap each layer of rods and form the stiffener webs and skin attachment. An optional block of rigid foam fills the space between the top and bottom of the stiffener. Spar caps with angular shape are formed from pultruded rods embedded in syntactic foam and interleaved with angle-ply laminates. The manufacturing concept chosen was to design for tooled surfaces at assembly interfaces or inside mold lines (IML) to minimize the requirement for shimming at assembly. The wing skin is placed over the stiffeners and spar caps using automated material placement techniques. The stiffeners and spar caps are cured integral with the skin but none of the angle or stiffener plies are interspersed with the skin plies. The wing rib would be formed out of a single flat sheet of thermoplastic material with oriented plies of long discontinuous fibers. The ribs are formed on a female tool assuring close tolerances to the skin and spar mating surfaces. Assembly of the skins to the ribs is by bonding. The front and rear spar webs are attached to the spar caps and ribs by bolts producing a wing that is fastener free on the aerodynamic surfaces. Increased design allowables are achieved by using a compliant "soft" skin with high stiffness or "hard" stiffeners and by reducing stress concentrations by installing fasteners in angle-ply laminates. Improved finished component quality is achieved by reducing the fiber waviness when using the pultruded graphite rods and by reducing the shimming required on mating surfaces.

**Significance:** A cost-effective concept for a civil tilt rotor wing has been developed. The multi-rib wing concept: has reduced part count; is designed and tooled for automated fabrication methods; has improved finished part quality; and increased material allowables.

**Future Plans:** Parametric studies are being conducted for a civil tilt rotor wing to determine internal structural loads for future component design. These studies will be used to determine structurally efficient and cost effective subcomponents for composite tilt rotor wings.

**Point of Contact:** Donald J. Baker, (Vehicle Structures Directorate, Army Research Office) Aircraft Structures Branch, (804) 864-3171

Figure 22a

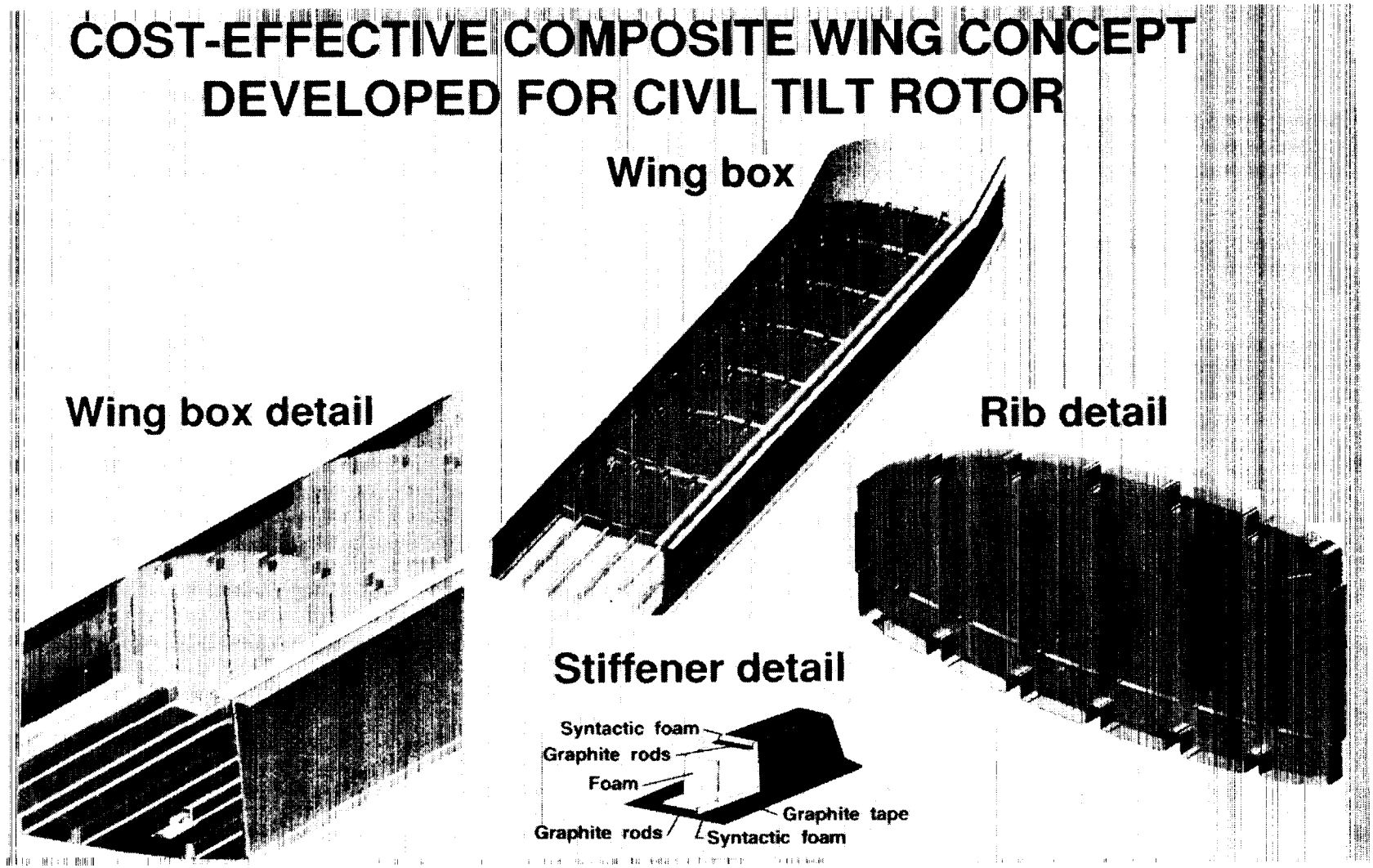
COST-EFFECTIVE COMPOSITE WING CONCEPT
DEVELOPED FOR CIVIL TILT ROTOR
Wing box
Wing box detail
Rib detail
Stiffener detail
Syntactic foam
Graphite rods
Foam
Graphite tape
Graphite rods
Syntactic foam

Figure 22b

## COST EFFECTIVE COMPOSITE FUSELAGE CONCEPT DEVELOPED FOR CIVIL TILT ROTOR

**Research Objective:** Develop cost-effective, advanced concepts for a civil tilt rotor center fuselage using innovative structural and material technologies to achieve structurally efficient designs.

**Approach:** Perform a preliminary design study of a civil tilt rotor center fuselage with the goals: to minimize part count; to develop a design and tooling concept suitable for automated fabrication methods; to improve finished part quality; and to increase material design allowables.

**Accomplishment:** As part of task assignment contract NAS1-18796, Bell Helicopter Textron, Inc. has completed a preliminary design study for the center fuselage of a 40-passenger civil tilt rotor aircraft. The fuselage concept chosen is a frame- and stringer-stiffened pressurized cylindrical shell and is illustrated in the attached figure. To minimize structural complexity and part count, structural members pass by each other on different planes rather than intersecting each other in the manner typical of the conventional frame- and stringer-stiffened skin arrangement. The fuselage skins are fabricated using ±45° graphite-epoxy tape with a layer of syntactic foam at the laminate mid-plane. The stringers are made from a single layer of graphite-epoxy pultruded rods on each side of a layer of syntactic foam. A pad-up of foam is added to the skin between the stringers at the frame locations to allow the frame outside diameter to be constant. The frame is a narrow hat stiffener which uses multiple layers of pultruded rods in the cap of the hat. Angle-ply tapes entrap each layer of rods and form the hat webs and skin attachment flanges. The concept was designed for tooled surfaces to be at assembly interfaces in order to minimize the requirement for shimming during assembly. Using this manufacturing concept, the center fuselage would be made from three types of parts: frame sections; skin panels that include the stringers; and longerons. The frame sections could be cost-effectively fabricated four at a time in an oven utilizing entrapped rubber mandrels to provide curing pressure. The skin panels could be fabricated by laying the stringers in recesses in the tool and then laying down the skin material using automated tape-placement equipment. The composite center fuselage consists of 18 frames, four skin panels and four longerons. All other parts such as skin and frame splice plates, small fittings, clips and brackets would be metal. Increased design allowables will be achieved by the use of soft skins (±45° plies) with hard stiffeners and putting fasteners in the angle plies thus reducing the stress concentration.

**Significance:** A cost-effective concept for a civil tilt rotor composite center fuselage has been developed. The frame- and stringer-stiffened pressurized shell concept is designed and tooled for automated fabrication methods. This concept also has reduced part count, improved finished part quality, and increased material design allowables.

**Future Plans:** Parametric design studies are being conducted for a civil tilt rotor composite fuselage to determine internal structural loads for future component design. Load introduction concepts and design allowables for the pultruded graphite-epoxy-rod/syntactic-foam-core concept are being developed. Results from these activities will be used to determine structurally efficient and cost effective subcomponents for composite tilt rotor fuselages.

**Point of Contact:** Donald J. Baker, (Vehicle Structures Directorate, Army Research Office) Aircraft Structures Branch, (804) 864-3171

Figure 23a

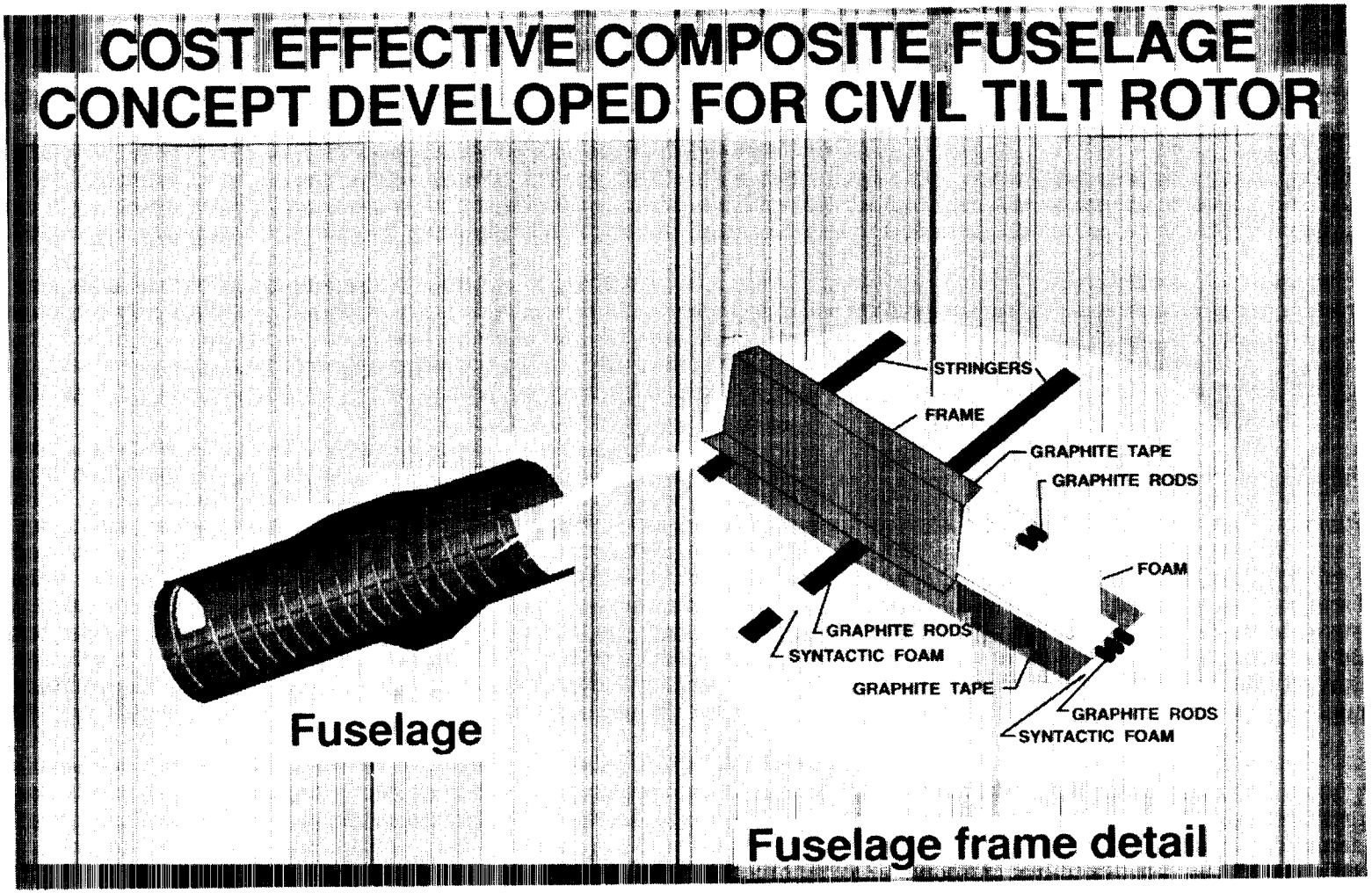
COST EFFECTIVE COMPOSITE FUSELAGE CONCEPT DEVELOPED FOR CIVIL TILT ROTOR
Fuselage
STRINGERS
FRAME
GRAPHITE TAPE
GRAPHITE RODS
FOAM
GRAPHITE RODS
SYNTACTIC FOAM
GRAPHITE TAPE
GRAPHITE RODS
SYNTACTIC FOAM
Fuselage frame detail

Figure 23b

## LANGLEY HEAT-PIPE CONCEPT SELECTED AS CANDIDATE FOR THE NASP WING LEADING EDGE

**Research Objective:** To design, fabricate, and test a reliable and lightweight refractory-composite/heat-pipe-cooled wing leading edge with failsafe features for the National Aero-Space Plane (NASP). The passive, heat-pipe concept is an attractive alternative to the current baseline actively-cooled wing leading-edge design which uses hydrogen fuel to convectively cool superalloy leading edges. The baseline leading-edge design also requires hydrogen cooling during descent when the vehicle is unpowered and does not require hydrogen for combustion. Thus, the hydrogen needed for descent cooling results in a substantial weight penalty for the vehicle.

**Approach:** The approach was to develop a wing leading-edge concept that would enable sufficient heat rejection by radiation to eliminate the need for active cooling for the expected NASP flight environment. The high-temperature heat-pipe-cooled leading-edge concept utilizes the high specific strength of refractory-composite materials at elevated temperatures to accommodate thermal and structural loads and provides a temperature capability above that of conventional refractory-metal heat pipes. Thin (0.010 in. wall thickness) refractory-metal D-shaped heat pipes are embedded within the leading-edge structure to transport the stagnation heat aft, where it can be rejected by radiation. The heat pipes are self contained and transport the heat very efficiently (nearly isothermal heat transport) without the need for external pumping. The heat pipes are sized to provide redundancy in the sense that if a heat pipe fails, adjacent working heat pipes can accommodate the additional heat load. In addition, the concept can rely on the local ablation of the refractory-composite material to insure structural integrity in the event of multiple heat-pipe failures. A three-dimensional, steady-state nonlinear thermal finite element analysis was used in the design study to predict maximum leading-edge temperatures. Variations in parameters such as the leading-edge radius, heat-pipe length, and refractory-composite weave architecture (2-D versus 3-D) were studied.

**Accomplishment:** The parametric study resulted in a leading-edge design which completely eliminated the need for active cooling during ascent and descent and was thus lightweight and much simpler than an actively cooled leading-edge design. The refractory-composite/heat-pipe-cooled wing leading-edge design is over 50 percent lighter than the baseline actively cooled leading-edge design and a competing all refractory-metal/heat-pipe-cooled wing leading edge and was thus selected by the NASP National Program Office for further development (fabrication and test) and funding under NASP Government Work Package No. 69.

**Significance:** The feasibility of providing a reliable and redundant refractory-composite/heat-pipe-cooled wing leading-edge design for application to the NASP is highly attractive since it is anticipated that the weight savings over the baseline actively cooled design will be over 8000 lbs. As a result of the significant weight savings, this heat-pipe concept is currently being investigated as a replacement for the baseline wing leading edge, as well as being considered for use on the nose and tail leading edges of the NASP.

**Future Plans:** A heat-pipe-cooled leading-edge subcomponent will be designed, fabricated, and tested to demonstrate and verify the concept.

**Point of Contact:** Charles J. Camarda, Aircraft Structures Branch, (804) 864-5436

# LANGLEY HEAT-PIPE CONCEPT SELECTED AS CANDIDATE FOR THE NASP WING LEADING EDGE

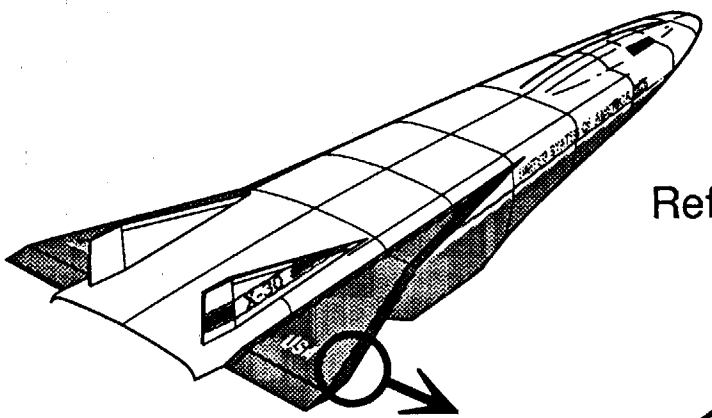

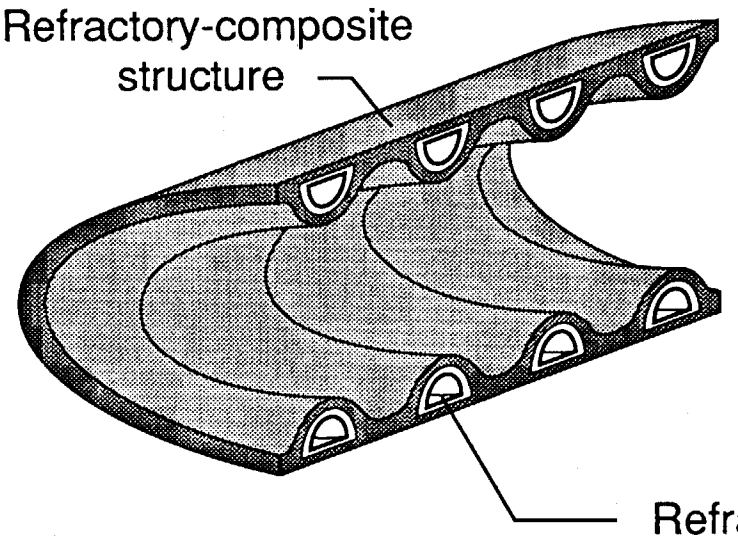


- Concept saves over 8000 lbs. in takeoff weight compared to baseline actively cooled wing leading-edge design
- Concept is currently being considered for baseline wing leading edge
- Concept is also being considered for the nose region and tail leading-edge sections of the vehicle

Figure 24b

## PRELIMINARY DESIGN THERMAL STRUCTURAL ANALYSIS REDUCES MODELING AND COMPUTATIONAL TIME FOR BEAM AND PLATE STRUCTURES

**Research Objective:** Discrete thermal and structural models are often dissimilar and require some form of mapping to transfer temperatures from the thermal model to the structural model. In addition, discrete structural elements like beam and plate elements have no analagous thermal elements which can be used to calculate the temperature distribution through the element thickness. The objective of the present research is to develop thermal elements which are compatible with structural beam and plate elements. Compatible thermal and structural elements can reduce modeling time, problem size, and the computational time required to obtain accurate thermal stresses.

**Approach:** Structural and thermal energy functionals are developed which include parallel formulations for internal energy and the energy associated with boundary conditions. The Ritz method is used to develop the governing equations for the thermal and structural elements. The resulting Ritz-based elements use similar functions to approximate temperatures and displacement fields for the thermal-structural elements. Results from the Ritz-based elements were compared with linear finite element results to examine solution accuracy as a function of degrees of freedom.

**Accomplishment:** Temperature and thermal stress results for a Ritz-based analysis of a heated beam are shown in the figure. The structure has mixed thermal boundary conditions and is fixed against translations and rotations at each end as shown in the upper sketch. Results from finite element thermal and structural analyses are also shown for comparitive purposes. Both sets of results were chosen from convergence studies which examined changes in temperature and stress as a function of degrees of freedom. Convergence studies for the Ritz-based element required only an increase in interpolation function order while finite element convergence studies necessitated mesh refinement and associated changes in loads and boundary conditions defined at nodes. The Ritz-based analysis requires only 12 degrees-of-freedom (dof) for accurate prediction of temperatures and 34 dof for accurate prediction of thermal stresses. The conventional finite element anlaysis requires 99 dof for accurate temperature calculations and 198 dof for good predictions of thermal stresses. The Ritz-based elements are capable of representing mixed boundary conditions including convection for a steady-state thermal analysis and prescribed displacements for structural analysis. Orthotropic and layered media can also be modeled with the Ritz-based elements.

**Significance:** The Ritz-based thermal-structural element decreases the modeling effort required by the analyst since the same model can be used for the thermal and structural analyses. In addition, the energy-based elements give comparable accuracy to finite element results while using significantly fewer degrees of freedom. The decrease in degrees of freedom afforded by the Ritz-based analysis can be very useful for solving thermal-structural problems where sensitivity calculations require multiple analyses per iteration. Finally, thermal loads are calculated more accurately with the Ritz-based approach since temperature functions are integrated exactly and transferred to the structural formulation as loads.

**Future Plans:** Application of the Ritz-based elements to model beam and plate assemblies is underway.

**Point of Contact:** James H. Starnes, Jr., Aircraft Structures Branch, (804) 864-3168

Figure 25a

# Preliminary Design Thermal–Structural Analysis Reduces Modeling and Computational Time for Beam and Plate Structures

Ends restrained against translation and rotation

$k_x = k_z = 0.5 \frac{Btu}{in\text{–}sec\text{–}^\circ F}$ $T_{ref} = 70\,^\circ F$

$\alpha = 0.00006 \frac{in}{in\text{–}^\circ F}$ $E = 10000$ ksi

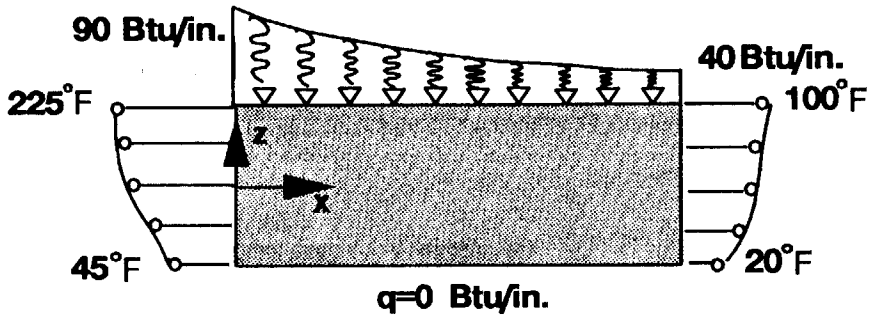


**Advantages of combined elements**

- reduced modeling effort –same model for thermal and structural analysis
- reduced degrees of freedom – higher order interpolation functions
- improved thermal load calculations – temperature function passed directly to structural analysis

## Steady–State Temperature Contours

Ritz–based element
• 12 degrees of freedom

Finite element
• 99 degrees of freedom

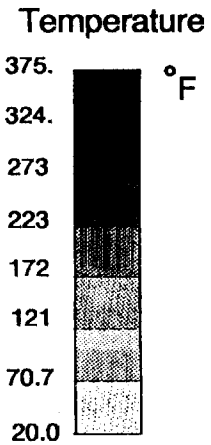


## Thermal Stress Contours

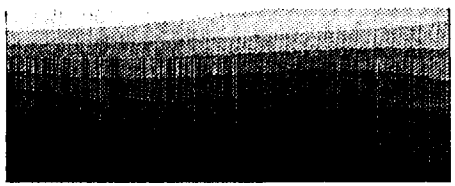

Ritz–based element
• 34 degrees of freedom

Finite element
• 198 degrees of freedom

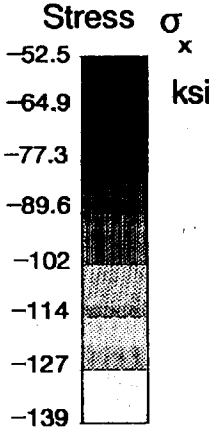


Figure 25b

# CONCEPTUAL STUDIES INITIATED FOR HSR WING STRUCTURES

**Research Objective:** To determine the internal structural configuration and calculate the structural response and weights for a preliminary High Speed Research (HSR) wing.

**Approach:** An internal structural arrangement was defined for a supersonic transport wing design supplied by the Advanced Vehicle Division at Langley. A finite element model was developed for the wing structure, and five aerodynamic load cases for subsonic and supersonic flight conditions were applied to the model. Approximations to Mach 2.4 thermal loads and to fuel, engine, and landing gear masses were also considered in the analysis. The wing panel skins were sized for two material systems, titanium and a quasi-isotropic organic composite material. Honeycomb sandwich construction was assumed for the cover panels, and sine-wave webs were assumed for the ribs and spars.

**Accomplishment:** The finite element model that was generated for the internal wing structure is shown in the upper portion of the figure. The wing upper surface cover panels are removed in this view. The internal forces (stress resultants) for the upper surface cover panels are shown for a Mach 2.4, 2.5g maneuver load condition in the lower right region of the figure. The thermal loads at this flight condition also contribute to the internal forces shown in the figure, but the contribution of these thermal loads to the cover panel stress resultants was found to be minor for the materials of this investigation. For both material systems, the longitudinal stress resultants ($N_x$) achieve their maximum compressive value near the leading edge discontinuity (or crank) in the wing. This load concentration near the leading edge spar is unfavorable and occurs because insufficient wing depth (i.e., bending stiffness) exists at the rear spar. The spanwise internal forces achieve their maximum compressive value at the locations where the main wing spars intersect the fuselage. Here again, the small depth of the rear spar limits the load this spar can transmit to the fuselage. The calculated unit weights of the upper surface cover panels sized to carry these internal loads are shown in the lower left region of the figure. The crank region has the heaviest panels for both material systems, but the organic composite wing panels are significantly lighter than the baseline titanium panels. Wing tip deflections, though not shown, were also calculated and found to be high for the sized wing structure.

**Significance:** This study illustrates the importance of structural input to a wing configuration design. A significantly lighter wing design would result if the thickness of the wing, especially at the rear spar, were modified to improve the internal load paths. Wing tip deflections would also decrease if the rear spar were made deeper. Since the results also show large gradients in the internal loads where the main spars meet the fuselage, an increase in the number of spars and a more accurate model of the structure at the wing-fuselage intersection appear necessary. The weight advantages of composite materials are also apparent from these results.

**Future Plans:** A new wing design with an improved thickness distribution will be obtained from the Advanced Vehicle Division. The internal structural geometry for this wing will be defined and a finite element model developed. This wing will be analyzed, and sizing methods based on structural optimization procedures will be applied to size the structure subject to deflection constraints in addition to local stress and buckling constraints.

**Point of Contact:** Stephen J. Scotti, Aircraft Structures Branch, (804) 864-5431

Figure 26a

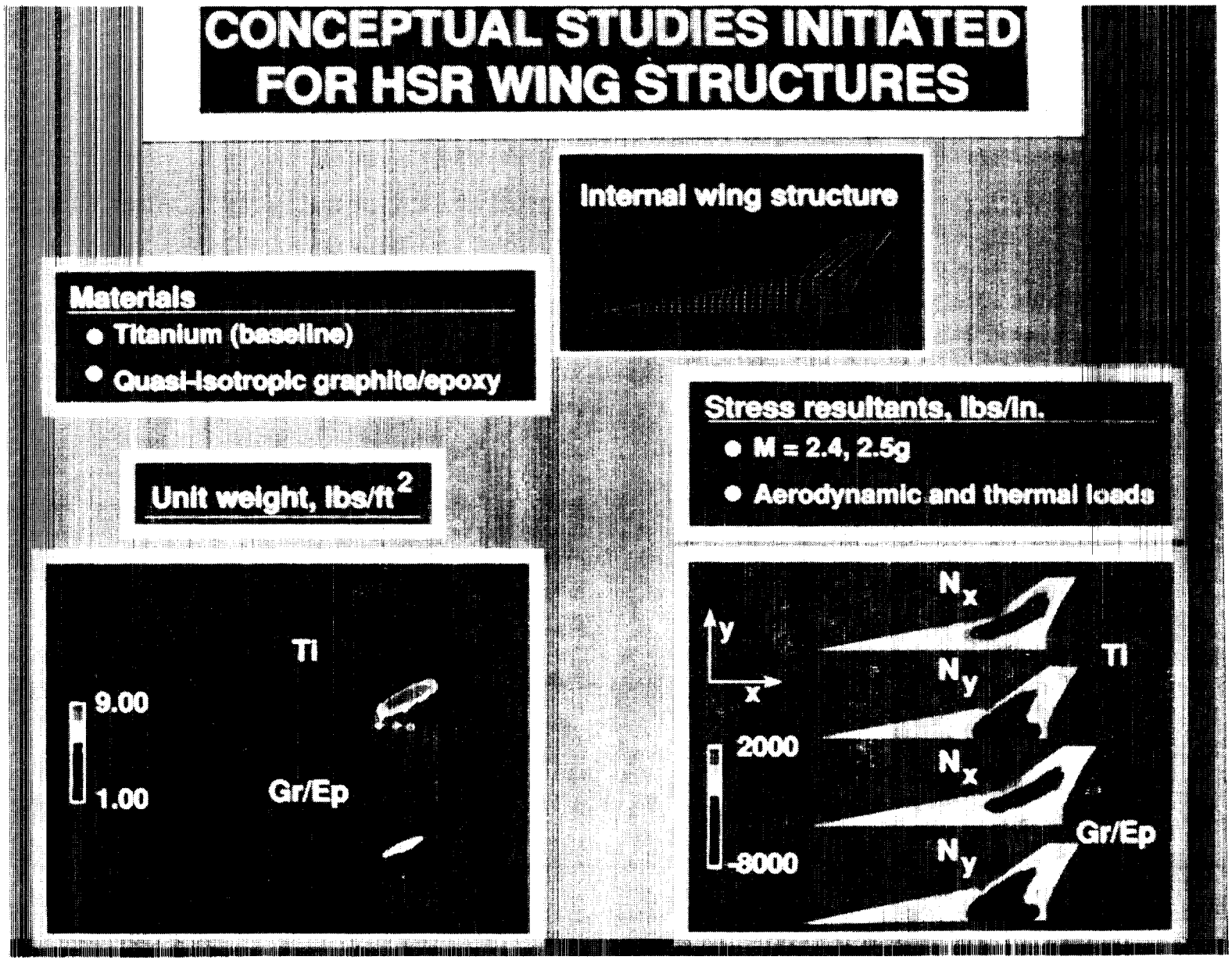
CONCEPTUAL STUDIES INITIATED FOR HSR WING STRUCTURES
Internal wing structure
Materials
• Titanium (baseline)
• Quasi-Isotropic graphite/epoxy
Stress resultants, lbs/in.
• M = 2.4, 2.5g
• Aerodynamic and thermal loads
Unit weight, lbs/ft$^2$
Ti
9.00
1.00
Gr/Ep
$N_x$
y
x
$N_y$
Ti
2000
$N_x$
-8000
$N_y$
Gr/Ep

Figure 26b

THIS PAGE LEFT INTENTIONALLY BLANK

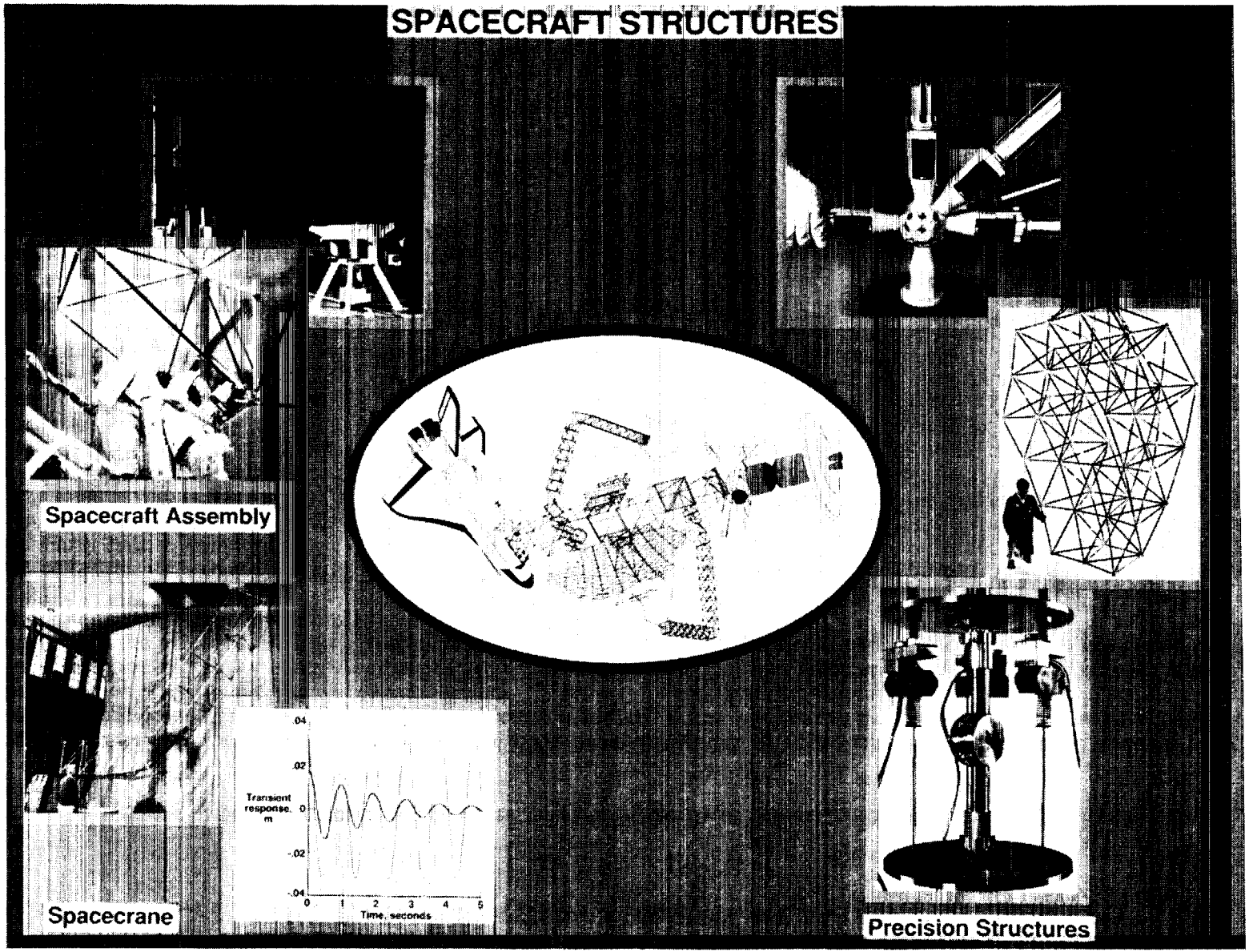


Figure 27

## LaRC ERECTABLE TRUSS HARDWARE ENABLES SPACE CONSTRUCTION FLIGHT DEMONSTRATION AND *INTELSAT* RETRIEVAL

**Research Objective:** To provide erectable truss joint hardware for the flight demonstration of Assembly of Structures by EVA Methods (ASEM).

**Approach:** The ASEM experiment is a demonstration of EVA assembly methods using truss members similar to the erectable baseline structure for Space Station Freedom. The flight experiment is managed by the McDonnell Douglas Space Systems Company, under supervision of the JSC-Crew and Thermal Systems Branch, for the WP-2 Space Station Freedom Project Office. The experiment flew as a secondary payload on STS-49, which was the ***INTELSAT*** rescue mission. The truss segment ( left side of the figure) was assembled on the Shuttle cargo bay sills using the LaRC erectable truss joint system (center of the figure), and an MPESS pallet was used to simulate attachment of a payload to the truss.

**Accomplishment:** The extremely short schedule available to design, fabricate, test, and integrate an experimental payload to meet the STS-49 launch date of April 27, 1992, dictated that all assets required by this effort be available from the beginning. Due to the Spacecraft Structures Branch participation in SSF truss structure development, the required capability existed at Langley Research Center. A total of 137 strut end joint assemblies was supplied to JSC which permitted three sets of experimental hardware to be assembled which were needed for neutral buoyancy training, certification and flight. The quality of the research hardware produced at LaRC was sufficiently high that it could be qualified for flight, resulting in a large production time savings since many of the needed joint components were already machined. Therefore, delivery of all three hardware sets was made on schedule. In addition to the truss hardware operating perfectly during the ASEM experiment, the availability of the ASEM truss hardware permitted placement of an EVA foot restraint over the cargo bay, enabling a three (3) astronaut manual capture of the ***INTELSAT*** spacecraft (right side of the figure) during an unplanned retrieval effort, after a previous rescue attempt by a single astronaut had failed.

**Significance:** The unique in-house design, engineering and fabrication capability of the Langley Research Center, developed to support space structures research activities, enabled the NASA to utilize a flight opportunity for astronaut training in EVA structural assembly methods which otherwise would have been missed. Furthermore, the utility and versatility of the ASEM truss hardware allowed STS-49 mission controllers to quickly develop, on-orbit, an alternative EVA scenario for the successful capture and repair of the ***INTELSAT*** spacecraft.

**Future Plans:** Continue development of one- and two-inch-diameter erectable truss joints for future in-space construction missions.

**Point of Contact:** Harold G. Bush, Spacecraft Structures Branch, (804) 864-3102

Figure 28a

# ERECTABLE TRUSS HARDWARE ENABLES SPACE CONSTRUCTION FLIGHT DEMONSTRATION AND *INTELSAT* RETRIEVAL

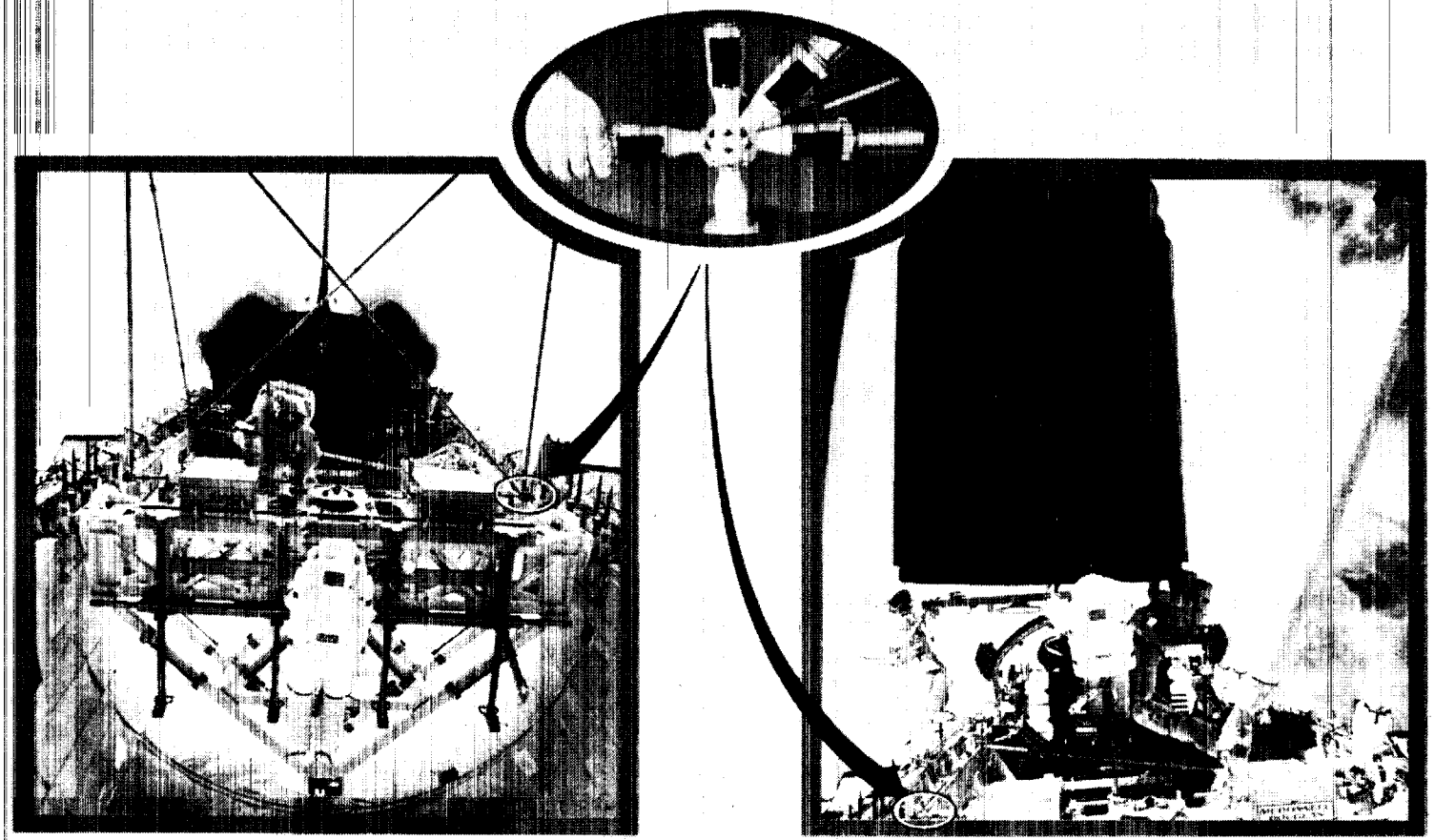

***ASEM*** **Flight Experiment**

***INTELSAT*** **Retrieval**

Figure 28b

# PRECISION SEGMENTED REFLECTOR PANEL-TO-TRUSS ATTACHMENT HARDWARE AND PROCEDURES VERIFIED IN NEUTRAL BUOYANCY TESTS

**Research Objectives:** To evaluate, in a simulated weightless environment, procedures and hardware for the attachment of precision reflector panels to a support truss structure, and to investigate one technique for the removal and replacement of a damaged panel.

**Approach:** Developmental prototypes of two panel-to-truss attachment joint concepts and a panel replacement tool were designed and fabricated. This hardware was evaluated for operation and Extravehicular Activity (EVA) compatibility in a simulated weightless environment. During EVA simulations, 31 neutrally buoyant struts were assembled into a portion of a tetrahedral truss, and three neutrally buoyant mock-up reflector panels were attached using both developmental joints. A reflector panel was also removed from the truss and replaced using a special purpose alignment tool which prohibits the panel from contacting adjacent panels in the reflector surface.

**Accomplishment:** The Spacecraft Structures Branch is developing technology to enable the on-orbit construction of large, high-precision reflectors for future Earth resource observation missions. A key aspect of this activity is the development of precision, EVA compatible, joint hardware for the panel-to-truss attachment. Through a Memorandum of Agreement with the McDonnell Douglas Space Systems Company (MDSSC), Langley engineers were allowed to perform EVA simulations in the MDSSC Underwater Test Facility (see attached figure), and evaluate two designs for the panel-to-truss attachment joint. During these simulations panel attachment operations were performed (see left photograph) as well as panel removal and replacement operations using a special purpose alignment tool currently under development (see right photograph). In most cases, the developmental hardware operated as expected. This resulted in measured assembly times which were within 10 percent of the times predicted using past EVA assembly experience. Both panel attachment concepts were found to be EVA compatible, although one concept was judged by the test subjects to be superior based on the ease of visually identifying the position of its locking handles and the ease of operation of these locking handles.

**Significance:** The most practical and reliable approach for the construction of large structures on-orbit is EVA assembly. A critical aspect of the EVA assembly of large segmented reflectors is the handling and integration of high-precision reflector panels without risking damage to the panel surface. The hardware currently under development allows all EVA operations, including panel removal and replacement, to be efficiently performed from behind the panel, thus minimizing the risk of panel damage.

**Future Plans:** Qualitative assessments of the panel-to-truss attachment joints and the panel removal tool will be incorporated in future hardware revisions. These improved designs will be used during EVA assembly simulations of a 14-meter diameter microwave radiometer reflector be conducted at the Marshall Space Flight Center Neutral Buoyancy Simulator in May/June 1992.

**Points of Contact :** Mark S. Lake,Spacecraft Structures Branch, (804) 864-4311
Walter L. Heard, Jr.,Spacecraft Structures Branch, (804) 864-3123

Figure 29a

# PRECISION SEGMENTED REFLECTOR PANEL-TO-TRUSS ATTACHMENT HARDWARE AND PROCEDURES VERIFIED IN NEUTRAL BUOYANCY TESTS

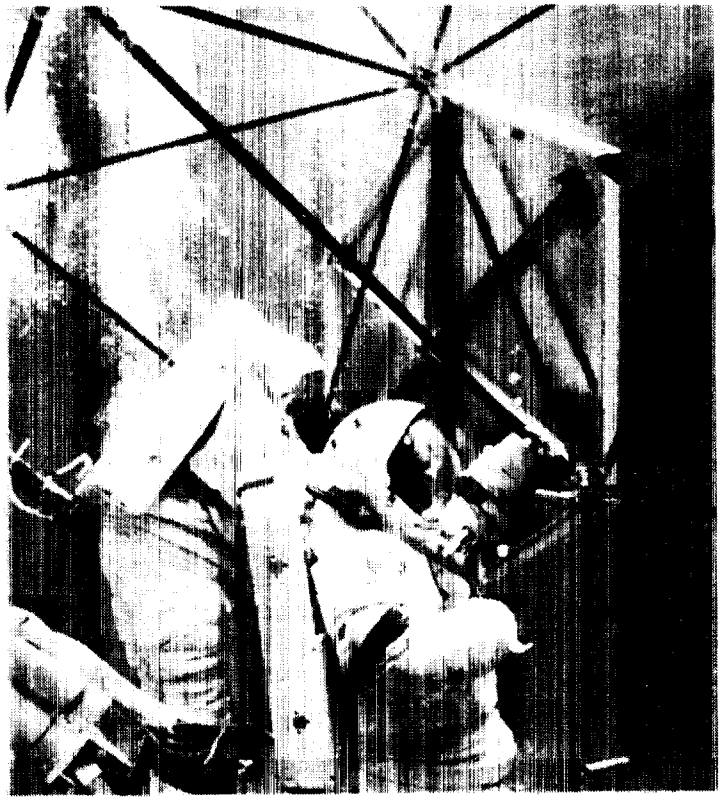

Panel Attachment

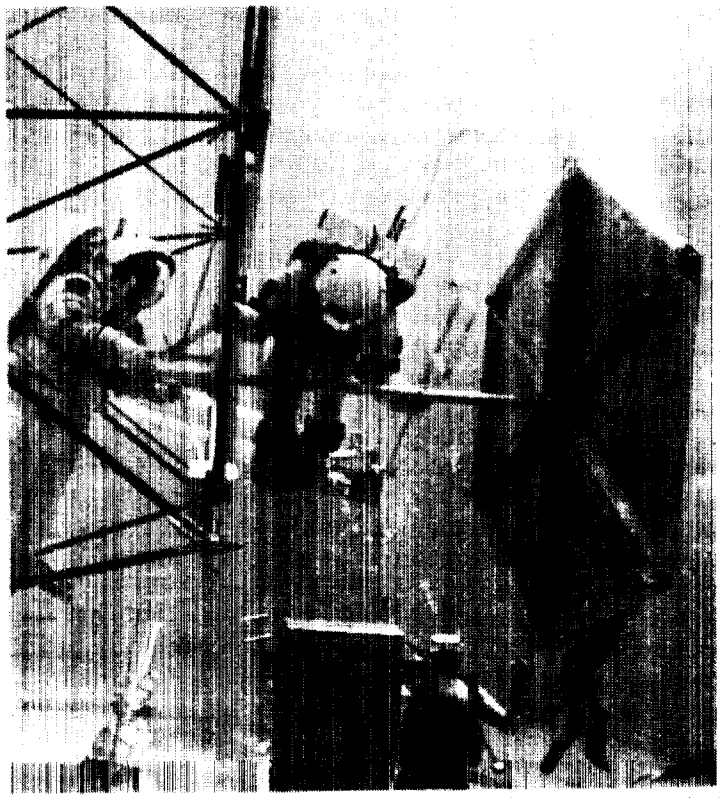

Panel Removal and Replacement

Figure 29b

## EVA ASSEMBLY PROCEDURE FOR 14-METER-DIAMETER PRECISION REFLECTOR VERIFIED IN NEUTRAL BUOYANCY TESTS

**Research Objectives:** To evaluate, in a simulated weightless environment, procedures and hardware for the assembly and maintenance of a large precision reflector including construction of a support truss structure, attachment of reflector panels, and removal and replacement of a damaged panel.

**Approach:** Computer graphic illustrations were prepared detailing an efficient EVA procedure and time predictions for assembly and maintenance of a fourteen-meter-diameter precision reflector. Assembly procedures and hardware were evaluated during simulated weightless environment testing. Assembly times were predicted using data from previous structural assembly tests, and these predicted times were compared with test results. Qualitative evaluations of the hardware were recorded for future hardware design revisions.

**Accomplishment:** A joint activity between the Spacecraft Structures Branch and the Antenna and Microwave Research Branch is leading to the development of a microwave radiometer model representative of a concept proposed for future Earth resource observation satellites. The primary reflector of the radiometer model is a fourteen-meter-diameter segmented surface supported by a precise truss structure. A key aspect of this activity is the development of EVA compatible hardware and efficient procedures for on-orbit construction and maintenance of this large reflector. Due to the double curvature and high surface precision of the reflector, each of the 315 struts and 84 nodes comprising the supporting truss has unique dimensions. Likewise, each of the 37 reflector panels has a unique shape. Nevertheless, an efficient EVA procedure was developed and verified which allowed the entire support truss and seven mock-up reflector panels to be assembled in approximately three hours. During these simulations, the developmental strut-to-node and panel-to-node joints operated as designed. However, minor hardware changes are being considered to improve EVA compatibility. Panel removal and replacement operations were performed from behind the panel using a special purpose alignment tool to minimize the risk of panel damage.

**Significance:** The most practical and reliable approach for the construction of large structures on-orbit is EVA assembly. Of critical importance to the efficient EVA assembly of large segmented reflectors is the storage and handling of unique hardware components. The current assembly procedure accomplishes this by devoting one EVA crew member to hardware management while the other crew member assembles the structure. With this mix of task assignments, it has been demonstrated that a precision reflector structure can be assembled at about the same rate as a uniform truss structure whose hardware components are interchangeable.

**Future Plans:** Qualitative assessments of the panel-to-node and strut-to-node attachment joints will be incorporated in future hardware revisions for improved EVA and robotic compatibility. Test results will be incorporated in the development of EVA and robotic procedures for the construction of a complete microwave radiometer spacecraft including feed-support mast and spacecraft bus.

**Points of Contact :** Mark S. Lake,Spacecraft Structures Branch, (804) 864-4311
Walter L. Heard, Jr.,Spacecraft Structures Branch, (804) 864-3123

Figure 30a

# EVA ASSEMBLY PROCEDURE FOR PRECISION REFLECTOR VERIFIED IN NEUTRAL BUOYANCY TESTS

NASA Langley Research Center

***Offset parabolic reflector assembled in approximately 3 hours. (315 struts, 84 nodes, and 7 reflector panels***

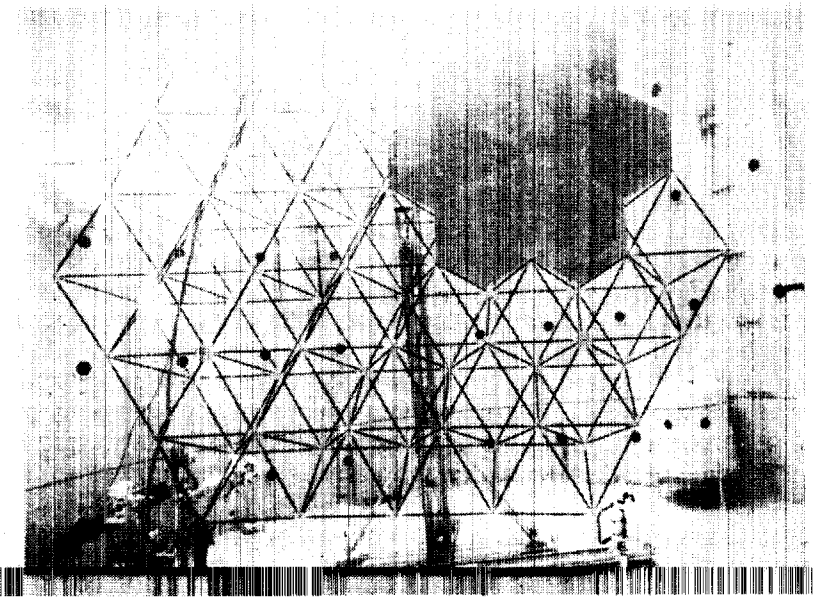

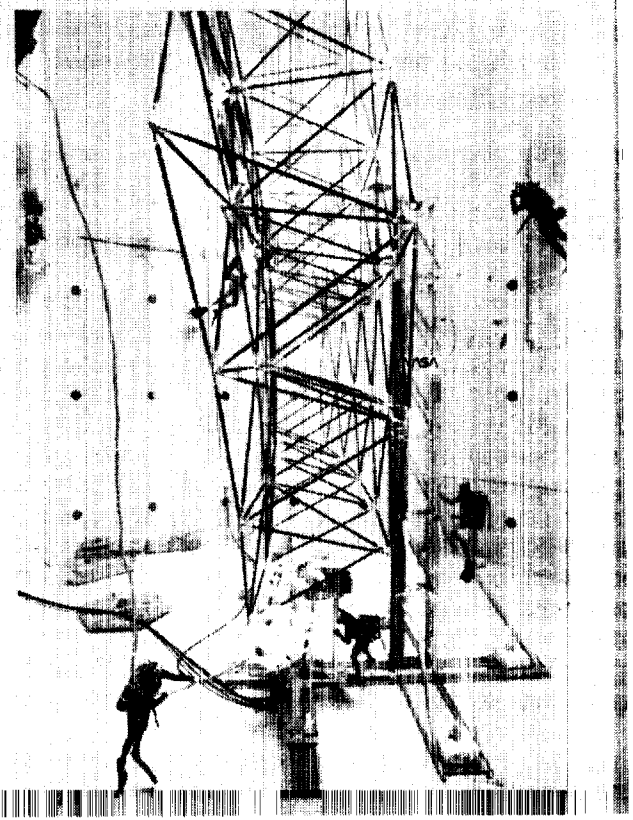

Figure 30b

## DEVELOPMENT OF A MACHINE VISION GUIDANCE SYSTEM FOR AUTOMATED ASSEMBLY OF SPACE STRUCTURES

**Research Objective:** To develop an operational vision guidance system capable of autonomously identifying a passive target in a cluttered environment and guiding a robot in Cartesian space to the target for installing struts in a space truss structure.

**Approach:** A combination of processing tasks which take advantage of a special target configuration is employed to identify the target within the field of view of a video image. The hardware components of the sensor guidance system consist of a miniature CCD video camera and illumination system that is mounted to the robot end-effector (fig.a), and a specially designed passive target that is mounted to the receptacle of the truss connecting joint (fig.b). The target consists of five retro-reflective dots that are arranged in a distinctive pattern to aid in target identification. The retro-reflective dot material has a high reflectivity which is greatest for incident illumination normal to its surface. The video image from the camera is stored in a frame buffer in gray level digital format. A technique based on histogram information is used to establish a gray level threshold and the video image is converted into a binary pixel array. This binary array is analyzed for contiguous pixel units (blobs) that are candidates for the desired target and the centroids of all blobs are located (fig. c). These blobs are first evaluated for their potential as the target dots based on their size and shape. For the blobs that pass this test, the centroids are used as vertices of triangles and all possible triangles (fig. d) are formed. These triangles are evaluated and compared on the basis of geometric similarities to known conditions of four triangles that are formed by the target dots. When a single set of five blobs is identified that match the target in size and shape, and the centroids match all geometric aspects, the location of these centroids is sent to a routine which computes the target position in Cartesian space relative to the robot end-effector (optical axis of the camera). If the target is not identified, the threshold is automatically adjusted until the target is either correctly identified or the operator intervenes.



**Accomplishment:** Laboratory tests and bench tests of the system have been conducted. The laboratory tests were conducted in the automated structural assembly test lab in an uncontrolled lighting environment. They indicated that the hardware and the software algorithms developed for the system can successfully discriminate the passive receptacle targets in a widely varying and cluttered video image throughout the required operational range. The bench tests indicate that the system is fully capable of providing the positional accuracy required for truss assembly operations.

**Significance:** The use of pre-taught robot arm locations for capturing and installing struts is inadequate for use as an in-space automated assembly system. The machine vision system permits the operator to simultaneously view the target and the processing operation to determine if the system is operating properly as opposed to other sensors that do not provide visual feedback. The system also has potential for other robot positioning applications.

**Future Plans:** To perform an end-to-end truss assembly with the robot under vision control and determine the impact on system efficiency and reliability. The system will also be incorporated into the installation of panels, a recently developed capability that is being implemented in the assembly process.

**Point of Contact:** P. Daniel Sydow, Spacecraft Structures Branch, (804) 864-3180

Figure 31a

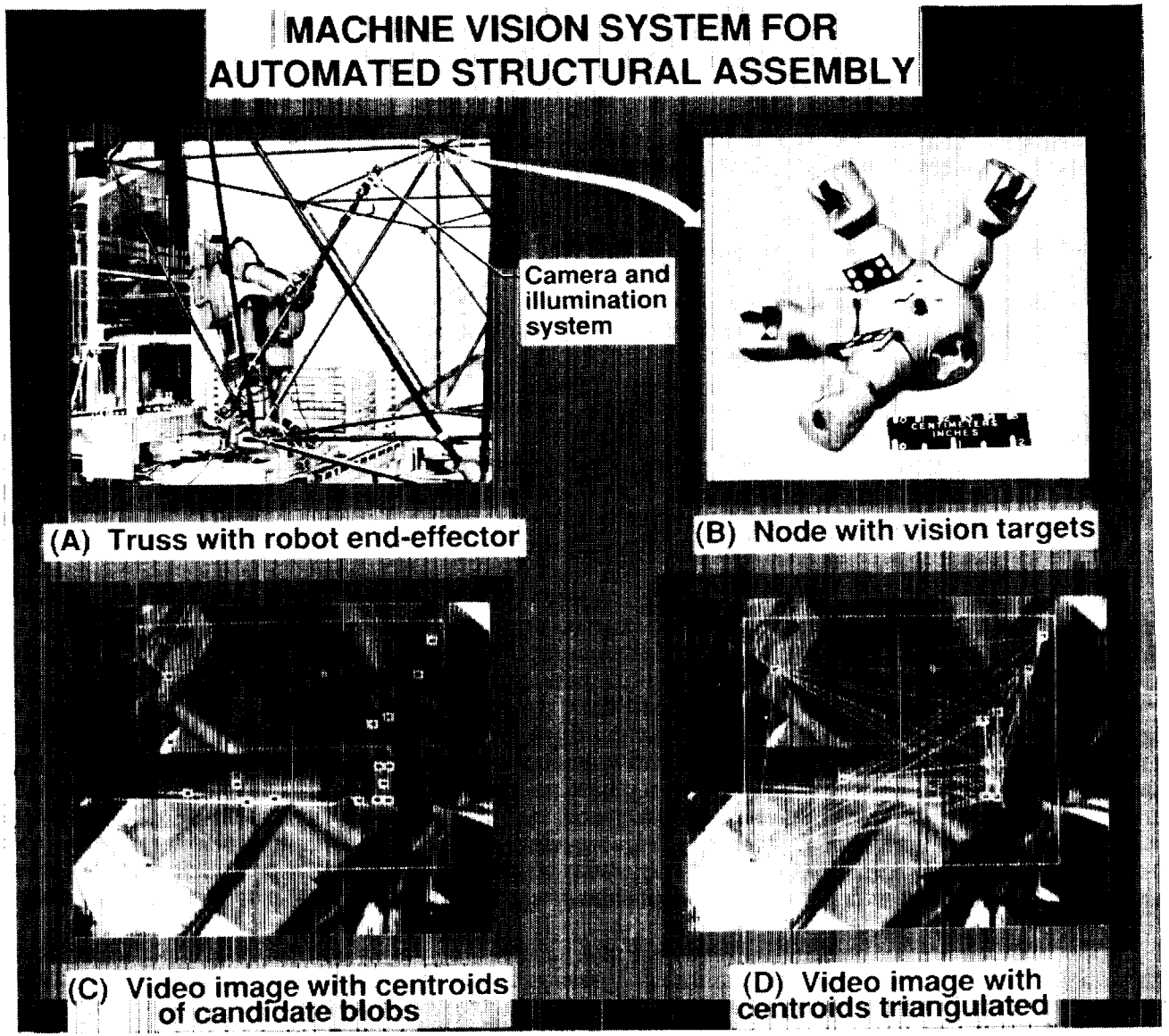
MACHINE VISION SYSTEM FOR
AUTOMATED STRUCTURAL ASSEMBLY
Camera and illumination system
(A) Truss with robot end-effector
(B) Node with vision targets
(C) Video image with centroids of candidate blobs
(D) Video image with centroids triangulated

Figure 31b

## STATIC AND DYNAMIC CHARACTERIZATION COMPLETED FOR SPACE CRANE REFERENCE TRUSS

**Research Objective:** The objective of this research is to experimentally determine the static and dynamic characteristics of the space crane reference truss configuration, and compare these characteristics with analytical predictions.

**Approach:** The Space Crane Articulated-Truss Test Bed (ATTB) is operational in B1148, and is being used to experimentally evaluate the static and dynamic characteristics of articulated-truss joint designs. To assess the predictability of various articulated-truss joint designs, a reference truss (RT) is used as a structural characterization baseline. The RT (see top left in the first accompanying figure) is a truss beam comprised of the same truss structure as the ATTB, but the articulated-truss joint is replaced with two bays of truss structure. The RT is cantilevered to the backstop in B1148, and constructed with 8 one-meter bays of the 1.0 inch erectable hardware that was developed for the Precision Segmented Reflector (PSR) Development program (Heard x43123). The RT static characteristics are determined by applying a load and measuring the corresponding deflections to obtain load-deflection curves. A linear actuator is used to apply the force to the RT, a load cell is used to measure the applied force, and direct current displacement transducers (DCDTs) are used to measure the deflections. The dynamic characteristics are determined by applying independent random forces at two locations on the RT and measuring the time response at the truss nodes with accelerometers. The modal analysis hardware is the 16 channel GENRAD model 2515 with the SDRC's Modal Plus Program - Data Acquisition Task software. The modal testing used 14 channels: one channel for each vibration exciter and the remaining 12 channels for 4 triaxial accelerometers.

**Accomplishment:** The RT load-deflection curve is shown on the bottom right of the first accompanying figure and exhibits a linear behavior over the load range. The load is cycled from 0 lbf to approximately 270 lbf, then to -270 lbf and returned to 0 lbf for three cycles. The load-deflection curve slope is 445 lbf/in and compares very well with the analytical prediction of 446 lbf/in. The RT dynamic characteristics have also been experimentally and analytically determined. The experimental frequency response functions (see one frequency response function in the bottom left of the second accompanying figure) indicate global truss vibration modes for first bending - 6.79 Hz and 7.00 Hz; first torsion - 24.84 Hz; second bending - 31.88 Hz and 33.15 Hz; first axial - 47.18 Hz; third bending - 77.04 Hz and 80.40 Hz; second torsion - 79.73 Hz. The corresponding analytical vibration frequencies are as follows: first bending - 6.77 Hz and 7.02 Hz; first torsion - 24.41 Hz; second bending - 31.38 Hz and 32.93 Hz; first axial - 46.60 Hz; third bending - 76.35 Hz and 80.85 Hz; second torsion - 76.03 Hz. The experimentally determined modal damping was less than 0.8 percent for the first five modes. Two analytical mode shapes are also shown in the second figure and are the fundamental and first torsion modes.

**Significance:** The superior structural performance of the 1.0 inch erectable hardware allows accurate analytical predictions for static and dynamic behavior.

**Future Plans:** The ATTB and RT will be used to evaluate passive damping hardware (D-struts), new articulated-truss joint concepts, and experimentally validate a closed-loop 2-D large-angle slew maneuver to be simulated using the Dynamic Analysis and Design System program.

**Points of Contact:** Thomas R. Sutter, Spacecraft Structures Branch, (804) 864-3109
K. Chauncey Wu, Spacecraft Structures Branch, (804) 864-3111

Figure 32a

# STATIC AND DYNAMIC CHARACTERIZATION COMPLETED FOR SPACE CRANE REFERENCE TRUSS

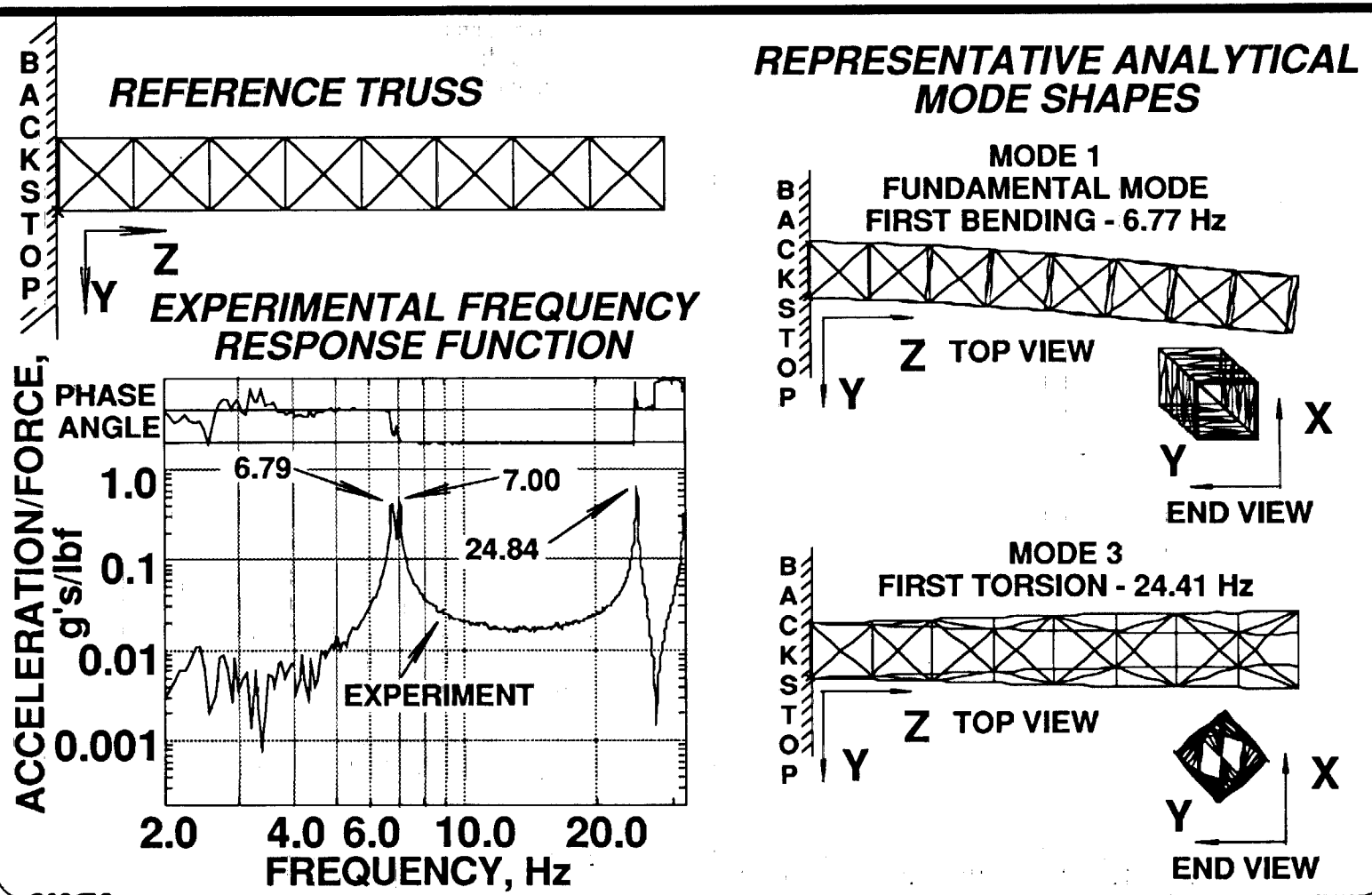


Figure 32b

## SIMULATION SHOWS PASSIVE DAMPING STRUCTURAL ELEMENTS EFFECTIVE IN REDUCING SPACE CRANE VIBRATION RESPONSE

**Research Objective:** The objective of this research is to simulate large-angle slew maneuvers of the space crane Articulated-Truss Joint Test Bed and predict the effect of passive damping on the tip transient response.

**Approach:** A planar model of the Articulated-Truss Joint Test Bed structure, shown in the accompanying figure, is generated using the DADS analysis software. The truss members and actuators are modeled as linear springs, with nodes represented by rigid bodies. The single degree-of-freedom (DOF) hinges necessary for large-angle articulation are modeled as revolute joints. The outboard boom is slewed through 1 radian in 5 seconds and held at that angle for an additional 5 seconds. The large-angle slew maneuver is implemented by extending the two linear actuators in the articulated-truss joint according to a pre-determined cosine profile. A 1000 kg tip mass is equally distributed to the 2 nodes at the outboard boom tip. Passive damping structural elements (D-Struts$^{TM}$) are modeled as linear dashpots in parallel with the root bay truss members. The tip transient response is evaluated with and without a 1000 kg tip mass and passive damping structural elements.

**Accomplishment:** Four analyses (with and without the tip mass, and with and without passive dampers) have been performed to evaluate the tip transient response. The tip transient response (defined as the difference from the rigid-body tip position) at the outboard boom tip are shown in the two plots in the accompanying figure. The large increase in deflections and reduction in fundamental frequency is evident with addition of the tip mass. Addition of the passive dampers removes the low-amplitude, high-frequency response for the case without the tip mass. The maximum deflection at t = 0.5 seconds is reduced by about 10 percent for the case with the 1000 kg tip mass. The settling time is greatly reduced by addition of the D-Struts, with the peak deflection reduced to 0.002 m by the end of the simulation at t = 10 seconds. This is 10 percent of the tip deflection at the end of the slew maneuver at t = 5 seconds.

**Significance:** NASA's exploration initiatives will require on-orbit assembly and construction of large spacecraft from components launched from earth. A dedicated construction facility will be necessary to perform these assembly tasks. These simulations may be used to predict the maximum tip deflections of the space crane which result from various slew rates and payload masses, resulting in minimum assembly time on-orbit.

**Future Plans:** Additional simulations with various tip masses and slew times over 5 seconds will be conducted to predict their effect on the tip transient response. Open-loop slewing of the Articulated-Truss Joint Test Bed in the B1148 Lab will also be performed to correlate experimental data with the dynamic simulations presented here.

**Point of Contact:** K. Chauncey Wu, Spacecraft Structures Branch, (804) 864-3111

Figure 33a

# SIMULATION SHOWS PASSIVE DAMPING STRUCTURAL ELEMENTS EFFECTIVE IN REDUCING SPACE CRANE VIBRATION RESPONSE

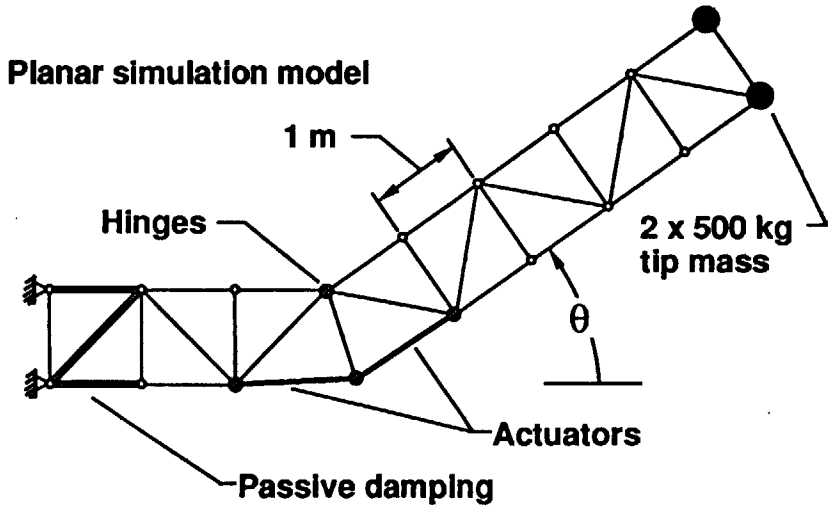


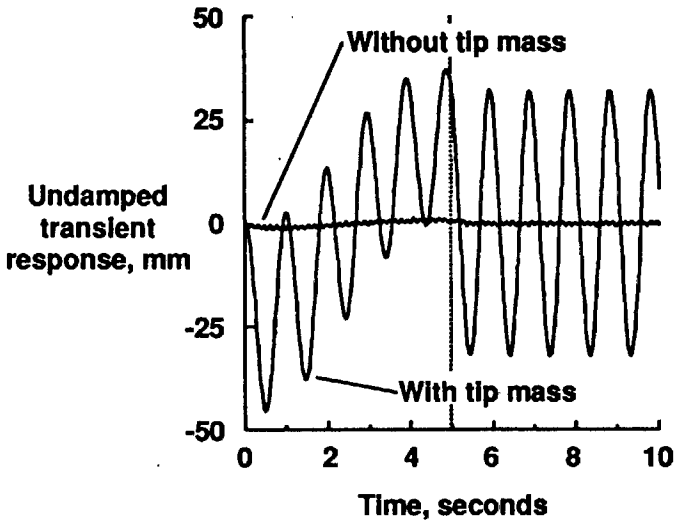


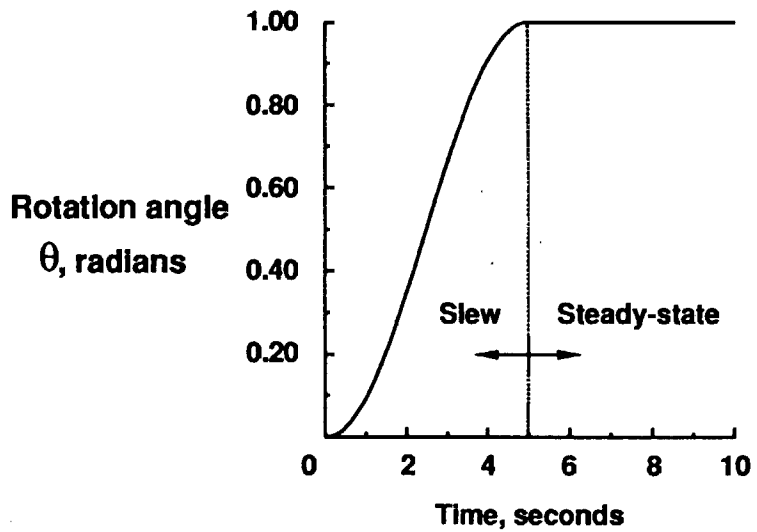


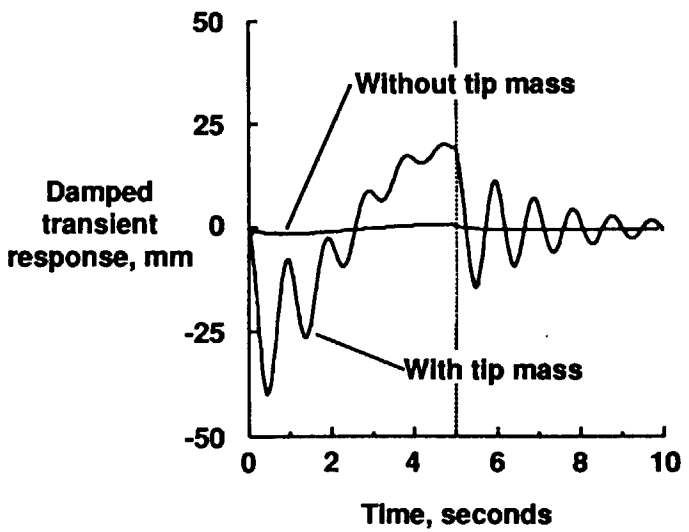


Figure 33b

THIS PAGE LEFT INTENTIONALLY BLANK

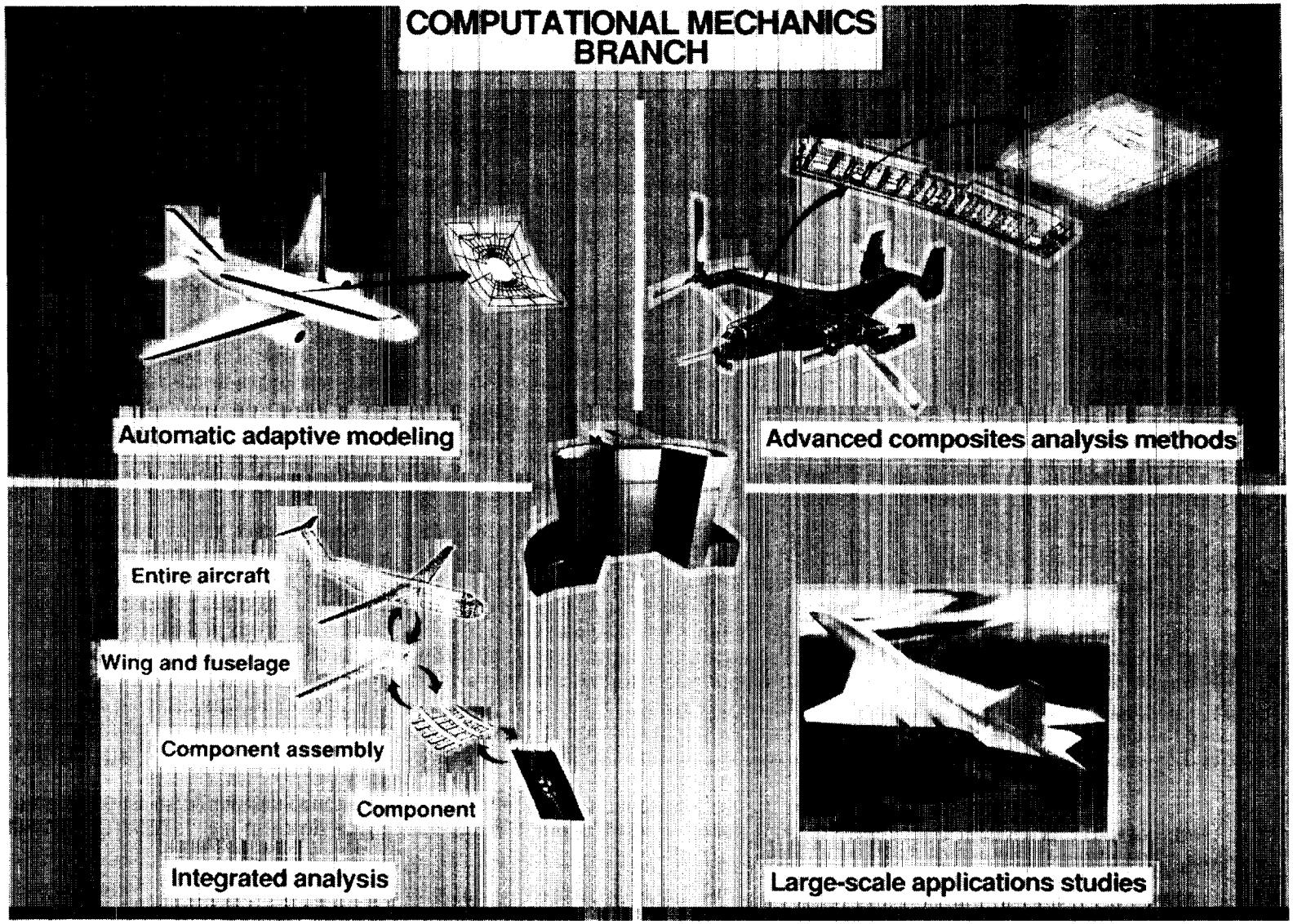


Figure 34

# FUNCTIONAL INTERFACE METHOD ACCURATELY JOINS INCOMPATIBLE FINITE ELEMENT MODELS

**Research Objective:** To develop and demonstrate a finite element based global/local analysis method for calculating detailed structural response using independent incompatible finite element models.

**Approach:** The global/local analysis of plate and shell structures has in the past been accomplished either by a two-step process, in which results from a relatively coarse model are applied as boundary conditions (*i.e.*, displacements or forces) on an independent detailed local model or by a one-step process in which local refinement is embedded in a single model analysis of the entire structure. The former approach does not take into account the interaction between the local and global regions, and the latter approach often leads to highly complex modeling due to the use of transition regions from the local refinement to the rest of the model. However, as demonstrated herein, the shortcoming of the latter approach can be overcome by using a newly developed functional interface method which joins two independently modeled regions. A functional form with its own free parameters is assumed for the behavior of the interface between the neighboring regions. Each region is joined to the interface using either a collocational formulation, a discrete least-squares formulation or an integral formulation. The function selected along the interface may be a single polynomial, or cubic, quadratic or linear splines. The computational strategy is implemented using the Computational Mechanics Testbed, COMET.



**Accomplishment:** A global/local analysis of an isotropic plate with a center crack loaded in axial tension has been performed. The problem is characterized by a stress singularity at the crack tip. A refined finite element model was used near the crack tip, and a much less-refined model was used for the remainder of the plate. The models are highly incompatible across the interface. The collocational formulation was used in this analysis with quadratic polynomials selected along the shorter segments of the interface and a cubic polynomial selected along the longer segment. The normalized stress intensity factor as a function of the crack length to width ratio is shown. The solid curve represents the reference solution found in the literature. The open circles represent the stress intensity factors obtained from the present analysis. The stress intensity factors are in excellent agreement with the reference solution.

**Significance:** The method described herein provides the analyst with increased modeling flexibility. Mesh transitioning between coarse and more refined finite element regions is not required. Grid points along the interface need not be coincident. These modeling features allow an analyst to easily substitute different local region models within the same global model. While the method is applied here to a problem with global/local behavior, it is also applicable to component synthesis. The application of this method to component synthesis is significant since component models are usually developed independently by different analysts and/or organizations.

**Future Plans:** The functional coupling methodology will be extended to more complex interface geometries and multiple critical regions.

**Point of Contact:** Jonathan B. Ransom, Computational Mechanics Branch, (804) 864-2924

Figure 35a

# Functional Interface Method Accurately Joins Incompatible Finite Element Models

## Cracked Plate

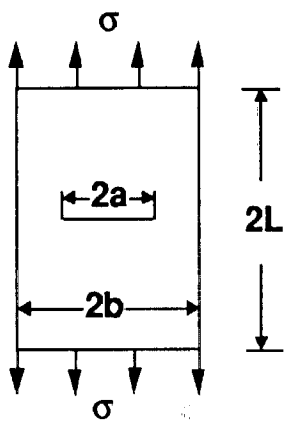


## Quarter Model

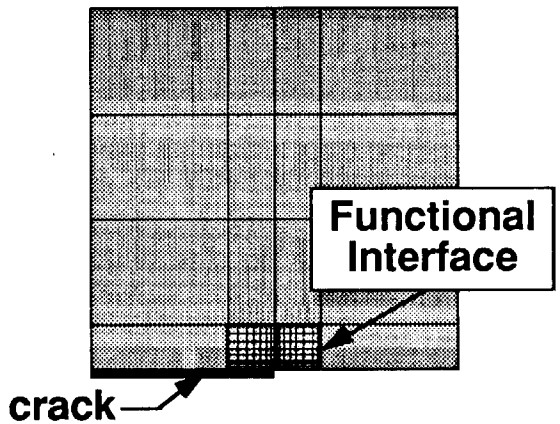


## Accuracy

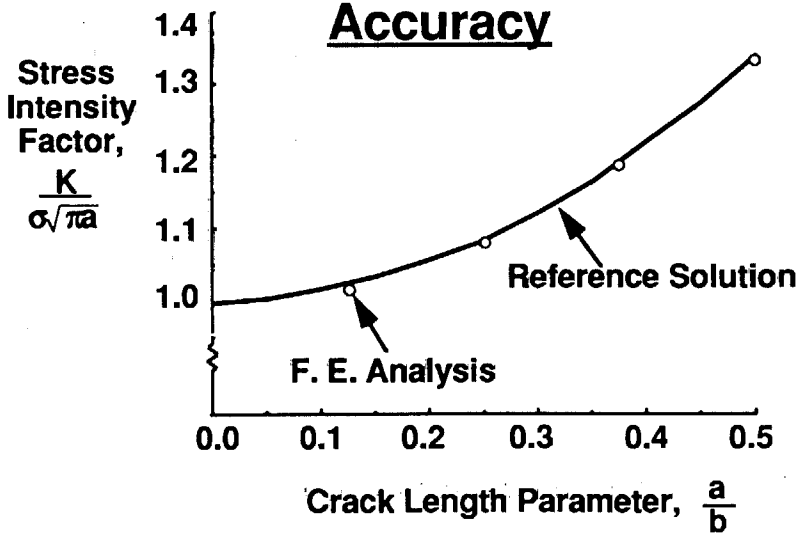


## Advantages

- No Tedious Transition Region Modeling
- Grid Points Along Interface Need Not Coincide
- Requires Fewer Degrees of Freedom than Model with Transition Regions
- Retains Accuracy

Figure 35b

## ITERATIVE METHOD DEVELOPED FOR CALCULATING FRACTURE PARAMETERS

**Research Objective:** Develop rapid analysis tool for calculating fracture parameters used to assess crack growth in planar structural components.

**Approach:** A rapid analysis tool has been constructed for calculating fracture parameters (e.g., stress intensity factors), for cracks in general planar structural components. This tool uses a newly developed iterative method which combines the boundary element method (BEM) for an uncracked finite component with cutouts under general loading conditions with a continuum solution for a cracked infinite component without cutouts. A schematic illustrating the iterative method is shown in the accompanying charts. First the BEM is applied to the uncracked component. Since the BEM requires only the discretization of the component boundaries, (including cutout boundaries), the modeling is easier than with finite elements which requires discretization of the entire component. Because the BEM step will not yield traction free conditions at the crack(s), the tractions predicted by the BEM step are removed by seeking the continuum solution for the equal and opposite tractions acting on the cracks of an infinite component. However, this results in unwanted tractions on the boundaries of the component. These are removed on the next iteration using the BEM. The iterative process continues until the BEM portion of the solution produces tractions on the crack surfaces which are negligibly small. The stress intensity factor for the crack is then the sum of the stress intensity factors obtained from all the iterations. Generally only five to ten iterations are required to obtain converged solutions.

**Accomplishment:** For verification, the iterative method has been applied to a plate under remote uniaxial tension having a crack emanating from a circular cutout in the plate for which accepted results appear in the literature. The variation of the stress intensity factor with crack length is shown for a crack emanating at 30 degrees from the transverse direction. Results are shown for Mode I and Mode II fracture; that is when the crack is driven by normal and shear stresses, respectively, at the crack tip. The excellent agreement with accepted results validates this new methodology.

**Significance:** Rapid analysis tools are needed for effective assessment of damage and fault tolerance in realistic components with cutouts and general loading conditions. Industry access to such tools allows assessment of component design integrity and life early in the design process.

**Future Plans:** Extension of methodology to configurations with multiple cracks.

**Point of Contact:** Jerrold M. Housner, Computational Mechanics Branch, (804) 864-2907

Figure 36a

# ITERATIVE METHOD DEVELOPED FOR CALCULATING FRACTURE PARAMETERS

## GENERAL 2-D CAPABILITY

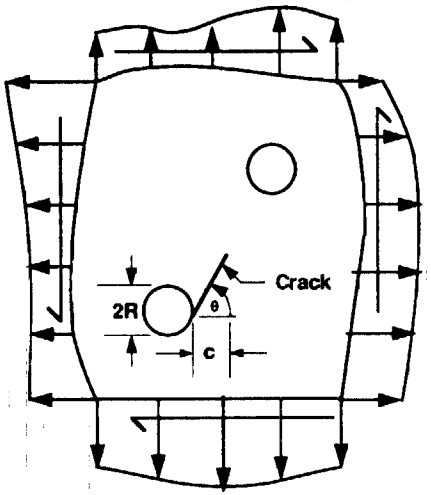


## ALGORITHM

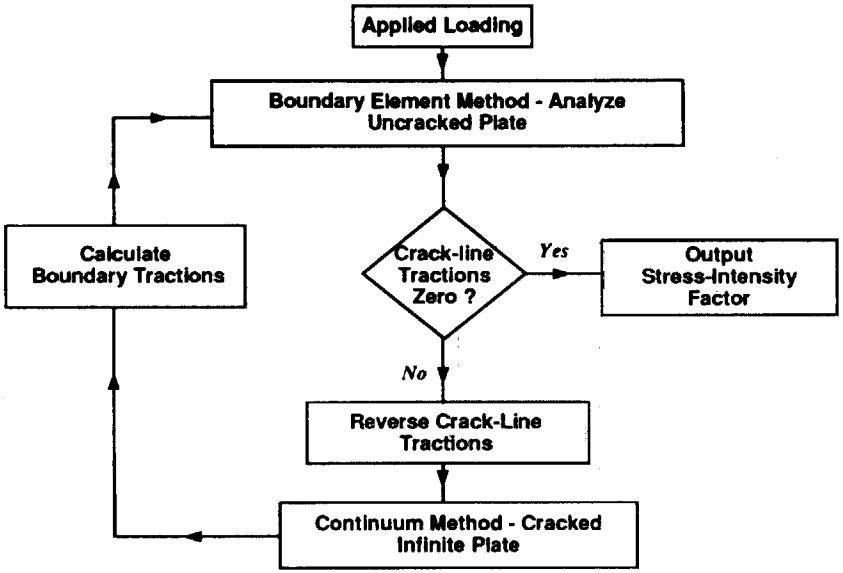


## VERIFICATION

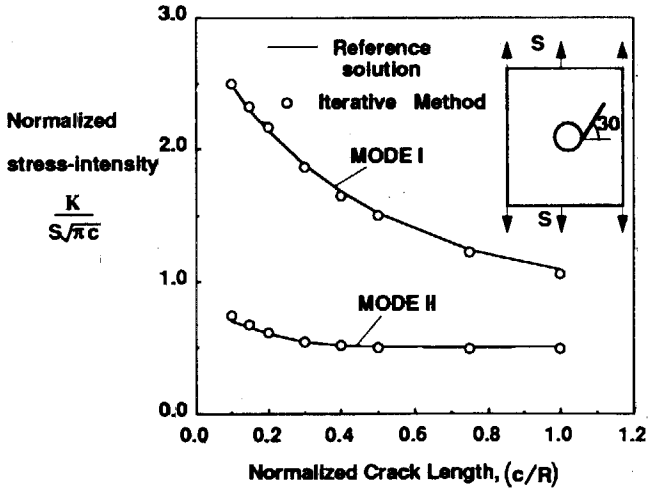


## EFFICIENCY

- **Easy to Model**
- **Rapid Execution of Parametric Studies**

Figure 36b

## PERFORMANCE OF ADAPTIVE MESH REFINEMENT DEMONSTRATED ON COMPOSITE FUSELAGE-LIKE COMPRESSION PANEL

**Research Objective:** Demonstrate performance of adaptive finite element mesh modeling on aircraft shell structural component.

**Approach:** A comparison is made of two automatic finite element mesh refinement techniques on a graphite epoxy curved fuselage-like compression panel containing a cutout. In one technique, the mesh is graded uniformally while in the other, it is graded adaptively at strategic locations. Each technique uses quadrilateral elements only, because for shell structures, these are more accurate and less sensitive to distortion than triangular elements. The initial mesh contains only four finite elements. The response is predicted at each progressive step of mesh refinement and refinement indicators based on stress intensity are used to determine when to remesh and for the adaptive refinement, where to remesh by identifying high stress gradient regions. A user selected tolerance is employed to terminate refinement.

**Accomplishment:** A comparison of the performance of the two techniques for predicting the stress concentration factor at the cutout is shown in the figure along with a published solution accepted as providing the true stress concentration. The model size (degrees-of-freedom) increases with automatic refinement for both techniques. The adaptive refinement technique requires less than 2000 degrees-of-freedom for accuracy because the meshing tends to zoom in on the high-stressed region around the cutout, whereas the uniform technique is still inaccurate even at 6000 degrees-of-freedom. The adaptive meshing "overshoots" the accepted solution due to the distortion of elements which naturally occurs in the transition region between the fine mesh near the cutout and the coarse mesh away for the cutout. This distortion of the quadrilateral elements from rectangular tends to degrade their accuracy.

**Significance:** Until now adaptive mesh refinement research for structural analysis has been primarily on flat models and to a lesser degree on three-dimensional models composed of brick elements. Very little has been done on shell structures which dominate aerospace vehicle structures. The coupling of membrane and bending effects with geometrical curvature make this a challenging problem requiring innovative meshing algorithms, strategies and refinement indicators. The excellent performance of adaptive meshing on a curved fuselage-like panel is significant for analysis and design of realistic composite aircraft structural components.

**Future Plans:** Extension to built-up structures is now underway and new techniques being developed should eliminate the need for transition regions with their inherent mesh distortion and performance degradation.

**Point of Contact:** Jerrold M. Housner, Computational Mechanics Branch, (804) 864-2907

Figure 37a

# Performance of Adaptive Mesh Refinement Demonstrated on Composite Fuselage-like Compression Panel

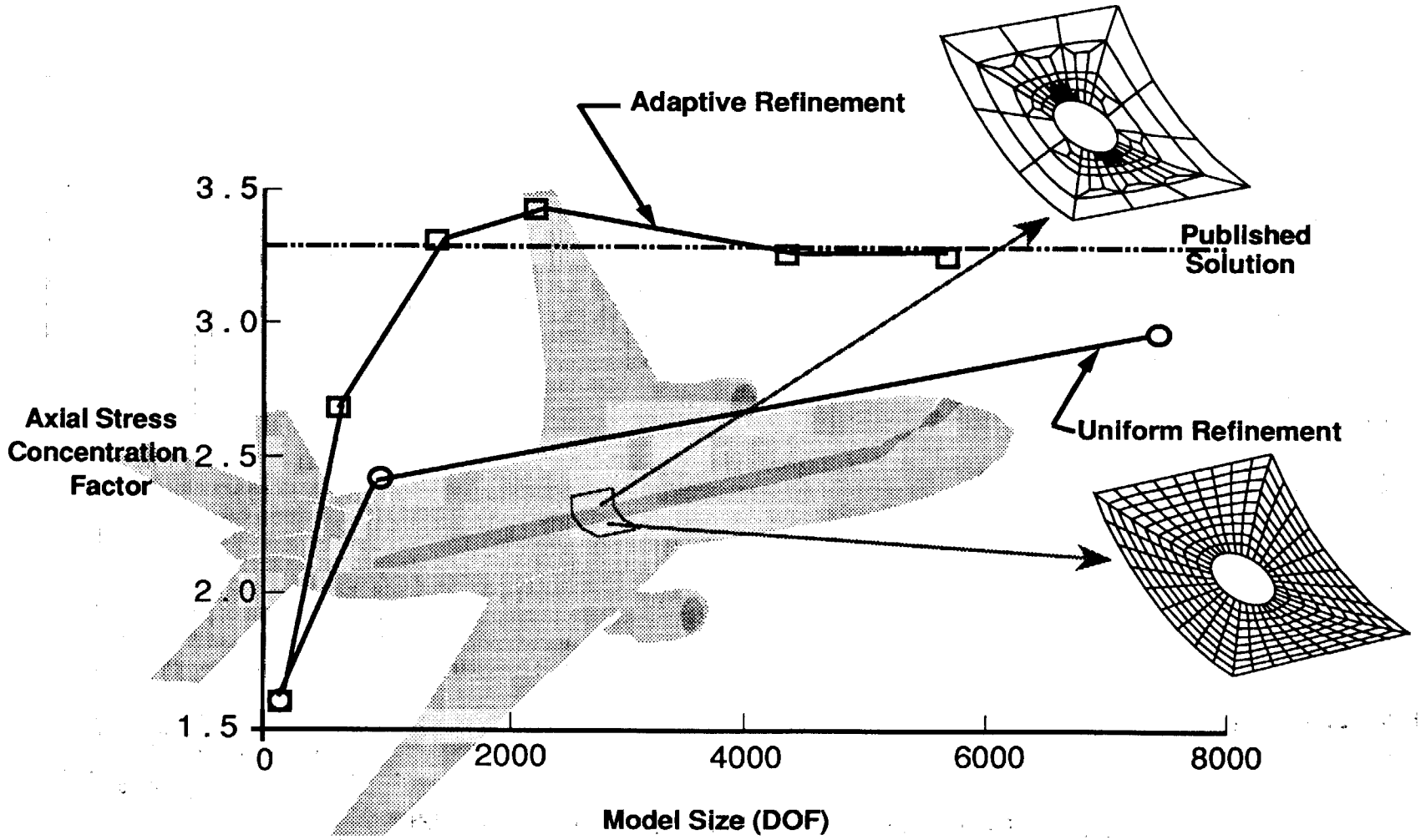


Figure 37b

## SUPERPOSITION ADAPTIVE REFINEMENT TECHNIQUE DEMONSTRATED ON BUILT-UP STRUCTURES

**Research Objective:** Using adaptive mesh superposition refinement technique, develop robust modeling capabilities for realistic built-up aerospace structures.

**Approach:** Automatic adaptive mesh refinement techniques are being developed to reduce the modeling effort of structural engineers and designers and to produce more accurate and detailed structural response predictions. A new adaptive mesh superposition technique has been developed to avoid distortion of quadrilateral and triangular elements (and their accompanying performance degradation) which usually arise in built-up structural analysis models using conventional automatic meshing techniques. In this method, a regular mesh containing little or no distortion in element shapes is used initially. As depicted in the upper left hand portion of the figure, refinement is done by superimposing a second (and subsequent) regular mesh(es) over the first. Refinement indicators identify where the superimposed finer meshes are to be placed and user selected tolerances indicate the desired solution accuracy. Unlike other adaptive refinement schemes now under development, the superposition-based meshing remains regular during the refinement process, provided the initial mesh is regular. The response of the structure is the sum of the responses of the superimposed meshes.

**Accomplishment:** The adaptive superposition-based refinement is shown applied to an aluminum blade-stiffened compression panel whose blades are discontinuous. Such discontinuities arise in realistic components due to various reasons such as cutouts or frame intersections. The presence of discontinuities generates stress concentrations and it is at these locations that failures usually initiate. This application therefore represents a realistic challenge for an adaptive modeling technique. The lower left-hand portion of the figure shows the initial coarse mesh which is regular in pattern. The lower right-hand portion illustrates the final mesh showing how the automatic meshing has zoomed-in on the stress concentrations caused by the abrupt termination of the stiffeners. A comparison of the color contours on the initial and final meshes indicate the improved resolution of the adaptive refinement. The upper right-hand portion of the figure compares the degrees-of-freedom needed by three different approaches to achieve the same accuracy. The uniform mesh case is used as a baseline. The conventional approach also produces a sequence of meshes with each subsequent one being more refined than the previous one, but the mesh superposition technique does not produce the usual distorted elements and hence, not having to correct for distorted elements, requires considerably fewer degrees-of-freedom.

**Significance:** The superposition-based adaptive refinement technique automatically creates an accurate finite element model for realistic complex aerospace structures. Such modeling refinement is needed for aerospace applications as it will lead to new design and analysis tools to reduce engineering time, thereby allowing lighter-weight design concepts to be readily assessed.

**Future Plans:** Apply superposition technique to large-scale HSCT model.

**Point of Contact:** Jerrold M. Housner, Computational Mechanics Branch, (804) 864-2907

Figure 38a

# SUPERPOSITION ADAPTIVE REFINEMENT TECHNIQUE DEVELOPED FOR BUILT-UP STRUCTURES

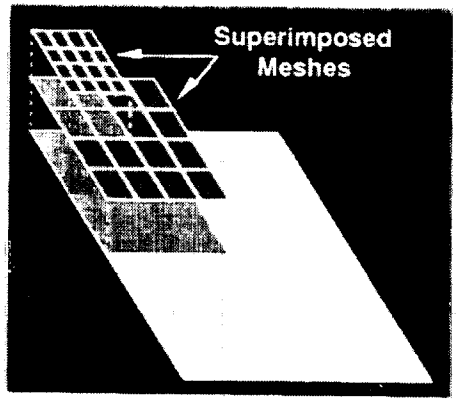


**Superposition Method**

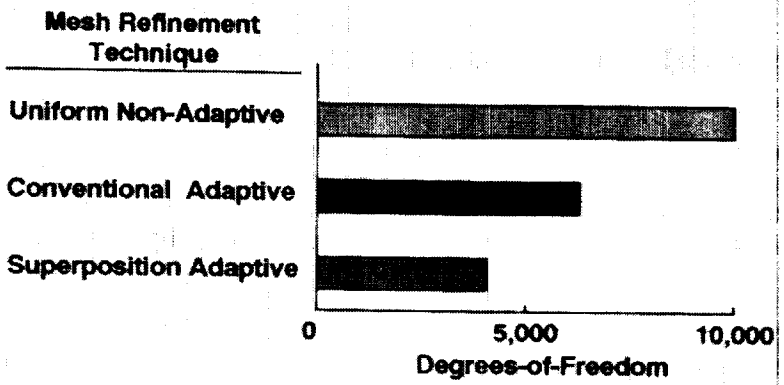


**Modeling Requirements**

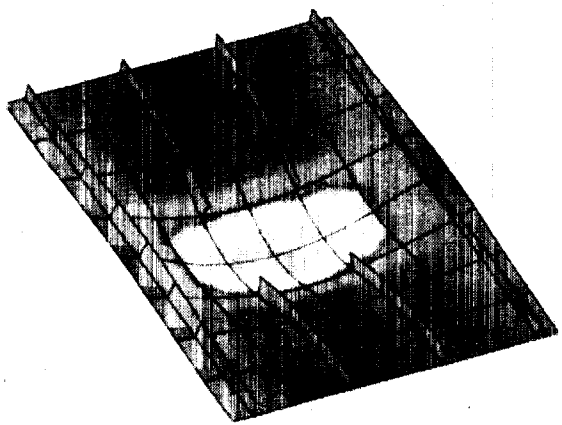

**Initial Mesh**


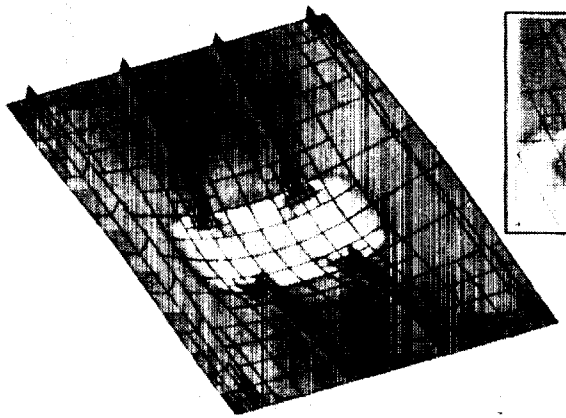

**Final Mesh**

**Compression Panel with Discontinuous Blade Stiffeners**

Figure 38b

## ADVANCED REDUCED-BASIS METHODS REDUCE COMPUTATIONAL REQUIREMENTS FOR LINEAR, TRANSIENT STRUCTURAL ANALYSIS

**Research Objective:** To compare two advanced reduced-basis methods, the force-derivative method (FDM) and the Lanczos method, as well as two widely-used methods, the mode-displacement method (MDM) and the mode-acceleration method (MAM) for solving linear, transient structural analysis problems.

**Approach:** The four reduced-basis methods: the FDM, the Lanczos method, the MDM and the MAM have been implemented on a CONVEX C220 high-performance computer using the COmputational MEchanics Testbed (COMET) as a general purpose finite-element code, and results from these methods have been compared for solutions to linear, transient structural analysis problems. The basis for comparison includes the number of basis vectors required to attain a desired level of accuracy and the associated computational time requirements. The approximate solutions obtained using the reduced-basis methods are also compared to a full-system solution obtained by integrating directly the full system of equations of motion of the system.

**Accomplishment:** The example in the figure is a simply-supported, discretely-damped multispan beam subject to a uniformly distributed load which varies as a quintic function of time. The displacement error norm, $e_u$, defined by the equation in the lower left-hand corner of the figure is used to evaluate quantitatively the accuracy of the approximate solutions relative to the full-system solutions. For purposes of comparison, an error limit of $e_u = 0.01$ has been selected, and the approximate solutions obtained using the reduced-basis methods are considered to be converged when the value of the error norm is equal to or less than this value. A plot of the displacement error norm, $e_u$, as a function of the CPU time in seconds is shown in the figure. The results are presented at time t=1.2 seconds. The horizontal line at a value of $e_u = 10^{-2}$ on the ordinate represents the value of the error limit. As indicated in the figure, the higher-order modal methods converge in approximately one-fourth of the time required for the full-system solution and approximately one-half of the time required for the Lanczos method and the lower-order modal methods.

**Significance:** For the structural problems studied so far, the FDM has been shown to be the most efficient method in terms of the number of basis vectors and the computational time required to provide converged solutions. Reducing the number of basis vectors or degrees-of-freedon can help reduce the cost of structural optimization by taking advantage of sensitivity algorithms specifically developed for problems with relatively few degrees-of-freedom. Since the methods have been implemented in a general-purpose finite element code, their application to larger, more realistic problems can be more easily investigated.

**Future Plans:** The methods will be compared for larger, more realistic problems, and their application to thermal problems will be investigated. The application of the methods to free-free structural vibration problems will also be studied.

**Points of Contact:**
David M. McGowan, Aircraft Structures Branch, (804) 864-4916
Susan W. Bostic, Computational Mechanics Branch, (804) 864-2910

Figure 39a

# ADVANCED REDUCED-BASIS METHODS REDUCE COMPUTATIONAL REQUIREMENTS FOR LINEAR, TRANSIENT STRUCTURAL ANALYSIS

$f(t) = 1000\ (t^4 - t^5)$

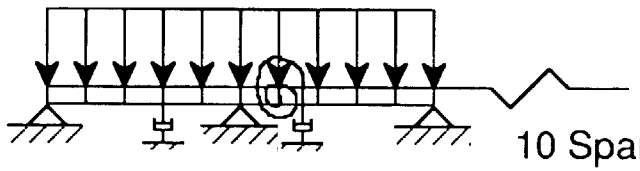

10 Spans

Discretely-damped multispan beam
(91 degrees-of-freedom)

Fundamental frequency = 1.571 Hertz

Solution of full system of equations of motion requires **45.5 CPU** seconds

$$e_u = \sqrt{\frac{(u - u_a)^T (u - u_a)}{u^T u}}$$

where:

u is the full-system solution
$u_a$ is the approximate solution

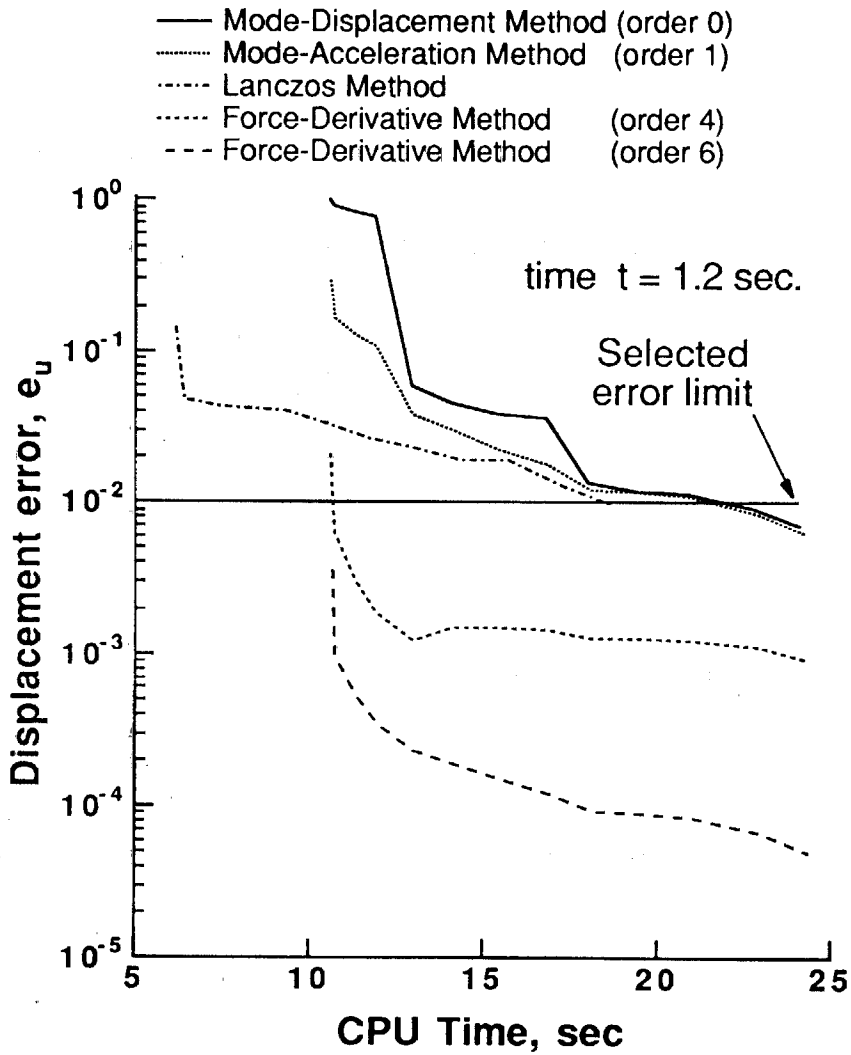


Figure 39b

## POTENTIAL IMPROVEMENT IN ELLIPTIC BOLTED COMPOSITE JOINTS DEMONSTRATED

**Research Objective:** Develop and apply rapid analysis methodology for predicting strength of bolt-loaded elliptical holes in composite joints.

**Approach:** A closed-form solution for bolt-loaded elliptical holes has been formulated based on laminate theory and anisotropic elasticity. Elliptical bolts may be fastened with an attached circular shaft and nut, and elliptic holes in composites may be made using water jet technology. The normal load distribution on the edge of the elliptical hole is represented by a cosine series. Unknown coefficients of the cosine series are determined by a boundary collocation procedure in which the bolt is assumed to be rigid. Bearing and hoop stresses along the loaded edge of the hole are obtained from this very efficient analysis procedure and compared with finite element solutions. Finally, a modified Tsai-Wu failure criterion was used to predict joint failure.

**Accomplishment:** The closed-form solution developed can be used as a rapid bolt joint design tool to efficiently perform parameter studies. Because of the closed-form character of the method, time consuming finite element modeling is avoided. Moreover, the closed-form solution for the bearing and hoop stresses along the loaded edge of the hole agree very well with converged finite element predictions. As is demonstrated in the figure, both analyses predicted that the maximum bearing stress along the hole loaded edge is substantially reduced if an elliptic-shaped bolt is used instead of a circular one. For the elliptical bolt considered in the figure, the reduction is 26 percent. This reduction of normal stress may result in the increase of joint strength and fatigue life. Failure analysis results for two selected joint configurations indicate that a joint designed for a bearing failure critical mode exhibits a 35.0 percent strength improvement while a joint designed for a shearing failure critical mode exhibited a 12.9 percent strength improvement.

**Significance:** With this rapid analysis tool developed, composite joints using elliptical-shaped bolts can be efficiently and accurately analyzed. The feasibility of increasing the joint strength by changing the bolt shape, as demonstrated in this study, may have application at locations where bolt-to-edge distance is insufficient for installing a larger diameter bolt.

**Future Plans:** Develop a hybrid method to couple this local closed-form analysis with global finite element analysis for aircraft structural design applications.

**Point of Contact:** John T. Wang, Computational Mechanics Branch, (804) 864-4818

Figure 40a

# Potential Improvement In Elliptic Bolted Composite Joints Demonstrated

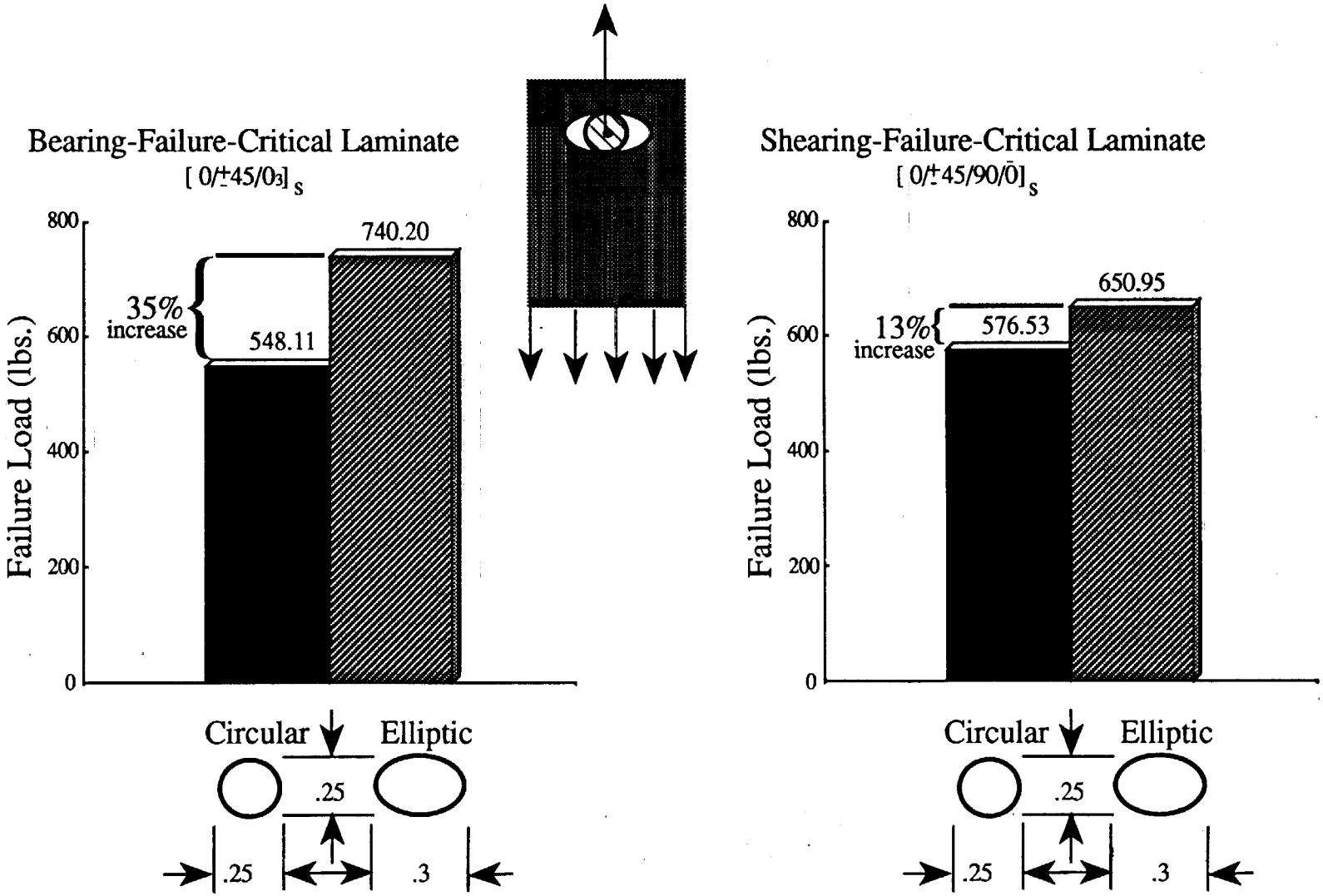


Figure 40b

## NONLINEAR FINITE ELEMENT ANALYSIS ACCURATELY PREDICTS STRAIN IN STIFFENED COMPOSITE WING PANEL

**Research Objective:** Validate and demonstrate the accuracy of nonlinear analysis methods on a realistic aircraft structural composite component for which there are experimental results.

**Approach:** Nonlinear structural analysis techniques were applied to a panel from the lower wing skin of the V-22 tiltrotor aircraft. The panel is made totally of graphite-epoxy composite material and contains design features such as ply drops, ply interleaves, axial stiffeners, transverse ribs, clips, brackets, and a large central elliptical access hole that greatly complicate modeling and analysis. Blueprints and drawings were supplied by Bell Helicopter as well as strain gage and other experimental data. From the blueprints, a very detailed finite element model of the panel was generated. Linear and nonlinear stress analyses were performed using a state-of-the-art finite element formulation and nonlinear solution strategy. First-ply failure techniques were applied to the results of the stress analyses and linear and nonlinear buckling analyses were performed to gain insight into the failure mechanism of the panel.

**Accomplishment:** As in demonstrated in the figure, excellent correlation between the nonlinear stress analysis and the experimental strain gage data was obtained. The nonlinear analysis accurately predicted the highly nonlinear response of the panel, where a traditional linear stress analysis did not. Even with the relatively coarse mesh surrounding the access hole, the finite element formulation (9-node assumed natural-coordinate strain element) accurately predicted the strains in the region. Traditional finite elements would have required a much higher mesh density to achieve a comparable level of accuracy. When a first-ply failure technique was applied to the stresses from the linear and nonlinear results predicted considerably more damage in the vicinity of the hole. The buckling load was only slightly decreased by the including the nonlinear effects since the panel response is globally linear through failure. The local nonlinearities around the cutout had little effect on the global buckling load of the panel.

**Significance:** With accurate finite elements and nonlinear solution strategies, post-buckling response of highly nonlinear structures can be determined. Accurate calculation of stresses and strains are critical to predicting failure modes and improving composite aircraft design.

**Future Plans:** Apply and extend techniques used in this research to progressive failure of laminated and textile composites.

**Point of Contact:** D. Dale Davis, Jr., Vehicle Structures Directorate, Army Research Laboratory (Computational Mechanics Branch), (804) 864-2916

Figure 41a

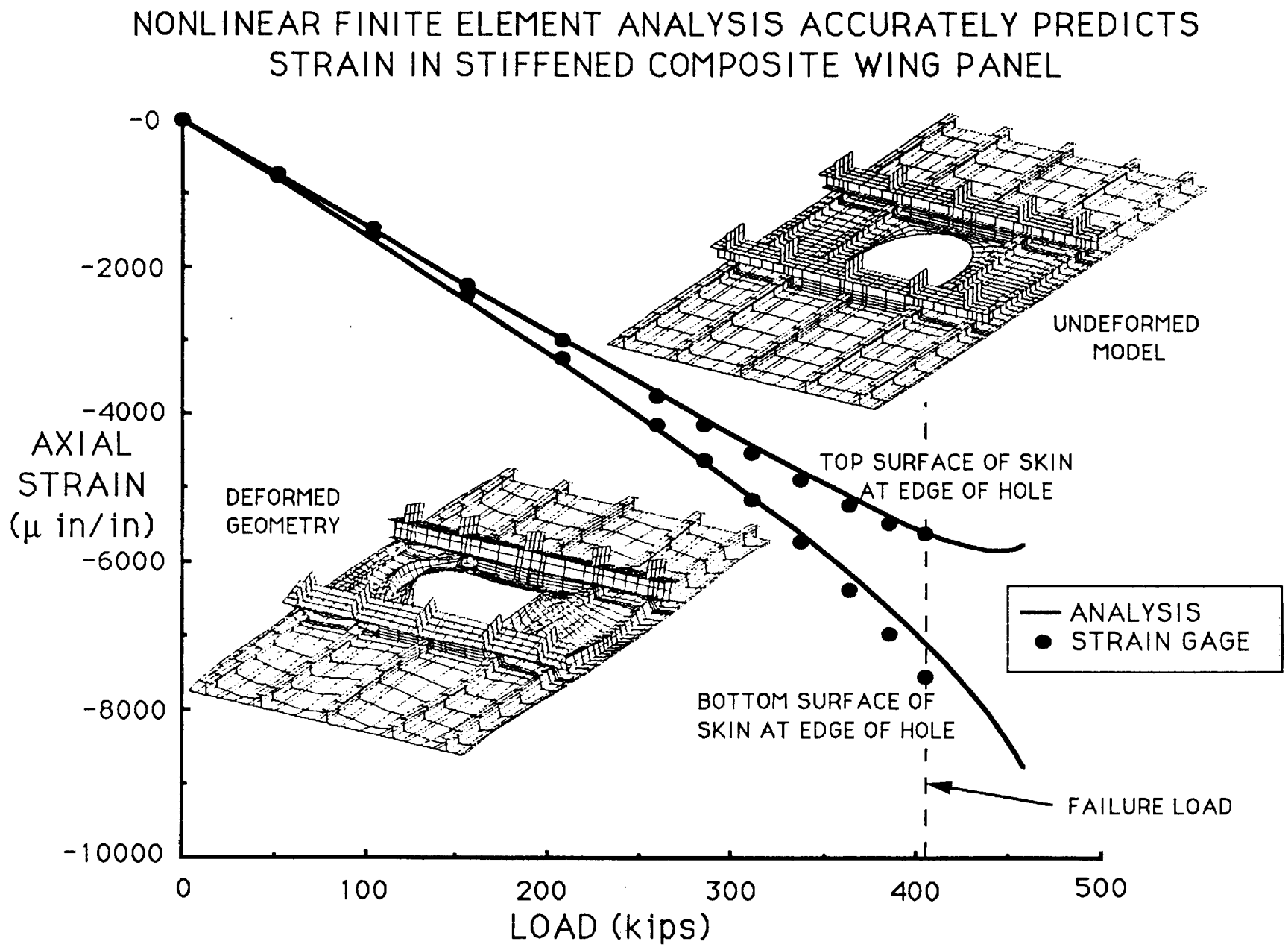
NONLINEAR FINITE ELEMENT ANALYSIS ACCURATELY PREDICTS
STRAIN IN STIFFENED COMPOSITE WING PANEL
-0
-2000
-4000
-6000
-8000
-10000
AXIAL
STRAIN
(μ in/in)
0
100
200
300
400
500
LOAD (kips)
UNDEFORMED
MODEL
DEFORMED
GEOMETRY
TOP SURFACE OF SKIN
AT EDGE OF HOLE
BOTTOM SURFACE OF
SKIN AT EDGE OF HOLE
FAILURE LOAD
ANALYSIS
STRAIN GAGE

Figure 41b

THIS PAGE LEFT INTENTIONALLY BLANK

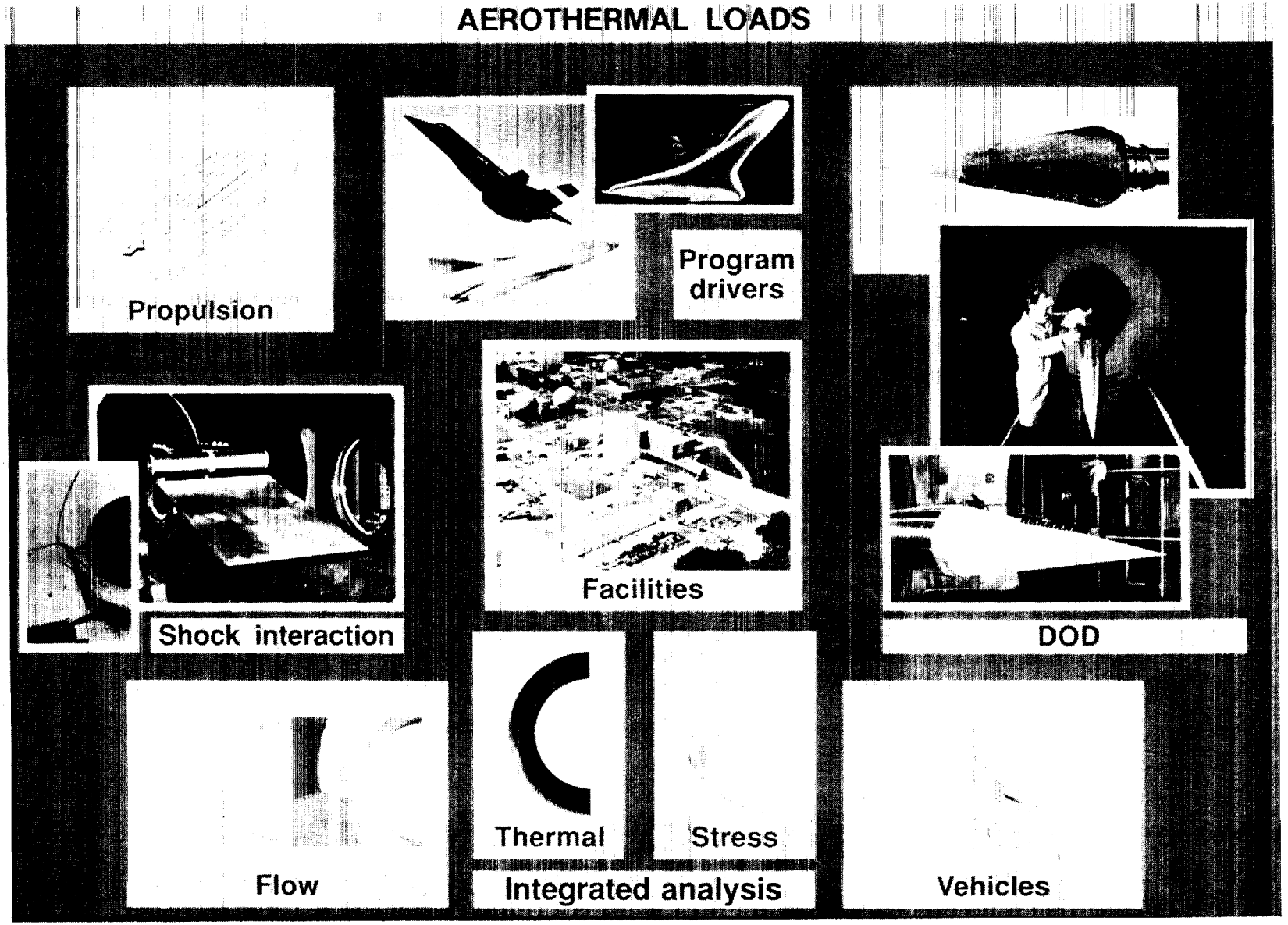


Figure 42

# A P=1 RUNGE-KUTTA DISCONTINUOUS GALERKIN METHOD APPLIED TO TRANSIENT COMPRESSIBLE FLOWS

**Research Objective**: Extend the Runge-Kutta Discontinuous Galerkin (RKDG) method to Euler equations

**Approach**: The RKDG method is a p-Finite Element Method which approximates the solution within an element using a polynomial of degree p. The (p+1)-order accuracy of the method in time and space was previously demonstrated for a scalar conservation law. The method was then extended to the Euler equations of compressible inviscid flow using linear elements (p=1). Several flow problems established that the method is capable of high resolution of discontinuities in the flow field without oscillations. An example of a transient flow problem with complex flow phenomena is illustrated at the top of the figure. A shock wave is moving into still air and intersects a wall that is oriented at an angle to the incident shock. The flow features that develop depend on the speed of the shock wave and the angle of the wall. The flow is self-similar in the sense that the flow pattern has the same shape at any time after the shock intersects the wall. As time progresses, the flow pattern is simply magnified. The density contours of the solution obtained on a uniform 32 X 192 element mesh using the RKDG method with linear elements is shown in the middle of the figure. Density contours which were calculated from interferogram images of experiments of Deschambault and Glass are shown in the bottom of the figure. Comparison of the numerical and experimental flow patterns show that the complex shock structure and slip surface are accurately predicted by the RKDG method.

**Accomplishment**: Successfully extended the RKDG method to Euler equations using p=1 elements and demonstrated its ability to capture complex flow features.

**Significance**: This work represents an important first step in the development of an adaptive p-Finite Element method for compressible viscous flows.

**Future Plans**: Extend the RKDG method to elements with p>1 for Euler equations. Include the capability to adaptively select the degree of the ploynomial approximation in an element. Extend the RKDG method to Navier-Stokes equations.

**Point of Contact:** Kim S. Bey, Aerothermal Loads Branch, (804) 864-1351

Figure 43a

# A P=1 RUNGE-KUTTA DISCONTINUOUS GALERKIN METHOD APPLIED TO TRANSIENT COMPRESSIBLE FLOW

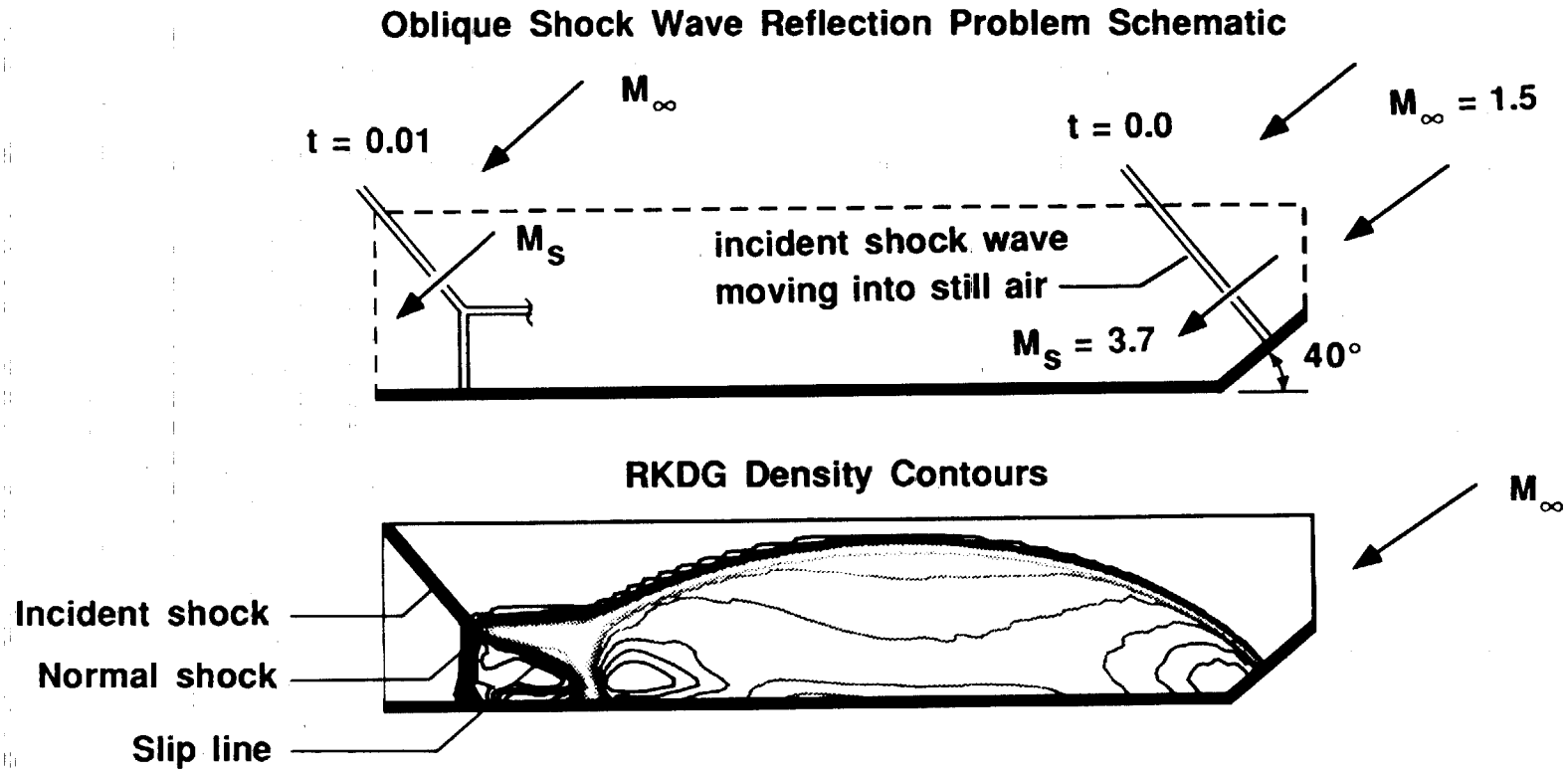


Figure 43b

# ADAPTIVE UNSTRUCTURED MESHING DEMONSTRATED FOR THERMAL STRESS ANALYSIS OF BUILT-UP STRUCTURES

**Research Objective:** Develop an adaptive unstructured meshing technique for thermal stress analysis of built-up structures.

**Approach:** An adaptive unstructured remeshing technique is combined with a finite element thermal stress analysis algorithm. The temperature and the Von Mises stress are selected as the key parameters, $\phi$, for constructing an adaptive mesh. At a typical node in an earlier mesh, the second derivatives, $\phi''$, of the two key parameters are computed. The higher quantity is selected to determine a new nodal spacing, h, for an adaptive mesh based on the equidistribution principle of error, $|\phi''|\, h^2 = |\phi''|_{max}\, h^2_{min}$, where $|\phi''|_{max}$ is the maximum absolute second derivative for the entire computational domain and $h_{min}$ is the specified minimum nodal spacing. Triangular membrane elements and triangular discrete Kirchoff bending elements are used in the adaptive unstructured mesh for predicting deformations and thermal stresses.

**Accomplishment:** The method is demonstrated by the thermal stress analysis of a representative scramjet engine inlet panel section. The structure experiences nonuniform heat transfer rates due to the interaction of planar shocks generated from the strut and cowl leading edges (top left figure). A portion of the structure consisting of intersecting panels and stiffeners is first discretized by a uniform finite element mesh (top right figure). Temperatures that vary quadratically from 700 °R at the centers of the two "hot spots" to 50 °R in the regions away from the two hot spots are prescribed. With this mesh, a thermal stress analysis is performed to provide a thermal stress solution. Using the adaptive remeshing procedure described earlier, a new adaptive mesh is constructed as shown in the lower left figure with cutouts to highlight the finite element discretization on the stiffeners. The new mesh has small elements in the high thermal stress regions to increase accuracy and larger elements in other regions to reduce the problem size and thus computational effort. The figure also shows that triangles provide smooth mesh transition from fine to coarse mesh regions which will further provide a more accurate stress distribution. The predicted thermal stress contours are superimposed on the deformed geometry in the right figure and the enlargement in the center which shows the details in the vicinity of the hot spots. As expected, the high localized temperatures result in compressive stresses (-25 ksi) at the two hot spots which causes the panels to expand and bend out of plane. In addition, a much higher tensile stress (+54 ksi) appears at the panel intersection to maintain equilibrium. If such high stress gradient regions are not anticipated prior to analyzing the problem, conventional meshing procedures would be inadequate, where as the adaptive unstructured meshing procedure will construct a minimum mesh size with good accuracy.

**Significance:** The adaptive unstructured meshing technique improves the solution accuracy and analysis efficiency without a priori knowledge of the solution.

**Future Plans:** Extend the adaptive unstructured meshing technique to thermal analysis in order to achieve a fully integrated thermal-structural analysis capability for built-up structures.

**Point of Contact:** Allan R. Wieting, Aerothermal Loads Branch, (804) 864-1359

Figure 44a

# ADAPTIVE UNSTRUCTURED MESHING DEMONSTRATED FOR THERMAL STRESS ANALYSIS OF BUILT-UP STRUCTURES

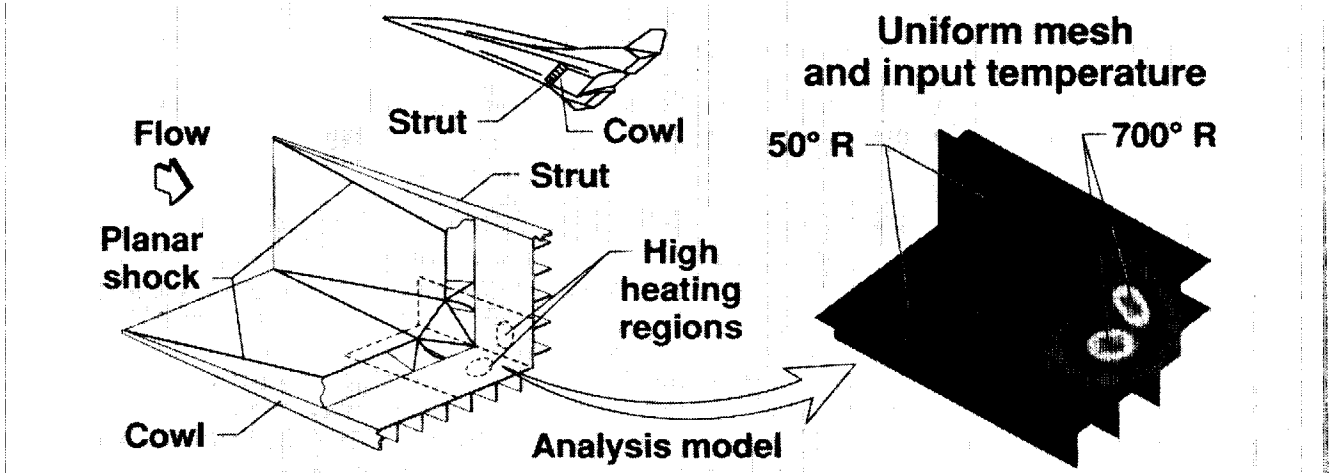


Adaptive mesh and computed longitudinal stress distribution

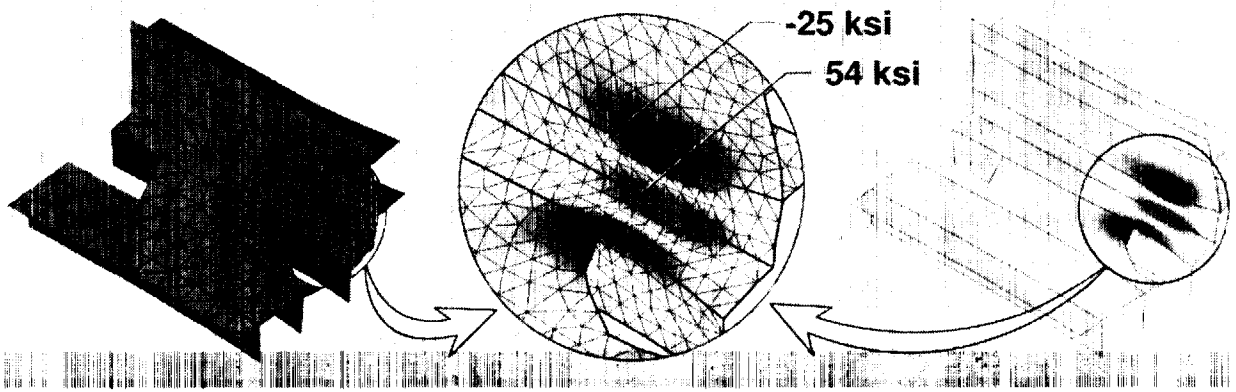


Figure 44b

# TRANSIENT ADAPTIVE MESHING IMPROVES ACCURACY AND EFFICIENCY OF PLATE THERMAL ANALYSIS

**Research Objective:** Develop an adaptive unstructured meshing technique for transient thermal analysis.

**Approach:** An adaptive unstructured remeshing technique is combined with a finite element thermal analysis algorithm. During the transient analysis process, the second derivatives of the temperature at the nodes throughout the computational domain are computed. The regions with the second derivatives that are higher than a specified threshold are reconstructed with finer or coarser elements according to the computed second derivatives. In the other regions, the meshes are untouched. The technique also places refined elements along the domain boundary to provide an accurate definition of the heating rate distribution. The accurate input of the heating rate distribution combined with the refined elements in the region near the heat source provides the increased accuracy of the method. The only a priori knowledge required is the speed at which the heat source moves, as this information is used to set the remesh interval.

**Accomplishment:** The efficiency and accuracy of the method is demonstrated by the transient thermal analysis of a plate subjected to a moving heat source. The simplified plate model (top figure) has an exact transient temperature solution that is used to determine solution accuracy. A standard graded structured mesh is used to assess solution efficiency. The plate is subjected to a square heat pulse of 50,000 Btu/ft$^2$-sec which translates at a speed of 2 in/sec from the left end to the right end of a one-inch-long plate. The temperature of the underside of the plate is fixed at 0 °F. The peak predicted temperature along the top surface of the plate is within 2% of the exact solution as shown in the left figure. This solution was obtained with the standard nonadaptive structured mesh that required 5,200 nodes and 9,400 CPU second as shown in the centered right figure. A solution of equivalent accuracy was achieved on a 200 node transient adaptive mesh that required 300 CPU second as shown in the top and the lower right figures. Both the standard nonadaptive structured mesh and the adaptive unstructured mesh provide an equivalent temperature solution accuracy within the plate as shown by the temperature contours in the right figures. Hence, the new method required 1/25th the number of nodes and 1/30th the number of CPU seconds.

**Significance:** The transient adaptive meshing technique significantly improves the solution accuracy and analysis efficiency compared to the standard finite element modelling technique with nonadaptive structured meshes.

**Future Plan:** Extend the adaptive unstructured meshing technique to both transient thermal and structural analyses of two- and three-dimensional structures subjected to time-dependent thermal and mechanical loadings.

**Point of Contact:** Allan R. Wieting, Aerothermal Loads Branch, (804) 864-1359

Figure 45a

# TRANSIENT ADAPTIVE MESHING IMPROVES ACCURACY AND EFFICIENCY OF PLATE THERMAL ANALYSIS

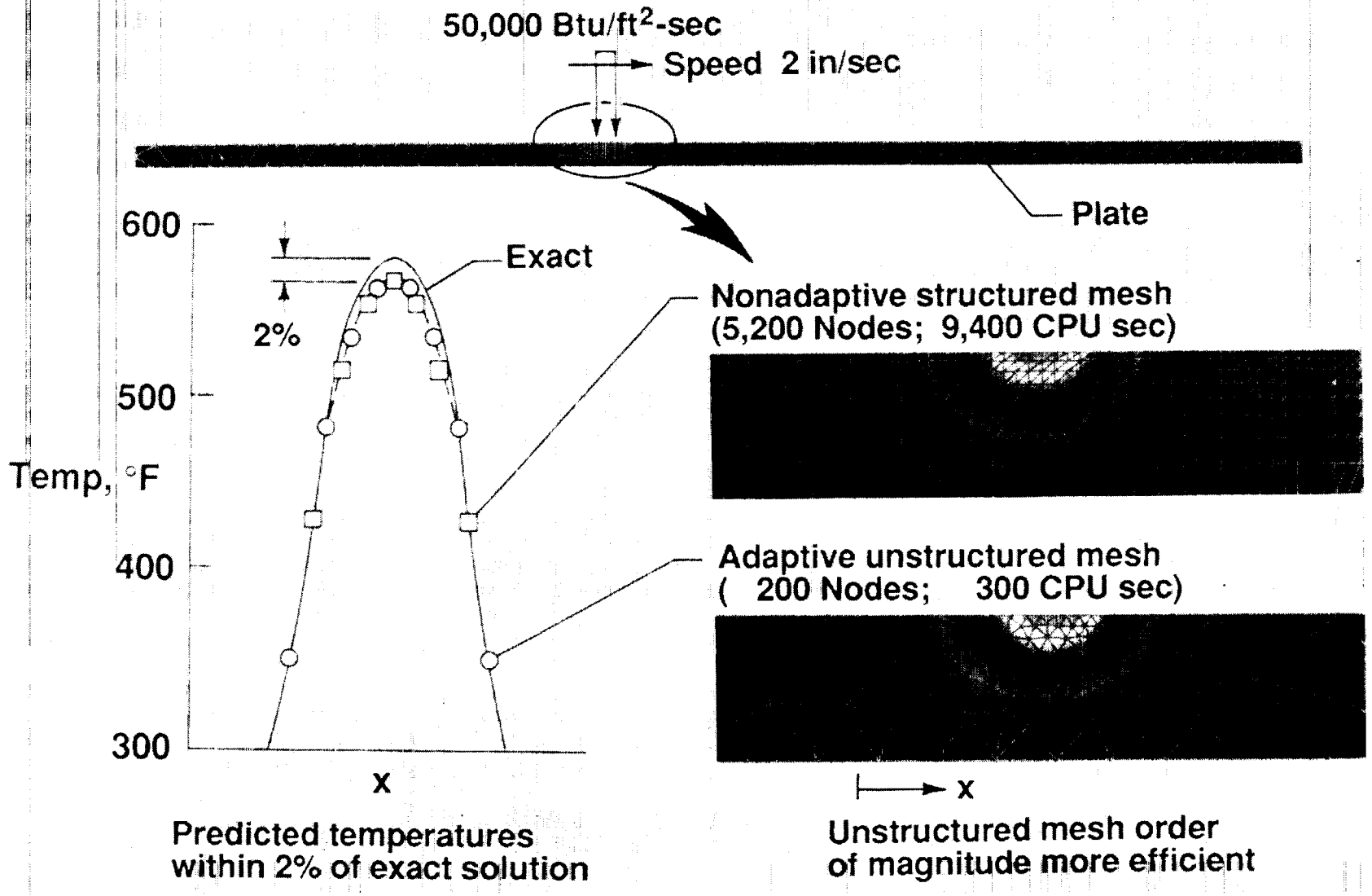


Figure 45b

## NEW SHOCK-SHOCK INTERFERENCE PATTERN IDENTIFIED CONCOMITANT SUPERSONIC JETS

**Research Objective**: Experimentally define the shock-shock interference patterns created by multiple oblique shock waves emanating from vehicle compression surfaces intersecting the bow shock wave of a cylindrical engine-cowl leading-edge. Define the heat transfer rate and pressure distribution associated with the shock-shock interference pattern.

**Approach**: The vehicle compression surfaces were simulated with a sharp leading edge 7.5° wedge, and interchangeable 5° or 6° wedges, which were mounted approximately 21 inches downstream of the leading edge of the first wedge. The 5° or 6° wedge was translated along the surface of the first wedge and the cylinder was translated horizontally or vertically to obtain different patterns. The experiments were in the Calspan 48-Inch Hypersonic Shock Tunnel at a Mach number of 8.0, total temperatures of 2800 °R, free stream unit Reynolds number of 1.5 x 106 per foot. The shock-shock interference patterns were determined analytically by constructing pressure deflection diagrams, that are based on oblique shock theory. A new shock-shock interference pattern consisting of concomitant supersonic jets was discovered. The predicted pattern is scribed on the schlieren photograph of the pattern in the figure. The first oblique shock wave intersects the bow shock wave creating the upper supersonic jet and the second oblique shock wave intersects the transmitted shock wave from the first intersection creating the second supersonic jet. The supersonic jets are separated from each other by a shear layer and from the subsonic flow by shear layers. The heat transfer rate distribution on the cylinder is compared with that for coalesced oblique shock waves in the right figure. The latter pattern is created when the two oblique shock waves coalesce at the bow shock wave intersection point and create a single supersonic jet. The heat transfer rate for the single jet is approximately twice that of the concomitant jets.



**Accomplishment**: Provided detailed heat transfer rate and pressure distributions on a cylinder for two-dimensional shock wave interference created by two incident oblique shock waves intersecting the cylinder bow shock wave. The peak heat transfer rate and pressure amplifications occur when the two incident shock waves coalesced before intersecting the cylinder bow shock wave. A new interference pattern, which consisted of two supersonic jets separated by a shear layer, was identified.

**Significance**: Provided first multiple shock-shock interference heat transfer rate and pressure data for the thermal structural design of engine cowl leading edges. Defined the interference patterns critical to understanding the fundamental fluid mechanics behind the aerothermal loads.

**Future Plans**: This experimental data base will be used in CFD code theory/test correlation activities.

**Point of Contact:** Allan R. Wieting, Aerothermal Loads Branch, (804) 864-1359

Figure 46a

# NEW SHOCK-SHOCK INTERFERENCE PATTERN IDENTIFIED
# CONCOMITANT SUPERSONIC JETS

**Shock-Shock Interference Pattern**

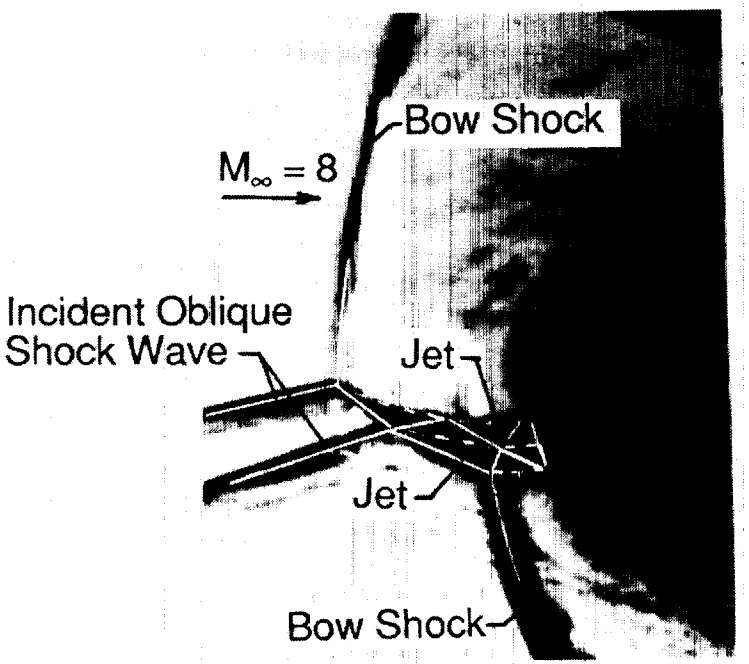


**Heat Transfer Rate Distribution**

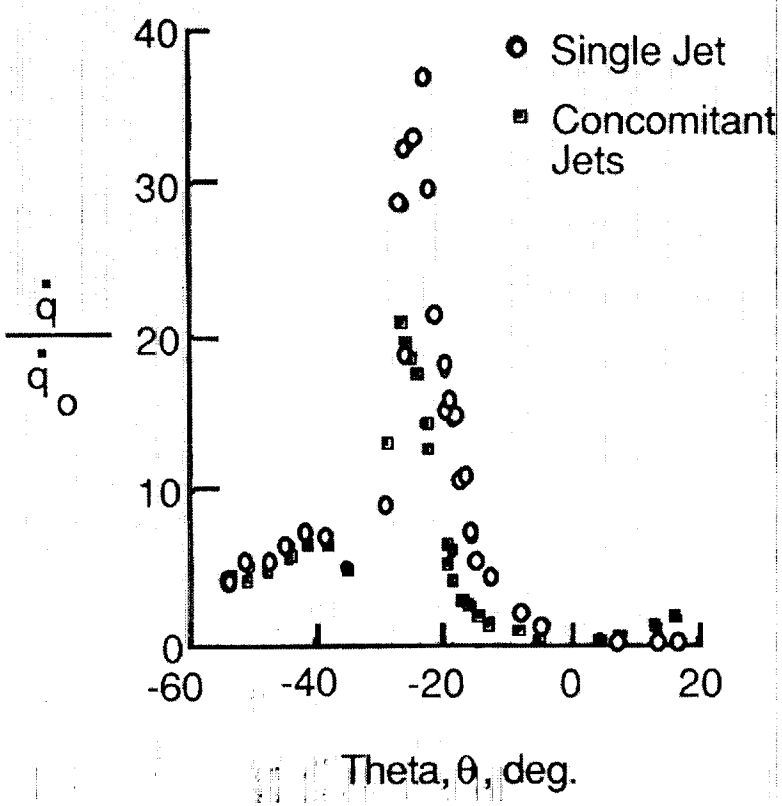


Figure 46b

## BLUFF AIRFOIL SHAPED FUEL INJECTOR IS EXCEPTIONALLY QUIET AND PROVIDES STABLE COMBUSTION

**Research Objective**: Develop and verify a stable methane injector for the LaRC 8-Foot High Temperature Tunnel (8' HTT) to operate in air or oxygen enriched air. Operation is over a pressure range of 200 to 4000 psia and a temperature range of 1500 to 4000 °R.

**Approach**: To test full scale injector segment in the Combustion Heated Test Facility (CHTF) combustion chamber, which is 1/4 the diameter of the 8' HTT combustor. The CHTF installation and salient features of the injector are shown on the left of the figure. The mixing and damping plate insures a homogeneous mixture of air and oxygen and decouples the supply and the combustion zones. The fuel manifold and bluff airfoil shaped injectors are streamlined to reduce turbulence and vortical flow . The fuel injectors incorporate a dual fuel plenum separated by a high pressure loss transfer slot to decouple the fuel delivery from the combustion dynamics. The short length fuel orifice keeps the Reynold's number of the fuel exit relatively low which enhances combustion stability. These features combined with a fuel velocity of between 400 to 600 ft/s create a stable detached flame that maintains the surface temperature below 800 °R.



**Accomplishment**: Developed an exceptionally stable methane injector system. The injector was operated to over a fuel equivalency range of 0.05 (lean) to 3 (rich). The peak pressure fluctuations were +/-1 psi (0.4%). The spectra was broadband with a spectral peak 4 orders of magnitude smaller than that of the existing 8' HTT combustor. This spectra approaches that of an ideal combustor and is rarely achieved.

**Significance**: This fuel injector provides a broad operation envelope. Demonstrated range varies from atmospheric to 2000 psia and temperatures from 900 °R to 4700 °R in methane/air and methane/air/oxygen mode. The low surface temperature will provide a long life. Operation over a wide range of fuel equivalency ratio reduces flameout possibility and enhances options to introduce O2 downstream of the main combustion zone. The latter provides a less sensitive mixture that reduces the risk of a deflagration to detonation transition.

**Future**: The use of the injector in the fuel rich mode would require further testing to verify complete mixing of the O2 with the combustion products for application in the 8' HTT. Design and fabrication of an injector for the 8' HTT is planned.

**Point of Contact:** Richard L. Puster, Aerothermal Loads Branch, (804) 864-1390

Figure 47a

# BLUFF AIRFOIL SHAPED INJECTOR IS EXCEPTIONALLY QUIET AND PROVIDES STABLE COMBUSTION

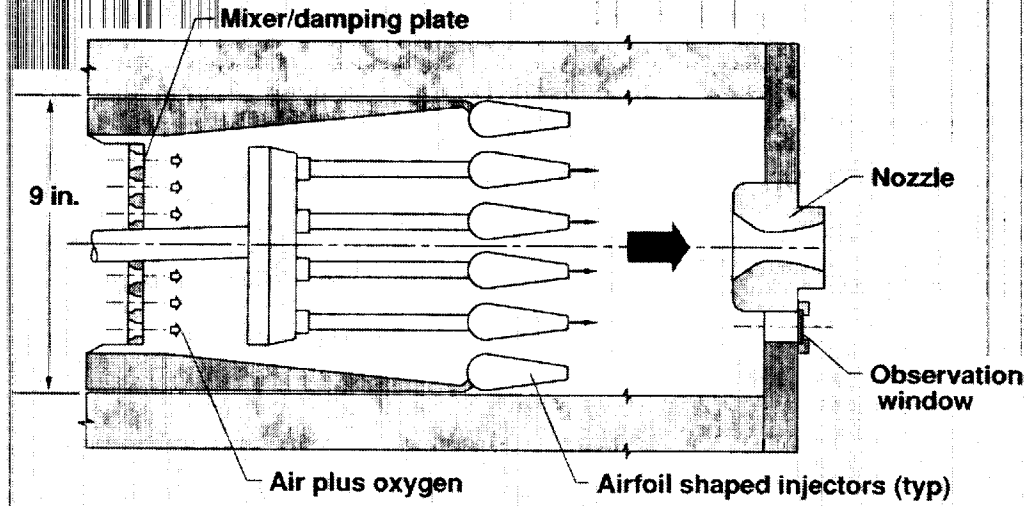


**Injector Installation**

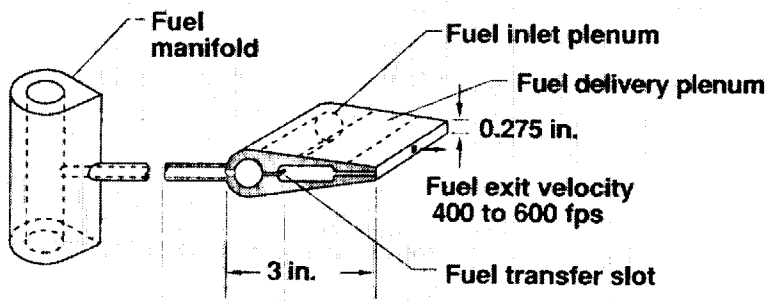


**Detail of Airfoil Injector**

## Fuel Injector

- Mixer/damping plate decoupled air/oxygen supply and combustor
- Streamlined components: low turbulence and vorticity
- Dual plenum fuel supply: decoupled fuel and combustor
- Operates over fuel equivalent ratio of 0.05 to 3.0: probability of flameout remote
- Pressure flucuation less than o.4%: stable
- Surface temperature less than 800 R: long life



Figure 47b

## COMPUTATIONS SHOW FLUID SPIKE EFFECTIVE IN REDUCING SHOCK-SHOCK INTERFERENCE HEATING ON A CYLINDRICAL LEADING EDGE

**Research Objective:** To assess qualitatively the effectiveness of a Mach 3 fluid spike in reducing the peak pressure and thermal loads due to a Type IV shock-shock interference on a 1/8 inch cylindrical body representing a leading edge of a hypersonic vehicle at a freestream Mach number of 8.

**Approach:** Computations are made using the set of computer codes Langley Adaptive Remeshing Code and NaviEr Stokes Solver (LARCNESS). Adaptively generated unstructured meshes are employed. Flowfields are computed for a freestream Mach number of 8 and an impinging shock generated by a 12.5 deg. wedge. Mach number in the fluid spike is 3, and the momentum ratio ($\rho_j u_j^2 w_j / \rho_\infty u_\infty^2 r$) is 0.253, where $\rho$ = density, u = velocity, j = fluid spike, $\infty$ = free stream, w = fluid spike orifice (0.005 inches), r = leading edge radius (0.125 inches). Two different locations ($\theta$ = 0 and -20 deg. on the leading edge) were considered for the fluid spike. The angle $\theta$ = -20 deg. on the leading edge corresponds to the location for peak heat-flux for a Type IV shock-shock interference in the absence of a fluid spike. Pressure and heat-flux distributions on the body with and without the fluid spike were compared.

**Accomplishment:** The fluid spike is found to displace the bow shock in front of the body, and modify the flowfield significantly as shown by the temperature contour plots in the figure. The peak pressure and heat-flux amplifications resulting from a Type IV supersonic jet shock-shock interference are reduced. The peak pressure amplification decreased from 8 to 4.5, and the corresponding peak heat-flux amplification decreased from 12 to 4.5 as shown in the figure. The secondary peak heat flux around $\theta$ = 0 degree on the cylinder is due to the entrainment of hot gases by the jet. The presence of the fluid spike altered the Type IV supersonic jet to a Type III shear layer and resulted in reduced heat flux on the surface. Similar results were obtained for the two locations of the fluid spike investigated ($\theta$ = 0 and -20 deg.).

**Significance:** The peak thermal load due to a Type IV shock-shock interference is very high and poses a serious problem in the design of leading edges of hypersonic atmospheric flight vehicles. Several methods, including swept leading edges and transpiration cooling, have been investigated in the past to reduce these thermal loads with limited success. The fluid spike presents an alternate method for this purpose. Computational results from the present qualitative study have provided encouraging results, and indicate that the fluid spike can be an effective device for the protection of leading edges from extreme thermal loads.

**Future Plans:** Make further computational studies to optimize the fluid spike configuration (location, orientation and number of fluid spikes on the leading edge, and the Mach number, mass and the momentum ratios in the fluid spike), and to determine quantitatively the reduction in maximum heat flux. Experimentally verify computational results and investigate the effect of a liquid fluid spike.

**Point of Contact:** Allan R. Wieting, Aerothermal Loads Branch, (804) 864-1359

Figure 48a

# FLUID SPIKE REDUCES PEAK SHOCK-SHOCK INTERFERENCE HEAT FLUX

TEMPERATURE CONTOURS

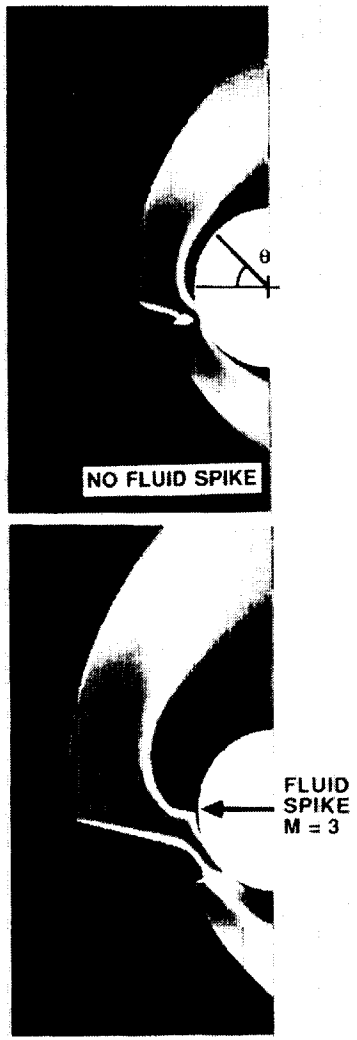


HEAT FLUX DISTRIBUTION ON THE CYLINDER

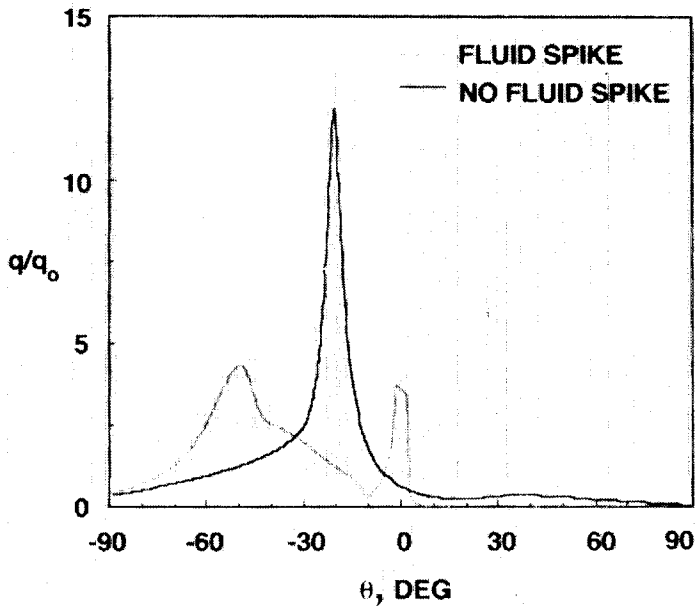


$q_o$ = UNDISTURBED STAGNATION POINT HEAT FLUX

Figure 48b

THIS PAGE LEFT INTENTIONALLY BLANK

# AIRCRAFT STRUCTURES RESEARCH

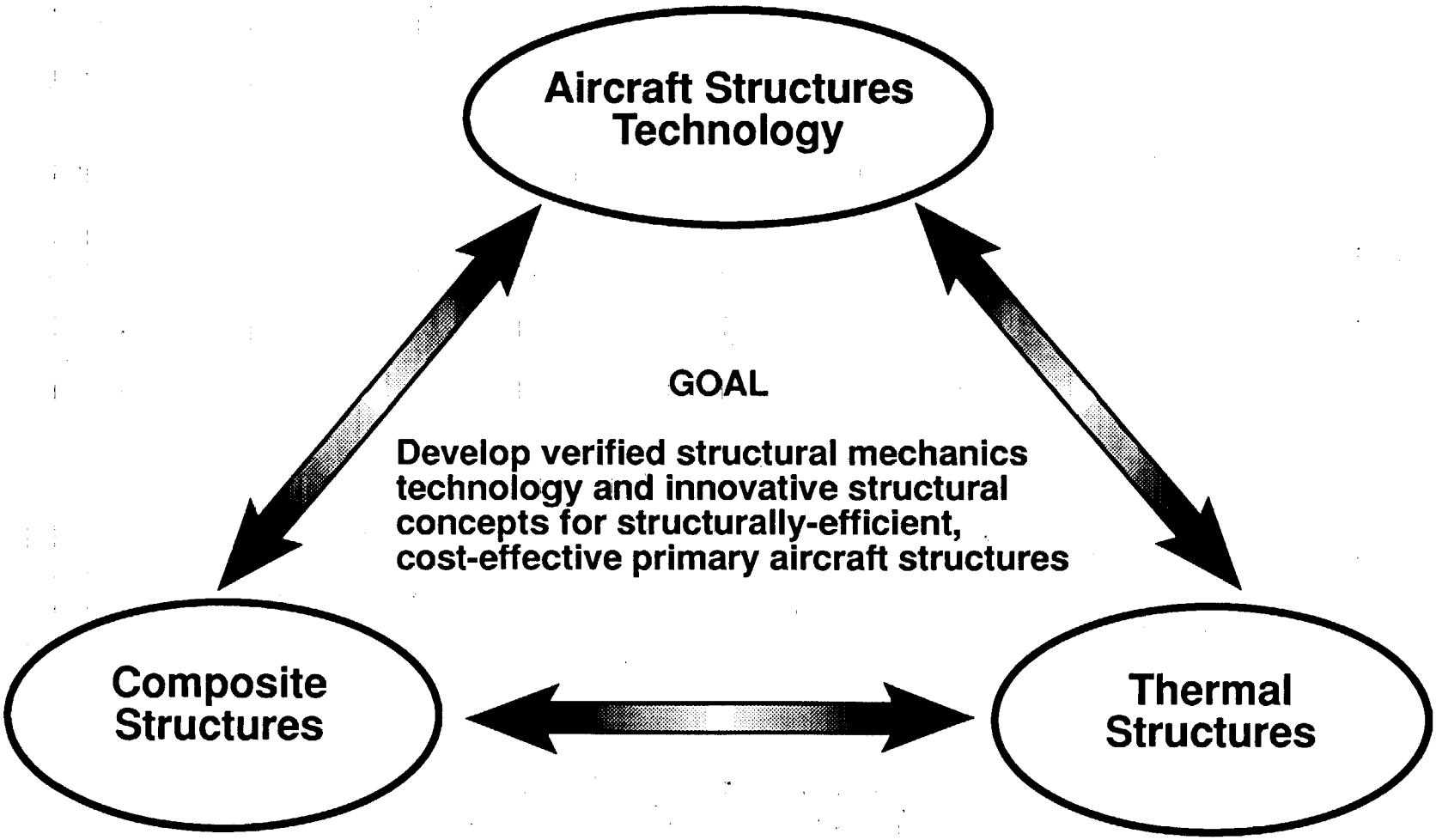


Figure 49

# Composite Structures

## Objective

**Develop advanced structural concepts and verified structural mechanics and design technologies for structurally-efficient, damage-tolerant advanced composite wing and fuselage structural components subjected to mechanical, pressure, and thermal loads**

## FY93 Approach

- Develop analysis, improve designs, and conduct experiments to determine the failure characteristics and damage tolerance of composite panels with stiffness discontinuities
- Develop analysis validated by experiments for predicting the damage resistance of composite laminates
- Conduct analyses and experiments for thin impact-damaged panels subjected to tensile and pressure loadings
- Determine bending gradient attenuation for anisotropic and orthotropic composite shells

## Key Milestones:

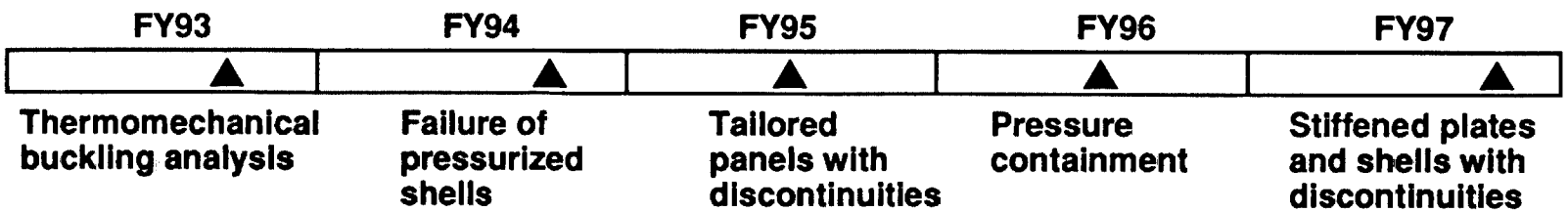


Figure 50

# Thermal Structures

## Objective

**Develop light-weight structural concepts and verified structural analysis and sizing methods that predict the structural and thermal response of airframe structures subjected to elevated temperatures**

## FY93 Approach

- Develop parameter estimation technique to predict thermal contact resistance of heat pipes imbedded within carbon-carbon
- Complete room temperature testing of carbon-carbon elevon
- Develop thin-film heater for very high local heating to a convectively cooled specimen

## Key Milestones:

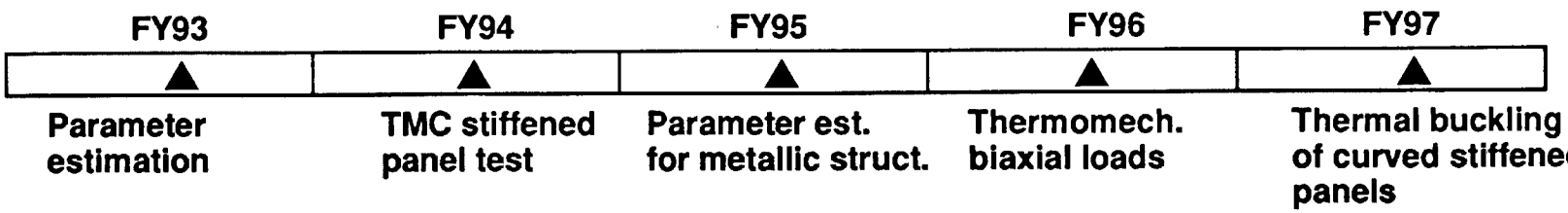


Figure 51

# Aircraft Structures Technology

## Objective

**Develop enabling structural mechanics technology for transport aircraft structures including advanced designs for composite and metallic structures, verified analyses, verified analyses, structural integrity, and failure prediction**

## FY93 Approach

- Install and complete operational check-out of pressure box test fixture
- Complete design and analysis of COLTS and D-Box test fixture
- Complete nonlinear analysis of stiffened fuselage shell with longitudinal cracks and subjected to internal pressure and bending loads
- Develop prototype nonlinear stiffened shell analysis for determing residual strength of structures with long cracks
- Conduct tests for damage tolerant composite sandwich panels subjected to compressive loading
- Develop bonded- and bolted-joint concepts for high speed civil transports

## Key Milestones:

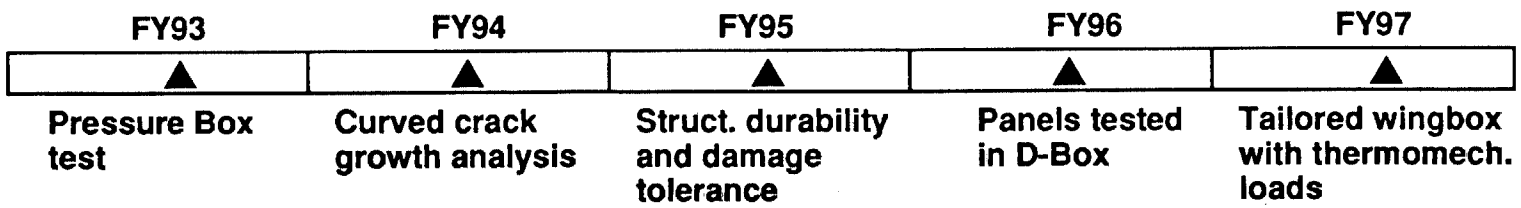


Figure 52

# SPACECRAFT STRUCTURES RESEARCH

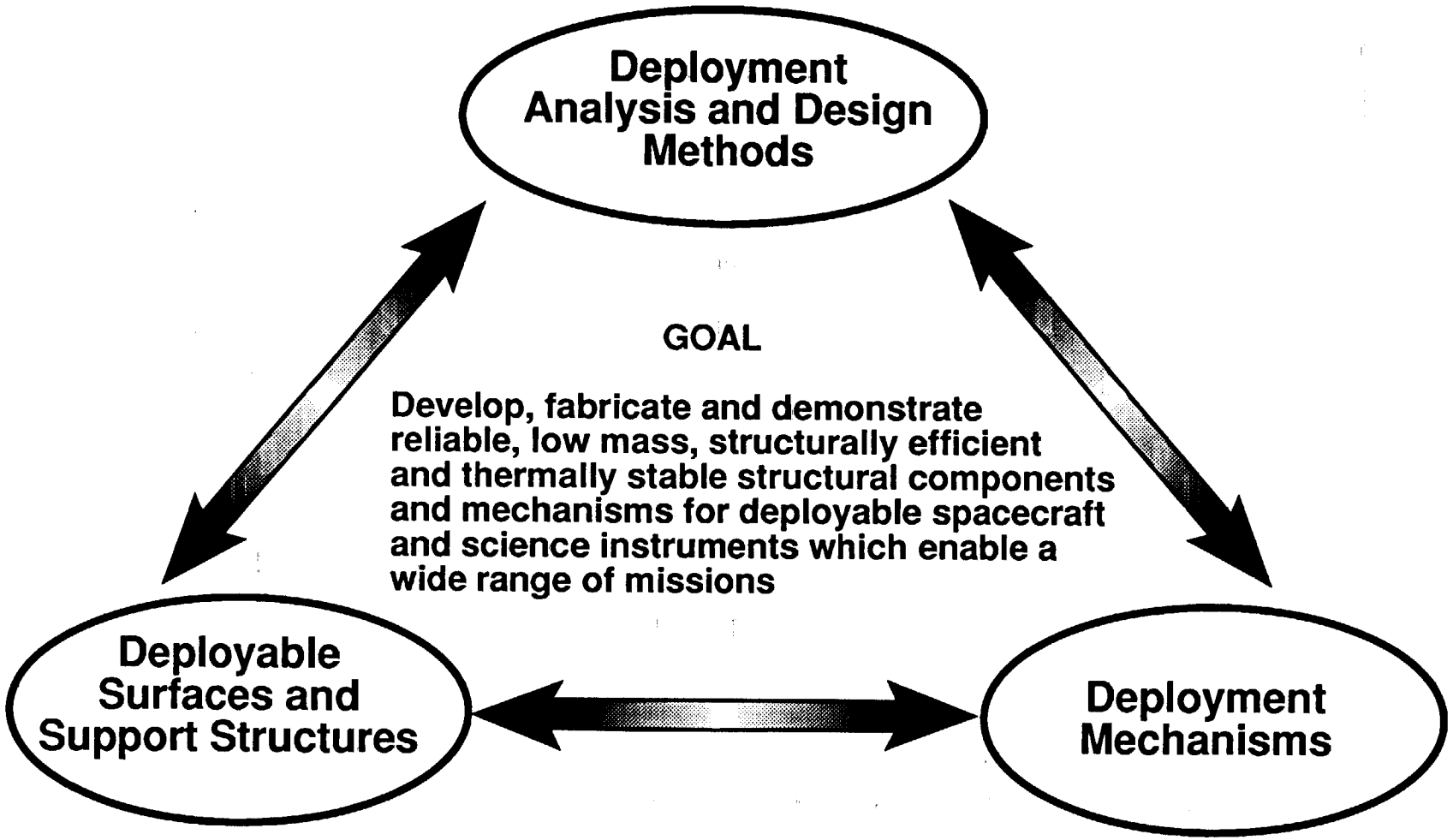


Figure 53

# Deployment Analysis and Design Methods

## Objective

**Develop analysis and design methods for identification of efficient, predictable, structural configurations for low mass, precision spacecraft components**

## FY93 Approach

- Acquire and evaluate time-accurate finite-element structural analysis method
- Initiate development of sensitivity analysis method for membrane reflectors

## Key Milestones:

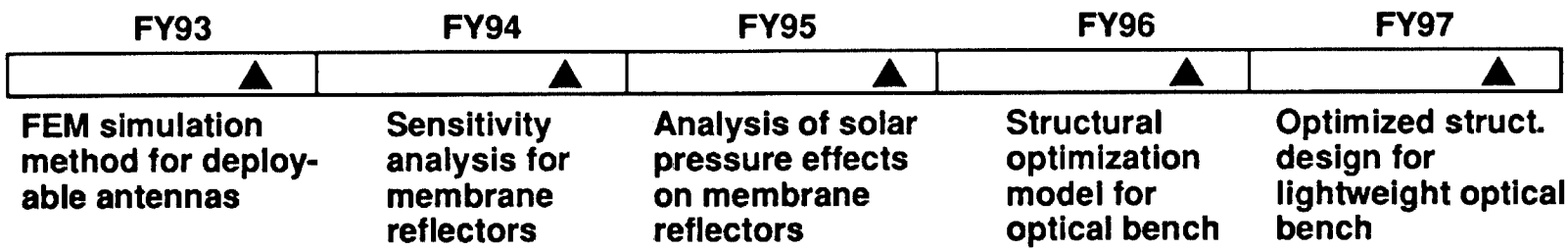


Figure 54

# Deployment Mechanisms

## Objective

**Design, fabricate and test kinematic and actuator mechanisms for low-mass, precision, deployable truss-supported reflectors**

## FY93 Approach

- Develop designs of deployment mechanisms for seven panel reflector
- Initiate design of linear, preloaded low friction revolute joints

## Key Milestones:

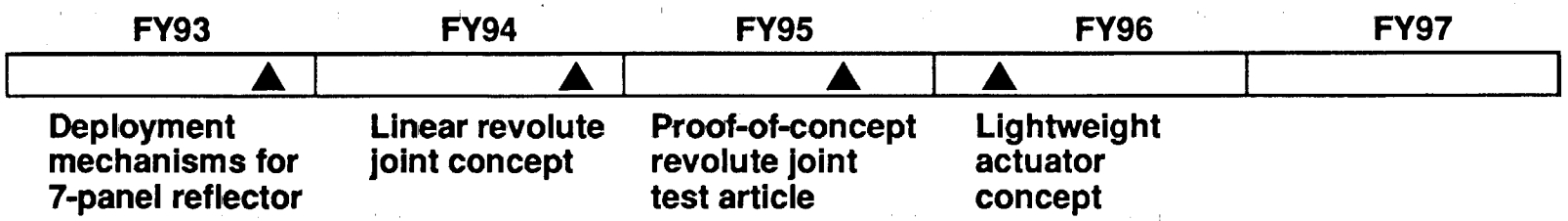


Figure 55

# Deployable Surfaces and Support Structures

## Objective

**Design, fabricate and demonstrate low mass, deployable and adaptive, surface panels and truss support structures for accurate position control and compact packaging**

## FY93 Approach

- Complete documentation of ASAL research program
- Complete documentation of erectable antenna research program
- Initiate development of sructural design concept for feed structure
- Initiate development of integrated panel design for test article

## Key Milestones:

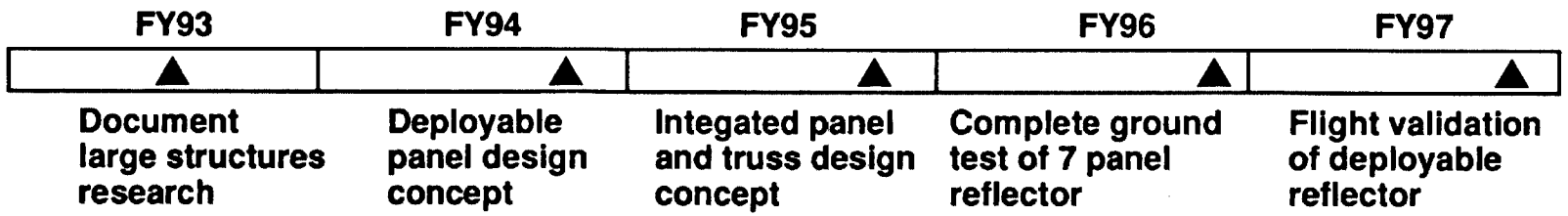


Figure 56

# COMPUTATIONAL MECHANICS RESEARCH

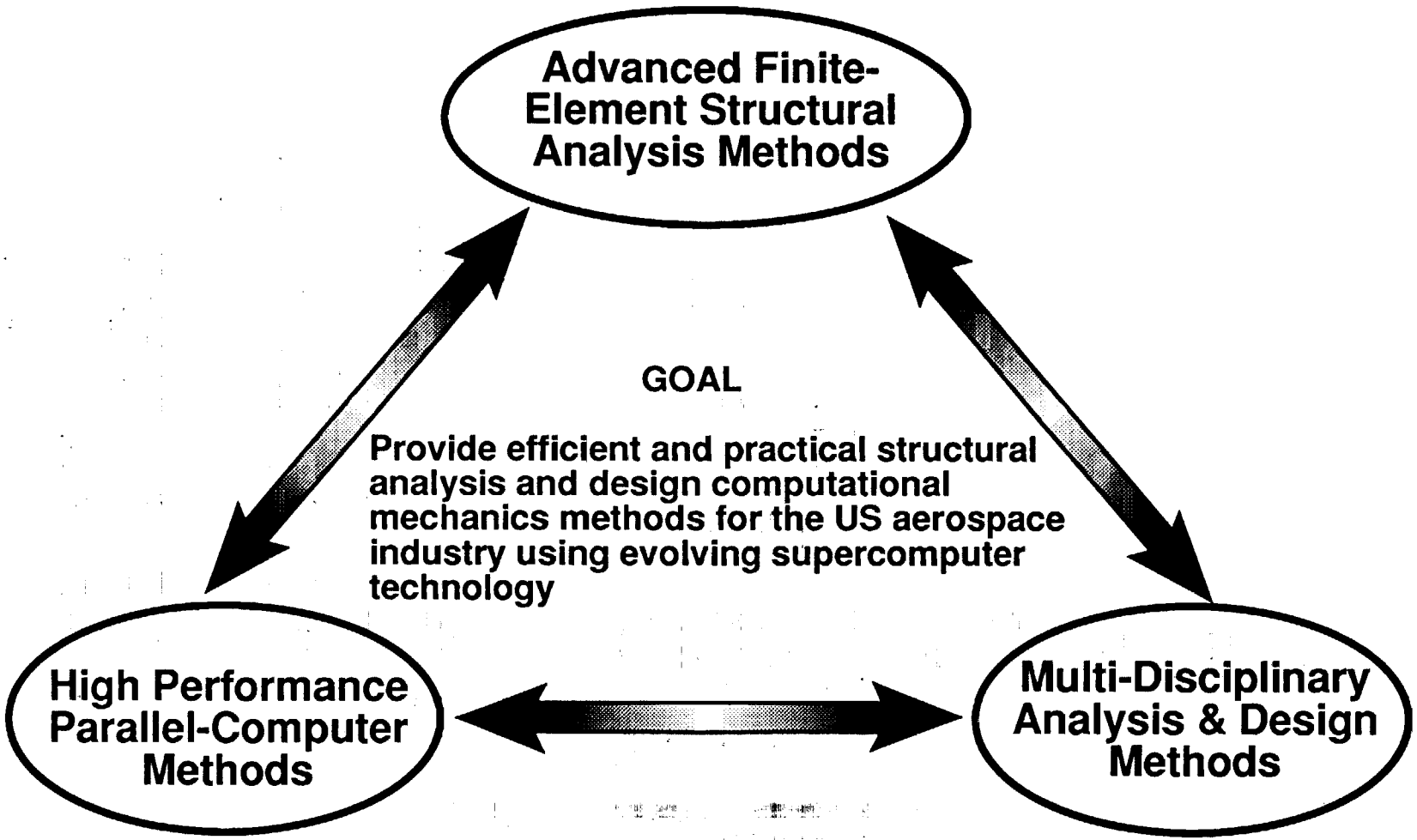


Figure 57

# Advanced Finite-Element Structural Analysis Methods

## Objective

**Develop advanced finite-element-based computational methods for predicting the structural response of complex aerospace vehicles subject to static, dynamic and thermal loads**

## FY93 Approach

- Formulate and implement interface elements in COMET code
- Develop high-order theories for composite plate and shell structures
- Develop 1D and 2D smoothing technique for stress and strain FEM results
- Verify ply discount progressive failure capability in COMET
- Integrate interface elements into COMET

## Key Milestones:

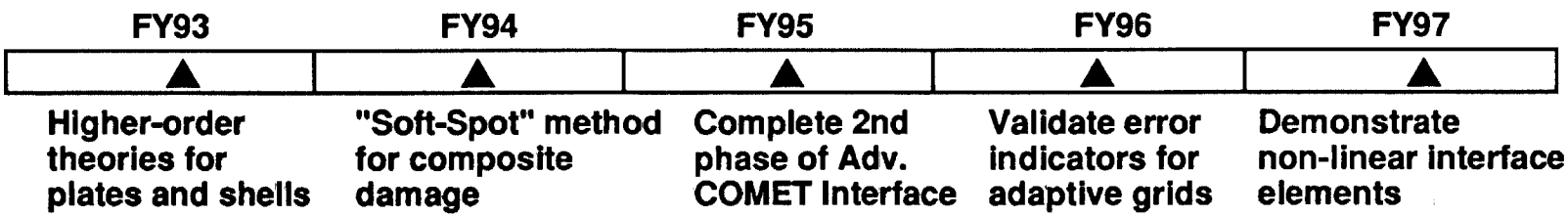


Figure 58

# Multi-Disciplinary Analysis & Design Methods

## Objective

**Develop efficient and robust computational analysis and design tools for integrated concurrent engineering applications**

## FY93 Approach

- Demonstrate reliability analysis on panels with imperfections
- Formulate interface requirements for coupled CFD/CSM methodology
- Define and assess interfacing procedures for coupling between CFD and FEM methods

## Key Milestones:

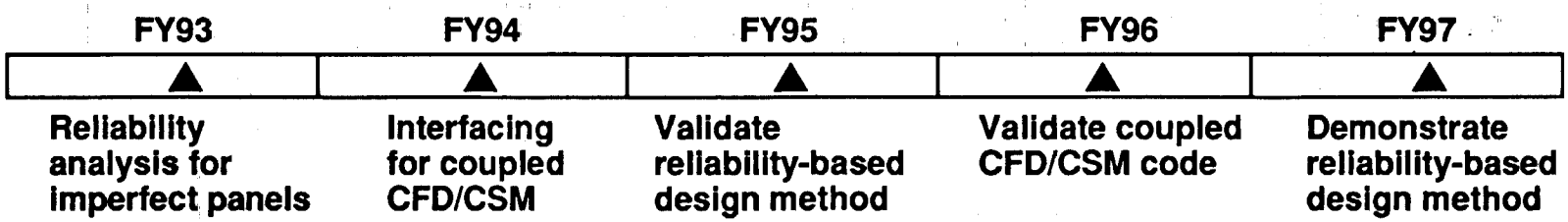


Figure 59

# High Performance Parallel-Computer Methods

## Objective

**Develop advanced structural analysis methods which exploit massively parallel computers to permit effective use of high-fidelity math models in the design and optimization of aerospace vehicles**

## FY93 Approach

- Demonstrate structural tearing/connecting sub-structuring algorithm on massively parallel computer
- Develop scalable solver of structural equations and demonstrate on large-scale HSCT model
- Develop and assess interfacing techniques for coupled fluid and structural meshes
- Organize and host Second Symposium on Parallel Computational Methods for Large-Scale Structural Analysis and Design

## Key Milestones:

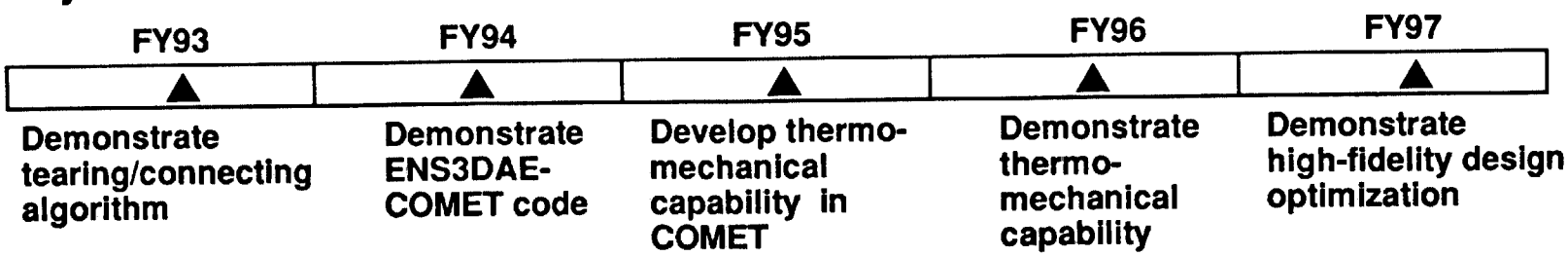


Figure 60

# AEROTHERMAL LOADS RESEARCH

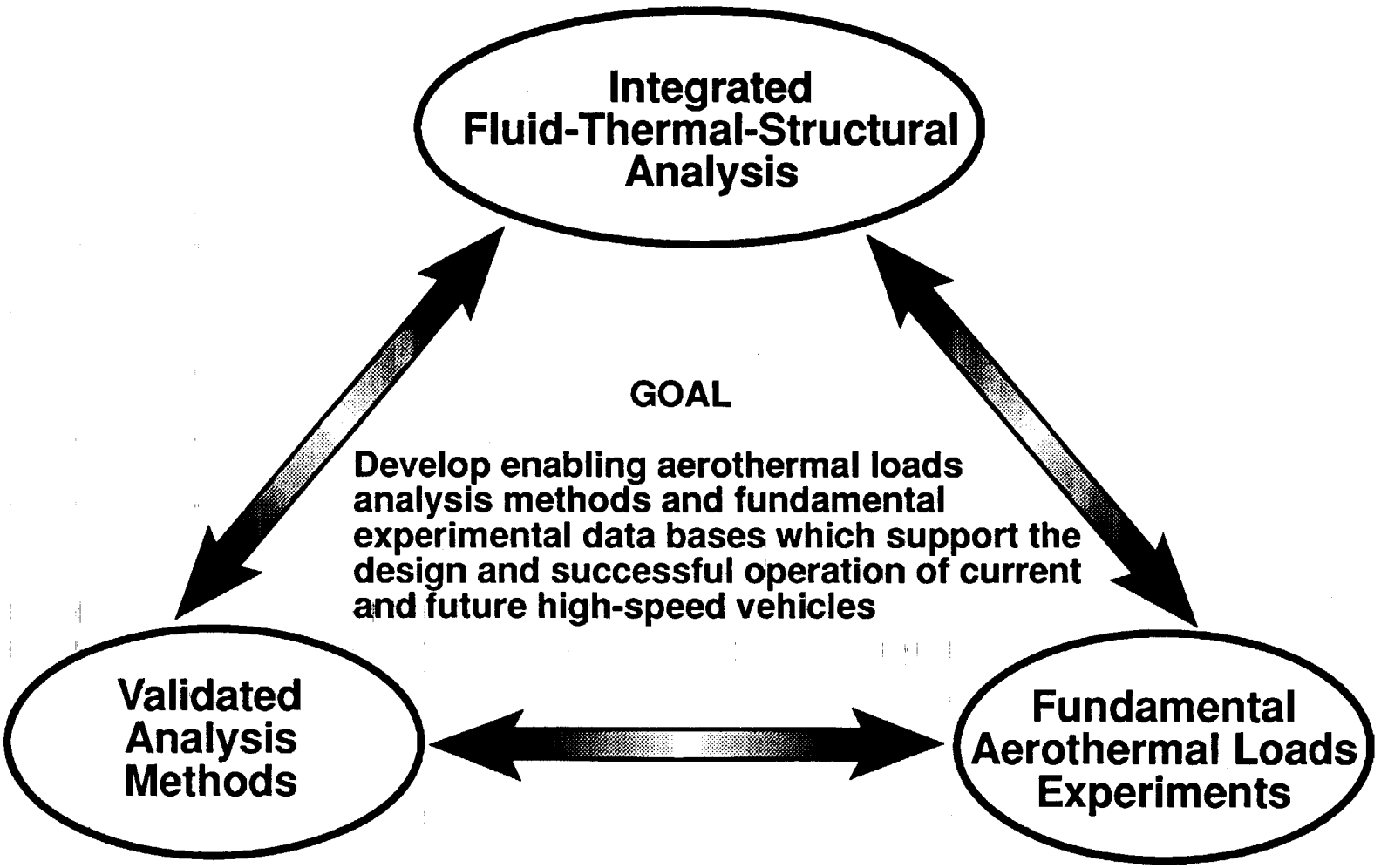


Figure 61

# Integrated Fluid-Thermal-Structural Analysis

## Objective

**Develop a unified, synergistic, computational fluid dynamics, heat transfer and structural mechanics numerical method to predict the aerothermostructural performance of high-speed vehicles**

## FY93 Approach

- Develop algorithm for variable density subsonic flow in typical cooled panels
- Develop fluid-thermal interface algorithm
- Develop coupled fluid-thermal algorithm for actively cooled structures
- Develop 3D adaptive unstructured mesh for thermal analysis
- Evaluate variable p finite-element algorithm for laminar flows

## Key Milestones:

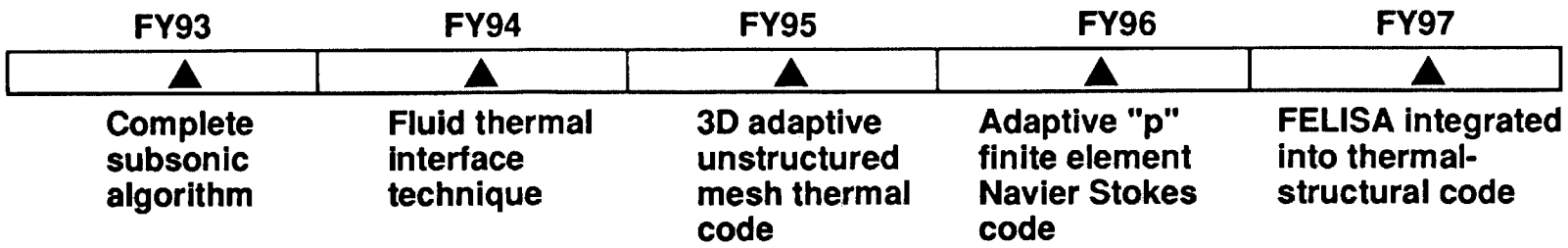


Figure 62

# Fundamental Aerothermal Loads Experiments

## Objective

**Develop experimental data base for aerothermal loads critical to the selection of material and thermal-structural concepts for low mass, high-speed vehicles**

## FY93 Approach

- Determine viability of hydrogen film-cooling for scramjet combustors
- Determine viability of fluid spike for reducing shock-shock interaction heating
- Determine effect of shear layer state on shock-shock interference heating levels
- Determine effect of leading-edge radius on shock-shock interference heating levels
- Assess non-continuum and non-equilibrium chemistry effects on shock-shock interference heating

## Key Milestones:

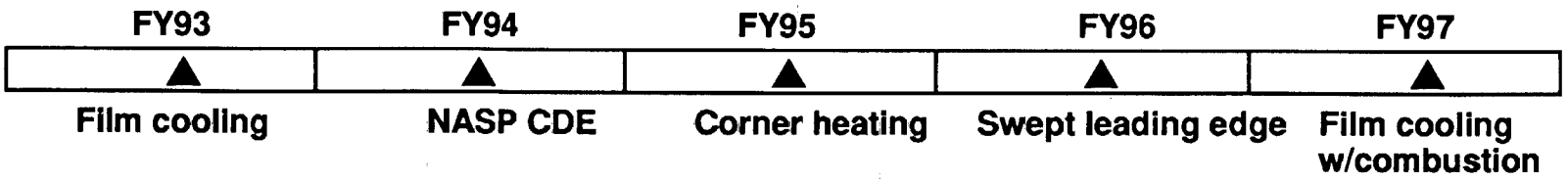


Figure 63

# Validated Analysis Methods

## Objective

**Provide efficient, validated, integrated fluid-thermal-structural numerical methods for prediction of aerothermal loads critical to high-speed vehicles**

## FY93 Approach

- Validate LARCNESS against laminar and turbulent shock-shock interference experiments
- Compare LARCNESS and DSMC methods for flight prediction of NASP cowl leading-edge loads
- Develop thermal-structural experimental data base for linear and non-linear behavior of plates
- Develop experimental model for corner flow shock interaction

## Key Milestones:

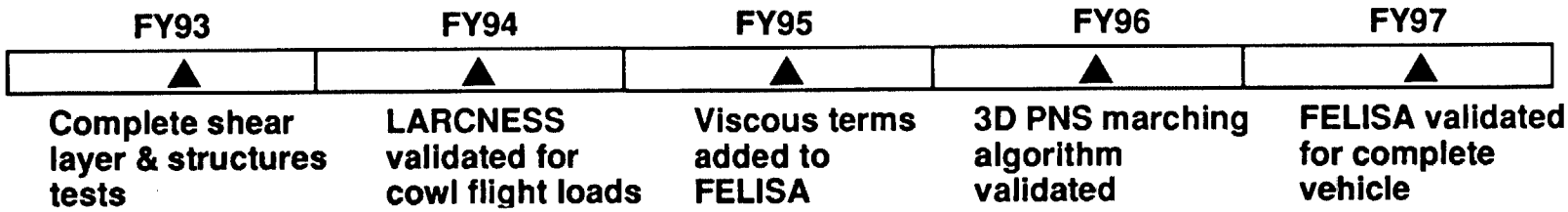


Figure 64

# REPORT DOCUMENTATION PAGE

*Form Approved*
*OMB No. 0704-0188*



| 1. AGENCY USE ONLY (*Leave blank*) | 2. REPORT DATE | 3. REPORT TYPE AND DATES COVERED |
|---|---|---|
| | November 1993 | Technical Memorandum |

**4. TITLE AND SUBTITLE**
Structural Mechanics Division Research and Technology Accomplishments for C.Y. 1992 and Plans for C.Y. 1993

**5. FUNDING NUMBERS**
WU 505-63-50-07

**6. AUTHOR(S)**
John B. Malone

**7. PERFORMING ORGANIZATION NAME(S) AND ADDRESS(ES)**
NASA Langley Research Center
Hampton, VA 23681-0001

**8. PERFORMING ORGANIZATION REPORT NUMBER**

**9. SPONSORING / MONITORING AGENCY NAME(S) AND ADDRESS(ES)**
National Aeronautics and Space Administration
Washington, DC 20546

**10. SPONSORING / MONITORING AGENCY REPORT NUMBER**
NASA TM-107752

**11. SUPPLEMENTARY NOTES**

**12a. DISTRIBUTION / AVAILABILITY STATEMENT**
Unclassified - Unlimited

Subject Category - 39

**12b. DISTRIBUTION CODE**

**13. ABSTRACT** (*Maximum 200 words*)

The purpose of this report is to present the Structural Mechanics Division's research accomplishments for C.Y. 1992 and plans for C.Y. 1993. The technical mission and goals of the Division and its constitutent research branches are described. The work under each branch is described in terms of highlights of accomplishments during the past year and plans for the current year as they relate to branch long range goals. This information is useful in program coordination with other government organizations, universities, and industry in areas of mutual interest.

**14. SUBJECT TERMS**
Accomplishments, research plans, structural concepts, structural mechanics, structural test, structural analysis, aerothermal loads

**15. NUMBER OF PAGES**
119

**16. PRICE CODE**
A06

| 17. SECURITY CLASSIFICATION OF REPORT | 18. SECURITY CLASSIFICATION OF THIS PAGE | 19. SECURITY CLASSIFICATION OF ABSTRACT | 20. LIMITATION OF ABSTRACT |
|---|---|---|---|
| Unclassified | Unclassified | | |